December 2018

Transient Analysis of a Coolant-to-Refrigerant Heat Exchanger to Provide Temporary High Performance in an Automotive Vehicle

Abhinav Ravi
University of Wisconsin-Milwaukee

TRANSIENT ANALYSIS OF A COOLANT-TO-REFRIGERANT HEAT EXCHANGER TO PROVIDE TEMPORARY HIGH PERFORMANCE IN AN AUTOMOTIVE VEHICLE

by

Abhinav Ravi

A Thesis Submitted in

Partial Fulfillment of the

Requirements for the Degree of

Master of Science

in Engineering

at

University of Wisconsin-Milwaukee

December 2018

ABSTRACT

TRANSIENT ANALYSIS OF A COOLANT-TO-REFRIGERANT HEAT EXCHANGER TO PROVIDE TEMPORARY HIGH PERFORMANCE IN AN AUTOMOTIVE VEHICLE
by

Abhinav Ravi

The University of Wisconsin-Milwaukee, 2018
Under the Supervision of Professor John Reisel

The objective of this thesis is to provide a numerical and experimental design tool to understand the heat transfer analysis of a coolant reservoir being chilled at a sub-ambient temperature with a goal of eventually providing a transient burst in performance. A high performance vehicle usually has a liquid charge air cooler that cools air before entering the engine. This liquid charge air cooler cools the air by using a specific coolant coming from the low temperature radiator. This study involves a coolant reservoir independent of the low-temperature radiator to provide coolant at a sub-ambient temperature to the liquid charge air cooler on a non-on-going basis. This causes the air in the liquid charge air cooler to be colder than usual, which provides a better volumetric efficiency that results in a higher performance in the engine.

The coolant in the reservoir heat exchanger that is being cooled by the refrigerant coming from the air conditioning unit in a vehicle is stagnant. Since this study is analyzing the coolant behavior and temperature, this thesis provides a comprehensive investigation on the natural convective heat transfer processes due to the motionless coolant being cooled.

A thermodynamic analysis coupled with a thermal resistance calculation provides a custom lumped capacitance model equation to show a relationship between the time

and coolant temperature. Results from this analytical calculation and experimental simulations using computational fluid dynamics software (Star CCM+) delivers a detailed understanding of the difference from cooling the coolant from the top compared to cooling the coolant from the bottom while understanding the importance of surface area for improved heat transfer.

TABLE OF CONTENTS

LIST OF FIGURES

LIST OF TABLES

LIST OF NOMENCLATURE

Symbol	Units	Definition
A	Meter^2	Cross Sectional Heat Transfer Area
c	$\frac{(\text{Joule})(\text{Kelvin})}{\text{Kilogram}}$	Specific Heat
g	$\frac{\text{Meter}}{\text{Second}^2}$	Gravity
h	$\frac{(\text{Watt})(\text{Kelvin})}{\text{Meter}^2}$	Heat Transfer Coefficient
L	Meter	Length
m	Kilogram	Mass
$\dot{Q}$	Watt	Heat Transfer Rate
R	(Watt)(Kelvin)	Resistance
r	Meter	Radius
T	Celsius	Temperature
t	Second	Time
th	Meter	Thickness
U	$\frac{(\text{Watt})(\text{Kelvin})}{\text{Meter}^2}$	Overall Heat Transfer Coefficient
V	$\frac{\text{Meter}}{\text{Second}}$	Velocity
$\dot{W}$	Watt	Work

Greek Symbol	Units	Definition
β	$\frac{1}{\text{Kelvin}}$	Thermal Expansion Coefficient
k	$\frac{(\text{Watt})(\text{Kelvin})}{\text{Meter}}$	Thermal Conductivity
ρ	$\frac{\text{Kilogram}}{\text{Meter}^3}$	Density
μ	$\frac{(\text{Kilogram})(\text{Second})}{\text{Meter}}$	Dynamic Viscosity

CHAPTER 1: INTRODUCTION

1.1 Motivation

There is and will always be a need for higher performance from automobiles. This improved performance may come in many forms, including better fuel efficiency, better energy efficiency, or better acceleration. Heat transfer issues often impact the performance of automobile components, and many companies seek to meet the demands of automotive companies with regards to thermal management. The focus of this work is to address potential customer needs regarding a specific need for high performance vehicles: power.

Power can mean anything from obtaining top speed from a racing car or an enhanced ability to successfully drive through a challenging off road trek. This thesis deals with the specific application of a high performance vehicle requiring an extra burst of speed for a short amount of time by using as much of the available resources provided, such as engine coolant and combustion air. Potential customer needs include both use in a for recreational vehicle or potentially competitive applications in a race car.

1.2 Background

A typical high performance vehicle contains a supercharger, charge air cooler, and an engine all in series to create combustion for performance as shown in Figure 1.1.

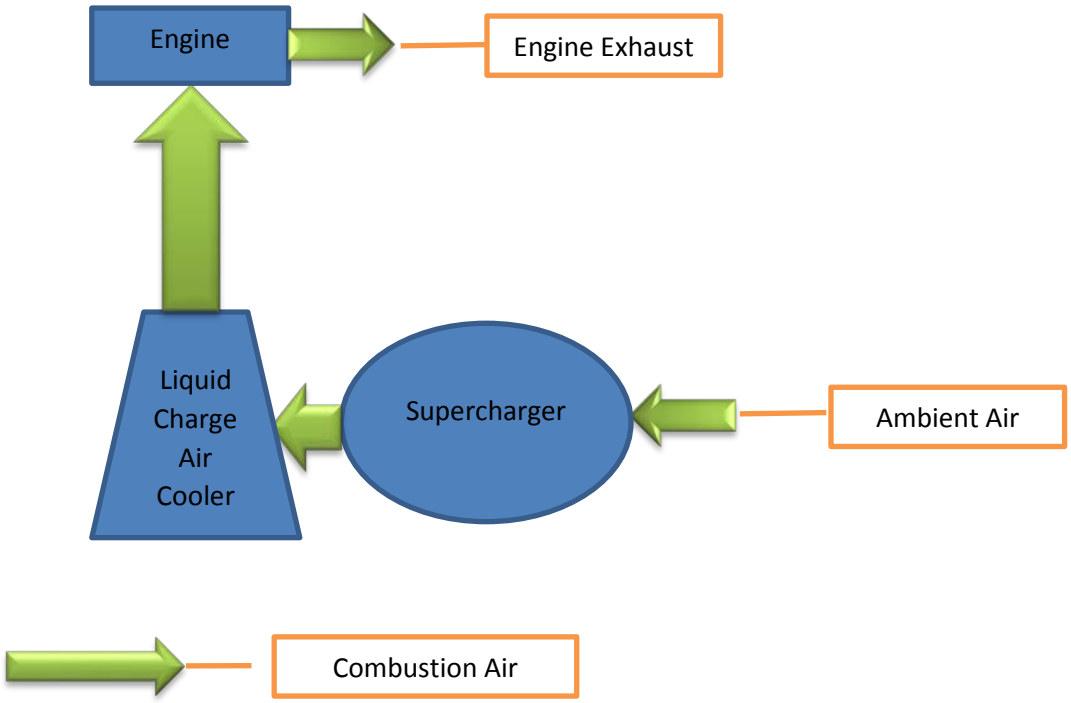

Figure 1.1: Supercharger – LCAC – Engine Loop

Outside or ambient air goes into the supercharger, which is used to increase the air mass flow rate into the cylinders to increase the power output of the engine. However, the supercharger achieves this by compressing the air, which results in not only an increased air pressure, but also an increased air temperature. A charge air cooler is needed to cool the pressurized air coming from the supercharger to a lower temperature. This increases the density of the air, which will ultimately increase the volumetric efficiency of the air intake of an engine.

In this particular case, the type of charge air cooler used will be a liquid charge air cooler. This means that inside the charge air cooler, a liquid coolant will provide the heat transfer means to cool the pressurized air coming from the supercharger. For that, the coolant should be at a relatively cool temperature. For the coolant to consistently be at a low temperature, a

dedicated Low Temperature Radiator (LTR) loop is used to cool the coolant with ambient air before it is delivered to the charge air cooler. This is illustrated in Figure 1.2.

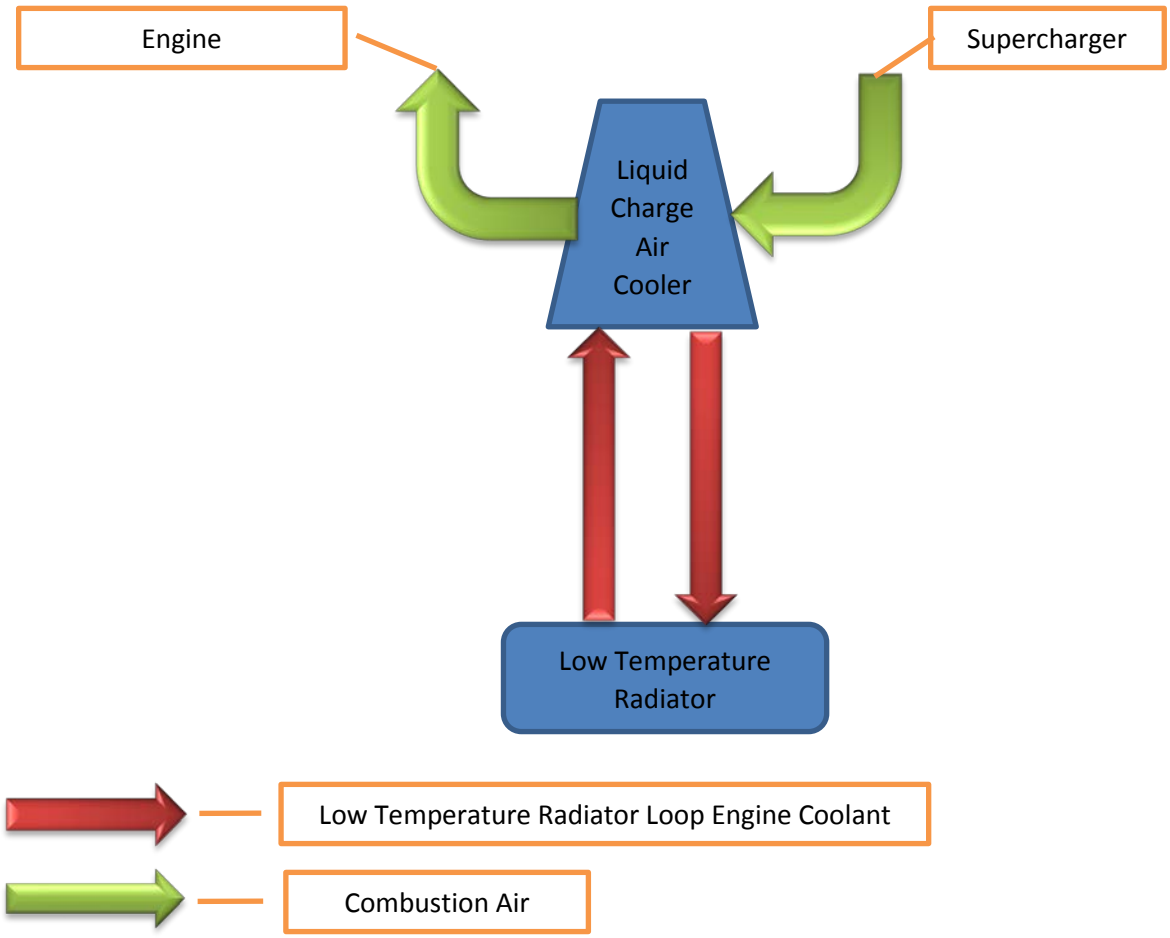

Figure 1.2: LTR-LCAC Heat Transfer Loop

This work introduces the addition of a coolant chiller that is independent of the low temperature radiator loop. The function of this chiller is to use refrigerant provided from the air-conditioning system (A/C) to chill a reservoir of coolant to a lower temperature than what could be achieved by only using the coolant from the LTR loop. This chilled coolant is only released to the charge air cooler during short, high power demands (such as rapid accelerations during racing). During these brief events, the coolant from chiller reservoir is used instead of the normal LTR coolant, and it will temporarily cool the pressurized air coming from the

turbocharger more than what would be possible with the LTR loop. This will further increase the power density and eventually greatly increase the volumetric efficiency of air going through the intake valve of the cylinder of an engine, which finally provides a transient increase in the power of the automobile. As shown in Figure 1.3, valves are used to decide if the coolant going to the liquid charge air cooler is coming from the LTR or the coolant chiller.

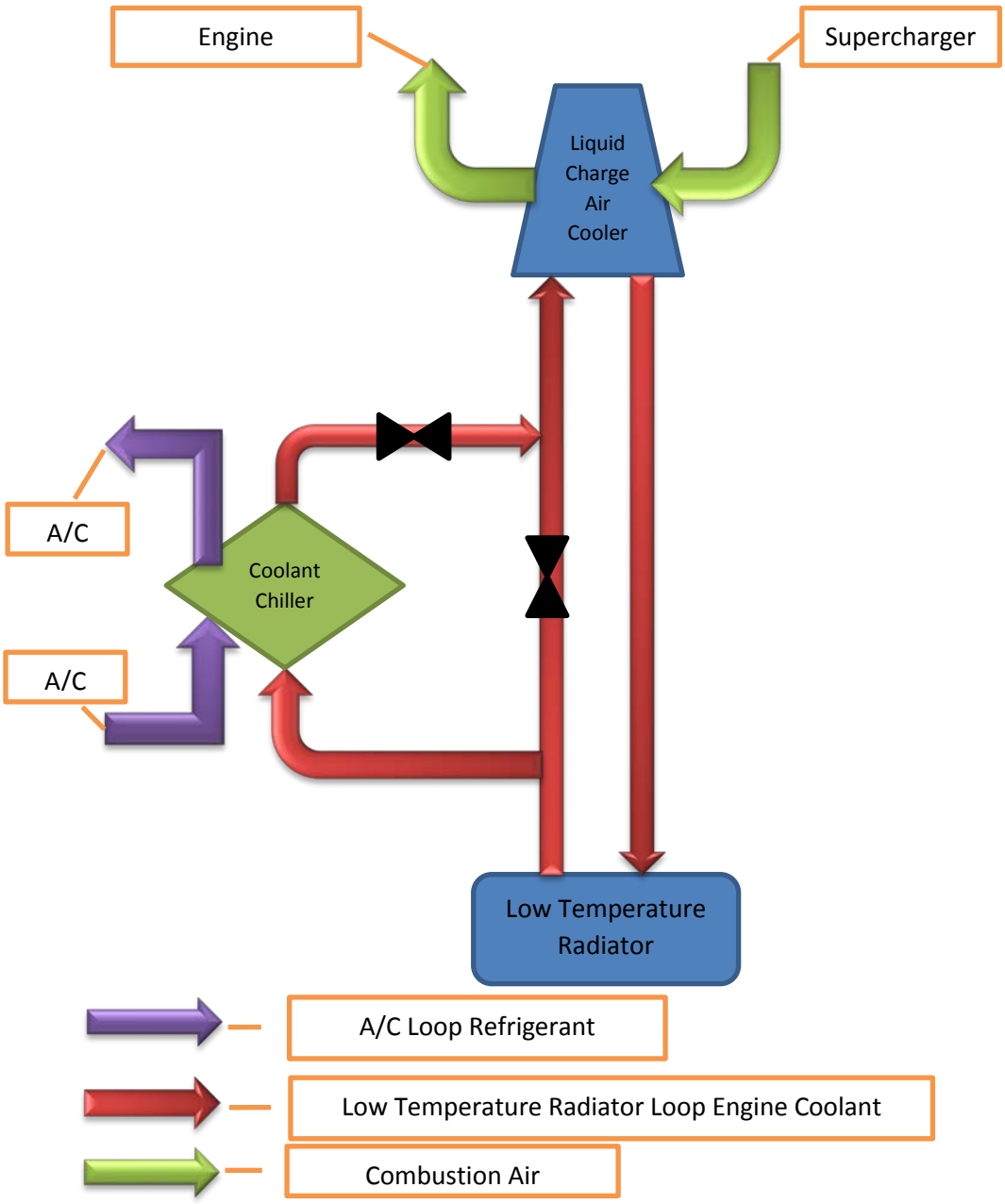

Figure 1.3: LTR-LCAC Heat Transfer Loop with Coolant Chiller

1.3 Objective

For the chiller to achieve a coolant at a sub ambient temperature, refrigerant from the vehicle's cabin A/C system is routed through the chiller. For this thesis, one assumption is that the engine coolant in the charge air cooler struggles to cool down significantly if this engine coolant is at a constant steady state flow going through the newly proposed coolant chiller. Attempts were also made to use this A/C loop to cool the flowing LTR loop, but it was found that the A/C system did not have sufficient capacity. Because of these two reasons, a stagnant pool of engine coolant in the coolant chiller is currently the optimal solution to significantly cool the temperature of this engine coolant. The coolant chiller with a constant steady flow of the low temperature refrigerant coming from the A/C loop provides the heat transfer for the coolant. This engine coolant should cool down as rapidly as possible during non-peak power operating times to be ready to be used when the user wants feature to be used.

The goal of this project is create a design model that compares the time and the temperature of the coolant to reach the sub ambient temperature inside the chiller by understanding and increasing the efficiency of the heat transfer of the coolant in the chiller.

To achieve this, several steps are involved:

1. Energy of the System: This is a 1-D model to understand a basic overview of the thermodynamic analysis of the constant volume chiller.
2. Heat Transfer Rate: Solving for the Heat Transfer Rate helps provide a relationship between the thermodynamic analysis and the overall heat transfer coefficient. The

heat transfer coefficient is calculated using a radial thermal circuit with custom correlations using CFD (Computational Fluid Dynamics) Simulations.

3. Lumped Capacitance Model: The variables from the Energy of the System and the Heat Transfer Rate ultimately provide a Lumped Capacitance Model. This model equation analytically predicts the coolant temperature for any given time throughout the heat transfer process.
4. Design Model for Multiple Iterations: This custom Lumped Capacitance Model is used with various structural changes to understand how various iterations to lead to differences in the coolant behavior and temperature.

Through this introduction, the importance and motivation on the study of an independent sub-ambient coolant reservoir in the LTR loop has been established. This background provides how components of high performance vehicles are typically designed and how this coolant chiller provides an advantage. The ultimate goal of transient high power comes from understanding the behavior of the engine coolant in this chiller going through heat transfer with a steady flow of refrigerant coming from the A/C department in a vehicle. The objectives assist in providing the process steps to understanding the coolant behavior going through heat transfer and providing a design model that can accurately predict the transient temperature of the coolant given the time and the structural design.

CHAPTER 2: LITERATURE REVIEW

A heat exchanger that has heat transfer between a stagnant coolant and a steady flow of refrigerant experiences both natural and forced convective heat transfer. Natural convection occurs in the stagnant coolant and forced convection is due to a steady flow of refrigerant. For this project, the coolant behavior and transient temperature is being studied. Therefore, there will be a heightened emphasis on the convective heat transfer properties and behavior of the coolant.

2.1 Engineering Applications of Natural Convection

Since natural convection has many applications in engineering, many studies discuss natural convection through both cooling and heating. Below is a sampling of studies that provide examples of this phenomenon. Analytical, numerical, and experimentation studies on

the transient natural convection of a warm crude oil contained in a storage tank that was being cooled in a cold environment was examined by Cotter and Charles [1]. This study provided a numerical simulation that shows a relationship between the viscosity of the crude oil and the natural convective cooling of the storage tank in a cold environment. The cooling shows that the tank cools to the ambient temperature asymptotically and the effect of the wall heat transfer coefficient on the rate of heat loss is most pronounced in the early stages of cooling. In terms of the viscosity, the rate of heat loss is significantly affected when the viscosity is temperature dependent.

Similarly, there is more research dealing with natural gas, since natural gas is getting increased attention as a potential clean fuel source. For this, the storage of liquefied natural gas (LNG) is crucial to understanding how LNG functions and can be used. An experimental and theoretical study on the natural convection in a liquid nitrogen tank provided the velocity and temperature profiles of various heat fluxes [2]. With this, a numerical simulation of natural convection was conducted in a liquid hydrogen tank going through a multiphase process, and provided the effect of thermal stratification in the tank [3]. This introduced studies in the natural convective effects on stagnant LNG at different Rayleigh Numbers [4]. This was then computationally conducted to prove that heat transfer rate is primarily affected by the liquid portion in a multiphase state [5]. Nakamoto *et. al* studied whether liquid phase semiconductor materials were being heated due to natural convection heat transfer in a CZ (Czochralski) furnace [6]. Their results demonstrated that the heat transfer was mainly due to the thermal conductivity of the inert gas involved.

Applications in geothermal engineering are also prevalent for natural convection. Stagnant water that is being heated by the outside hot dry rock that is underneath the earth was studied [7], while understanding the effects of borehole heat exchanger systems that are used as heat sinks underneath residential and commercial buildings have been studied thoroughly in terms of thermal conduction [8], forced convection [9], and for this thesis, natural convection [10]. These studies provide analytical and numerical design tools to understand the conductive and convective heat transfer considered in determining the borehole thermal resistance. These tools provide a theoretical foundation for further performance simulation and analysis.

Natural convective heat transfer plays a critical role in cooking, specifically for electric ovens. Laminar and turbulent natural convective studies in an enclosure containing a thermal load were conducted [11]. This paved the way for computational models to simulate natural convection heat transfer in electric ovens for various cooking cycles [12].

Natural convective heat transfer studies are also prevalent for reactor containing liquid metals, specifically in a hot molten core. Cooling of the molten core is investigated to understand its performance under long-term thermal load. Theoretical studies of natural convective heat transfer were studied using the surrounding fluid as air [13]. With this, analytical natural convective studies with varying Rayleigh Number was examined [14]. Using the theoretical and analytical models, various design model studies were performed, such as the addition of rectangular grooves [15], the use of square cylinders [16], the use of a semi-circular cavity [17], and a full cylindrical cavity [18]. Apart from the theoretical and analytical

models, numerical and experimental studies of molten core going through natural convection were conducted [19].

Finally, electronic components are becoming more and more prevalent as the impetus behind natural convective heat transfer studies. To understand these natural convection environment, initial numerical studies on natural convection cooling of two configurations of heat sources were examined [20] and of heat sources mounted on one of the vertical walls of a cube array [21]. This allowed for experimental studies for natural convection cooling for several heat sources in a vertical rectangular [22]. This showed that the heat transfer coefficient is strongly affected by the number of heat sources. Using this as a fundamental foundation, a numerical study was investigated to examine thermal interactions and natural convection cooling between heat fluxes generated by electronic devices mounted on a vertical printed circuit board (PCB) [23].

These various examples show the breadth of natural convection heat transfer in engineering applications. This provides a basis of how various industries have studied natural convection. However, to fully understand natural convection, the fundamentals of the topic should be investigated.

2.2 Fundamental Studies Conducted on Natural Convection

Natural convection was addressed by G.K. Batchelor in 1954, when he discussed the heat transfer across double-glazed windows at different temperatures [24]. Soon after, laminar transient natural convection of liquids in partially filled cylindrical coordinates was studied [25].

This study involved the Boussinesq approximation, which assumes all properties of the fluid being constant except for density. Since then; theoretical, numerical, and experimental studies for the basic understanding of natural convection in a container or cavity have been provided to further study Rayleigh Number and Grahshof Number in relation to the characteristic length [26]. From this, analysis on transient natural convection inside enclosures with differently heated sidewalls was studied [27]. These studies showed that the heat transfer rate was oscillatory during the transient period leading to the steady state. This was due to a fluid in constant convective motion due to recirculating regions of the stagnant fluid being heated. Kublbeck looked further into this study and went ahead to compare differentially heated sidewalls to one side wall non-uniformly heated while the other walls are left adiabatic [28]. This study proved that the one side wall that was non-uniformly heated produced a periodic flow structure compared to the differentially heated sidewalls. From this, a study by Vasseur and Robillard expanded on the idea of transient natural convection inside an enclosure with one wall being uniformly heated but not at constant temperature [29]. This study showed that a higher density fluid provides more motion in the fluid going through the natural convective heat transfer. Nicolette and Yang explore a different topic in the sense that instead of looking into transient heating, they look into transient cooling natural convection of single-phase fluids filled inside a square enclosure with one vertical wall cooled with the other three walls being adiabatic [30].

In parallel to the previous studies on the natural convection of fluids that are circulating and are in constant motion, theoretical and numerical investigations for a natural convective transient analysis of an already stratified fluid were being researched [31]. Studies continue

down this field of stratification, specifically for a fluid that is initially homogenous that turns stratified [32]. Kwak specifically studied the transient natural convective cooling down process of a fluid in a cylindrical container with the maximum temperature density allowed.

The reason that a literature review of both constant motion and stratification of a fluid undergoing transient natural convective heat transfer is done is because this provides a prediction of what the results of the experimentation could be. This project involves cooling a fluid from the bottom and from the top. Past literature provides a reasoning that cooling a fluid from the bottom could provide stratification and cooling from a fluid will more likely provide a constant circulating motion based on the density of the fluid. This is due to the natural behavior of hotter fluid continuously rising over cooler fluid.

For this thesis, analytical and numerical studies will be done to calculate natural convection in various structural interior designs. With that in mind, further literature was reviewed to understand numerical and analytical natural convection studies for various design forms. Similar to this thesis, computational fluid dynamics (CFD) was used to solve the problem of natural convection heat transfer around horizontal rectangular cylinders of isothermal surface temperature [33]. A numerical study of the same problem with the major axis horizontal was also solved [34]. Using this, a numerical study of natural convection around a square horizontal cylinder in an enclosure was studied [35] and a numerical study of natural convection around a square cylinder in a vertical channel was investigated [36]. In parallel with this, a numerical study of laminar natural convection heat transfer from an isothermal sphere was examined [37]. With all this research, a CFD technique was used to study the laminar

natural convection heat transfer from uniformly heated horizontal cylinders of a triangular cross-section, where thermal layers are obtained for various Rayleigh Numbers.

Since this thesis involves annuli design, further literature of natural convection in annuli design was studied. Experiments were performed to study natural convection heat transfer in vertical and electrically heated annular concentric parallel tubes [38]. Similar to this thesis, development of a correlation for the average Nusselt number and the Rayleigh provided an indirect correlation between the radius ratio and the Nusselt Number. Continued experimentation was done to determine the average and local heat transfer due to natural convection from the outside air to the surface of an isothermal cylinder of different diameters and lengths at various inclinations in both the laminar and turbulent regions [39]. Numerical analysis of natural convection in an annulus between two vertical concentric cylinders with the inner cylinder heated and the outer cylinder cooled was performed [40]. This provided the heat transfer coefficient of natural convection as functions of the Rayleigh number, radius ratio, and the temperatures of the heating and cooling wall surfaces. Continued numerical studies of natural convection in annuli design were done with the use of water as a working fluid in a vertical open-ended channel with constant wall heat flux [41]. This provided further experimental and numerical analyses for single-phase natural convection thermally induced flow of water in an internally heated vertical annulus [42]. For the experimentation, CFD was used to come to the conclusion that the heat flux leads to the increase in the heat transfer coefficient and the Nusselt Number.

Additional literature studies were reviewed for the study of reservoirs and the effects of natural convective heat transfer. A study was performed on the transient response of the fluid

in a vertical cylinder after a step change in the temperature wall until the stratification stage is reached [43]. This led to the analysis of long-term behavior of the cooling process in a vertical cylinder with fixed wall temperatures [44]. Further investigation of the cooling of a vertical storage tank was conducted to consider both the tank and insulation material [45]. This provided transient cooling of a laminar fluid initially rest inside a vertical cylinder to eventually find a correlation between the Nusselt number and the transient mean fluid temperature [46].

2.3 Studies on Ethylene Glycol Experiencing Natural Convective Heat Transfer

The literature that has been reviewed provides the fundamentals for natural convection and how the fluid behaves accordingly. However, this project delves into a specific fluid that is common in automotive engines: ethylene glycol mixed with water. Benchmark and numerical readings of containers filled with stagnant air were studied [47]. This study showed the similarities between the average and local Nusselt Numbers for air going through natural convective heat transfer. Soon after, experimental investigations for a container filled with water going through natural convection were calculated [48]. Schmidt argued that the flow for water was mostly stratified throughout this process. Since then, there have been many numerical [49], analytical [50], and experimental studies [51]. comparing the natural convection of the air and water.

However, there has not been much research done on ethylene glycol-water mixture. Mahdavi et al. did experimentally and numerically compare the nature of water and ethylene

glycol-water mixture flow in a cavity [52]. This study shows there was more uniformity of temperature in the walls and inside the heat exchanger for the ethylene glycol-water mixture filled cavity compared to the heat exchanger that just had water. This study was done for horizontal rectangular containers and vertical cylindrical containers.

2.4 Current Influence for this Thesis

This thesis involves the study of a stagnant coolant that is being chilled by a constant stream of refrigerant. This literature review has provided various topics that show what has been previously done in this area to provide a base to research and analyze this project.

Initially, it was important to understand the study how various industries have used natural convection heat transfer to show an in-depth look into how analytical, numerical, and experimental studies are processed and analyzed. The literature review includes fluids in storage tanks, such as crude oil and liquid natural gas. Natural gas also plays a role in geothermal engineering, such as borehole heat exchangers, and cooking, such as electric ovens. Finally, we can also see this heat transfer phenomenon in the cooling of electronic components and in nuclear technology, such as the cooling of molten core.

Understanding how multiple industries have used natural convection in practice, it was important to understand the fundamentals of natural convection heat transfer from a general overview. This included the effect of Rayleigh Number for laminar vs turbulent flow, the heating and cooling of a system, the effect of density and gravity, and the fluid flow studies. Fluid flow studies were analyzed for this particular project due to the effects of circulating motion and

stratification that will be caused due to the design of the heat exchanger being studied. Due to the unique design of heat exchanger, additional literature was reviewed to show the studies on natural convection in an annuli design. Additionally, detailed numerical and experimental studies for natural convection were examined, since this project involves CFD work using Star CCM+ software and numerical relationship studies specifically involving time and temperature.

With the fundamentals of natural convection heat transfer being studied, it was important to understand the primary fluid that is being cooled due to natural convection. The fluid being used for this project is an ethylene glycol-water mix. With that, it was important to understand the studies that have been done in this field, even though there has not been much work specifically done on that fluid.

This literature review provides an investigation of what has been studied, how others have defined concepts and studies, and to provide evidence for the continued research in this field. Having this information shows various perspectives of this subject and how the influence is shown in the rest of this project.

CHAPTER 3: METHODOLOGY

3.1 Overview

The motivation, background, and objectives behind this thesis have been discussed in the previous chapter. This chapter will delve into the methods that were employed to achieve the overall intent, which is to integrate a design model that can provide different relationships of the coolant temperature and time. Following the objectives for this project, the energy of the system is the first process to be analyzed.

3.2 Energy of the System

Thermodynamic analysis is imperative to understanding the relationship between the internal energy and the heat transfer rate of the system . For this study, it is assumed that the chiller will be a closed system consisting of a rigid aluminum container. This means that the

system is at constant volume. As shown in Figure 3.1, the coolant is considered to be stagnant, while the heat transfer is coming from a chilled refrigerant flowing at steady state.

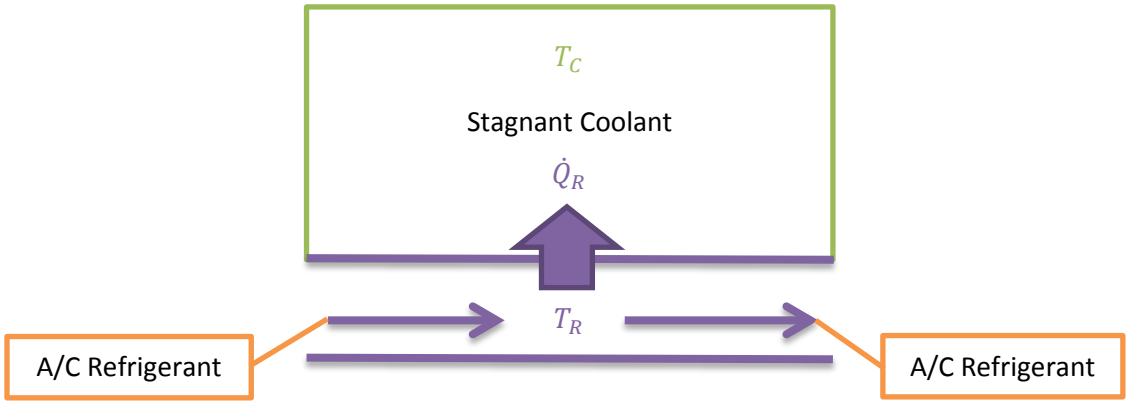

Figure 3.1: Closed System Model

For Figure 3.1, the first law of Thermodynamics for a closed system is used. Assuming that the changes in potential energy and kinetic energy are negligible, the equation for this is:

$$\frac{dU}{dt} = \dot{Q} - \dot{W} \tag{3.1}$$

In Equation (3.1), dU represents the change of rate of the internal energy in the system, dt represents the change of rate of time in the system, $\dot{Q}$ represents the overall heat transfer rate in the system and $\dot{W}$ represents the overall rate of work in the system. It is assumed that there is no work being done to the system or coming from the system, so $\dot{W}$ can be set equal to zero. Also, since this work involves the study of the coolant behavior, the heat transfer acting upon the system needs to be accounted for. In this case, the heat transfer acting upon the system is the heat transfer coming from the refrigerant portion, which can be referred to as $\dot{Q}_R$. Therefore, the equation for the first law of Thermodynamics for a closed system can be reduced to

$$\frac{dU}{dt} = \dot{Q}_R \tag{3.2}$$

For a constant volume scenario, $\frac{du}{dT}$ becomes c_v with dT representing the change of rate of temperature. du represents the change of rate of the internal energy of the system without the mass component, m, and c_v is the specific heat of the coolant at constant volume. This means that $\frac{dU}{dt} = m\frac{du}{dt}$, where dt represent the change of rate of time, which provides the equation:

$$\frac{dU}{dt} = mc_v dT_c \tag{3.3}$$

provided that the specific heat is considered constant.

T_c represents the temperature of the coolant.

Combining Equation (3.2) and Equation (3.3), the equation for the thermodynamic portion of this study is:

$$\boldsymbol{\dot{Q}_R = mc_v \frac{dT_C}{dt}} \tag{3.4}$$

3.3 Heat Transfer Rate

i. Overall Heat Transfer Coefficient

The thermodynamic analysis helps provide a relationship between the heat transfer rate $\dot{Q}_R$, the coolant temperature of the coolant T_c, and the time given, t. To be able to understand $\dot{Q}_R$, the heat transfer rate equation is used:

$$\dot{Q} = UA\Delta T,$$

or for this study,

$$\dot{\boldsymbol{Q}}_{\boldsymbol{R}} = \boldsymbol{UA}(\boldsymbol{T}_{\boldsymbol{C}} - \boldsymbol{T}_{\boldsymbol{R}}) \,. \tag{3.5}$$

In Equation (3.5), U represents the overall heat transfer coefficient, A represents the cross-sectional heat transfer area, and T_R represents the temperature of the refrigerant. The UA from Equation 3.5 can be calculated using the Thermal Resistance Equation:

$$\frac{1}{UA} = R_{total} \,. \tag{3.6}$$

Here, R_{total} represents the summation of resistances for all materials/components involved. In this study, the materials involved are the coolant R_C, the refrigerant R_R, and the aluminum R_{AL} in between the coolant and refrigerant.

ii. Radial Thermal Resistance Circuit

Since the aluminum is a solid, R_{AL} will be solely from heat conduction where a resistance equation for aluminum solid is typically:

$$R_{Al} = \frac{th_{Al}}{k_{Al}A_{Al}} \,. \tag{3.7}$$

where th_{Al} represents the thickness of the solid aluminum material, k_{Al} represent the thermal conductivity of the solid aluminum material, and A_{Al} represents the surface area of aluminum resistance.

Since both the refrigerant and coolant are fluids, R_C and R_R involve convective properties which means that a resistance equation for the coolant will usually be:

$$R_C = \frac{1}{h_C A_C} \tag{3.8}$$

Similarly a resistance equation for the refrigerant is:

$$R_R = \frac{1}{h_R A_R} \tag{3.9}$$

In these equations, h_C represents the heat transfer coefficient of the coolant and A_C represents the surface area of the coolant. Similarly, h_R represents the heat transfer coefficient of the refrigerant and A_R represents the surface area of the refrigerant.

However, for this particular study, there is a manufacturer's preliminary design concept that was used as a basis for this study. This design was modeled as shown in Figure 3.2.

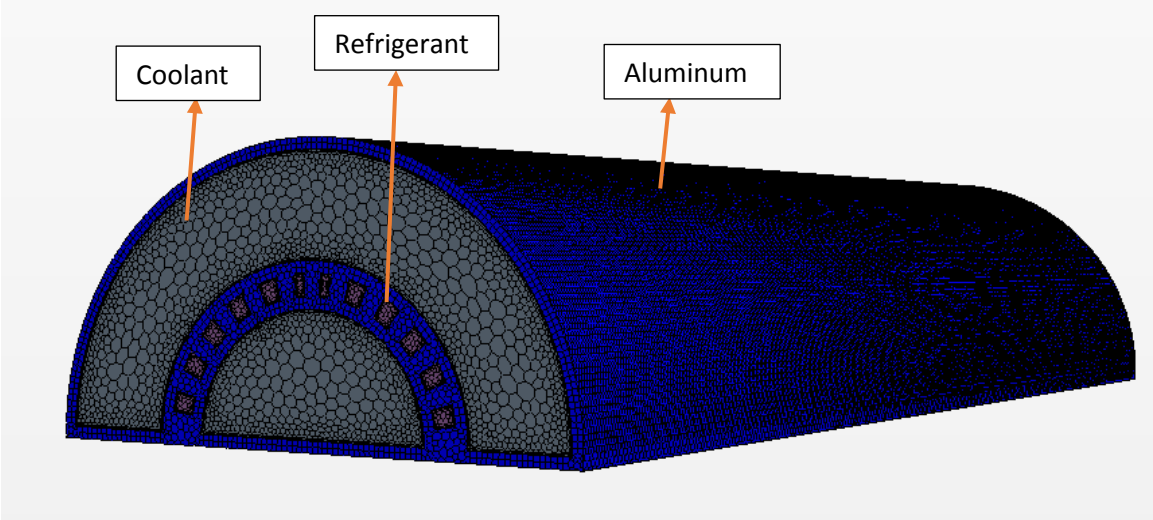

Figure 3.2: Initial Design of the Coolant Chiller

In Figure 3.2; the blue represents aluminum, the gray represents stagnant coolant, and the orange rectangular boxes represent a steady flow of refrigerant coming and go to the A/C department. This design shows that this study should be considered in radial coordinates instead of Cartesian coordinates. Since this is the case, the resistance equations are changed accordingly. For radial coordinates,

$$R_{AL} = \frac{\ln(\frac{r_2}{r_1})}{2\pi k_{Al} L_{Al}} \tag{3.10a}$$

$$R_C = \frac{1}{h_C 2\pi r L} \quad (3.10b)$$

$$R_R = \frac{1}{h_r 2\pi r L} \quad (3.10c)$$

As mentioned earlier, the reason the resistance equation for the aluminum is different than the resistance of the coolant and refrigerant is because the aluminum is conductive heat transfer only due to a solid material, while the coolant and refrigerant are fluids.

For this particular design, the bottom stagnant coolant will be designated as C1 and the bottom stagnant coolant will be designated as C2, as shown in Figure 3.3:

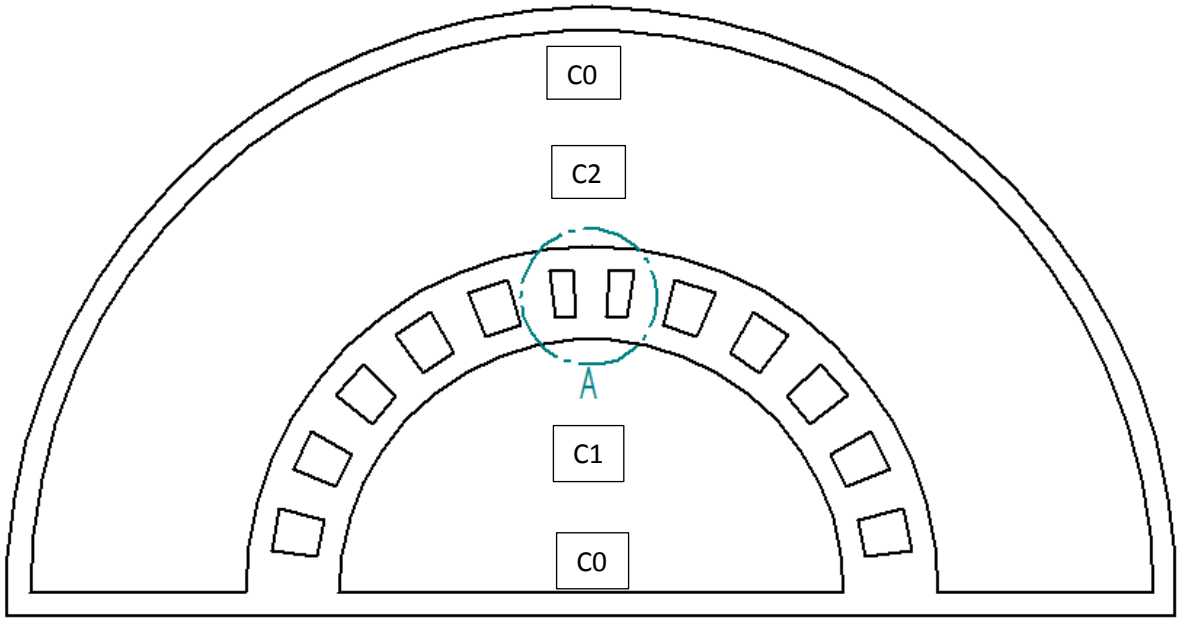

Figure 3.3: Front View of Initial Coolant Chiller Design with Material Designations

Also, the bottom part of the refrigerant is designated as R1, while the top part of the refrigerant is R2. Similarly, the bottom part of the aluminum is designated as Al1, while the top part of the aluminum is Al2. Figure 3.4 gives a more detailed look of the middle part of

Figure 3.3. This is addressed by “Detail A” expanded out in Figure 3.3. Figure 3.4 categorizes the Aluminum and Refrigerant portions.

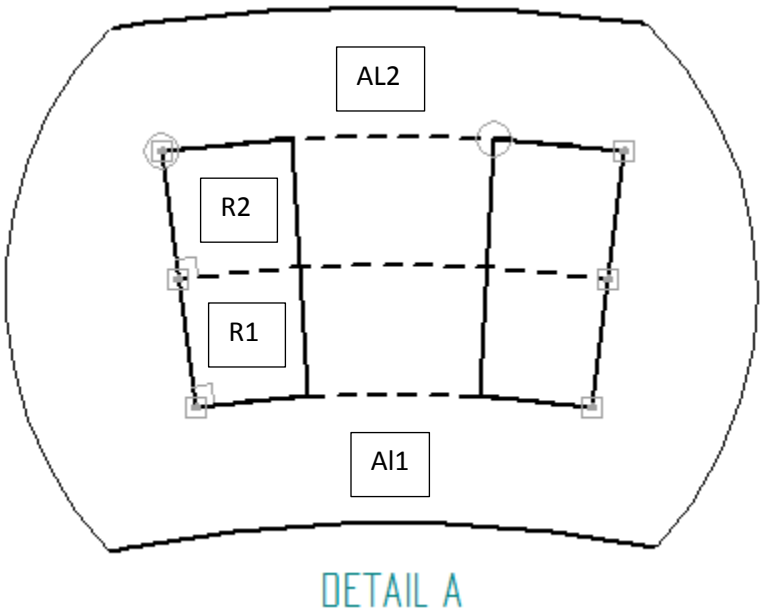

Figure 3.4: Detailed View of Figure 3.3 for Material Designation

The variables for the coolant dimensions are shown as r1, r2, r3, r4, and r5. These variables are shown can be seen in Figure 3.5.

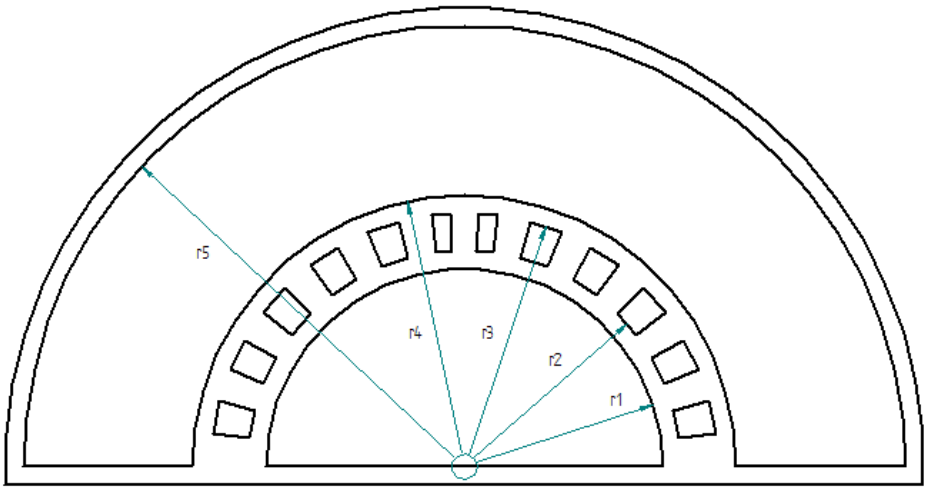

Figure 3.5: Front View of Initial Coolant Chiller Design with Radii designations

With these variables provided, the resistance equations from Equation 3.10 for the coolant, refrigerant, and aluminum can be updated to

$$R_{C1} = \frac{1}{h_C 2\pi r_1 L} \quad , \tag{3.11a}$$

$$R_{AL1} = \frac{\ln\left(\frac{r_2}{r_1}\right)}{2\pi k_{Al} L_{Al}} \quad , \tag{3.11b}$$

$$R_{R1} = \frac{1}{h_r 2\pi r_2 L} \quad , \tag{3.11c}$$

$$R_{R2} = \frac{1}{h_r 2\pi r_3 L} \quad , \tag{3.11d}$$

$$R_{AL2} = \frac{\ln\left(\frac{r_4}{r_3}\right)}{2\pi k_{Al} L_{Al}} \quad , \tag{3.11e}$$

$$R_{C2} = \frac{1}{h_C 2\pi r_4 L} \quad . \tag{3.11d}$$

To find R_{tot}, it was originally thought that the summation of the resistance was due to a thermal resistance circuit in series as shown in Figure 3.6.

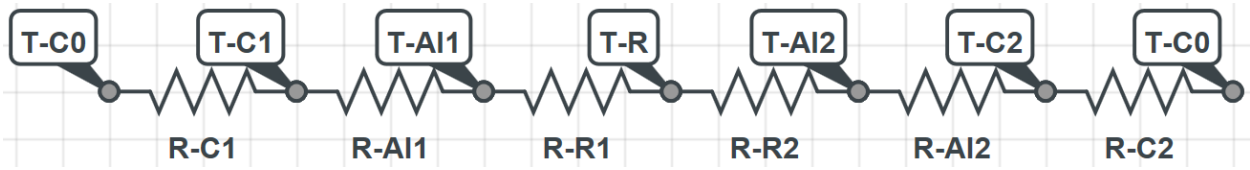

Figure 3.6: Radial Thermal Resistance Circuit of Frontal View of Coolant Chiller in Series (Incorrect)

The reason for this thinking is that this is developed from comparing the circuit to Figure 3.3 and starting from the bottom of the frontal view to the top. Even though this looks logical, it is inaccurate because the transient temperature of the overall coolant should be the same, which is not shown in the thermal resistance circuit in series. Starting from the refrigerant to the bottom coolant and the top coolant in parallel to get a uniform overall transient

temperature of the coolant is accurately shown through a thermal resistance circuit in parallel as shown in Figure 3.7.

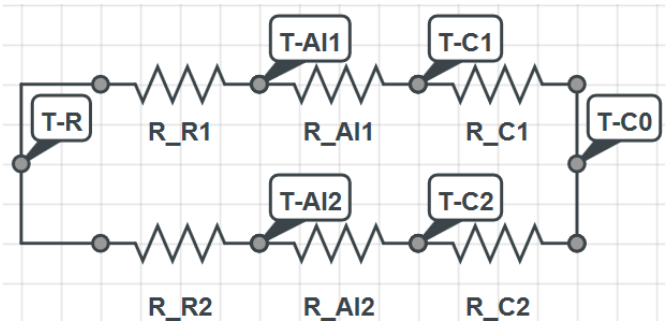

Figure 3.7: Radial Thermal Resistance Circuit of Frontal View of Coolant Chiller in Parallel (Correct)

R_{tot} can be solved from

$$\frac{1}{R_{tot}} = \frac{1}{R_{C1}+R_{AL1}+R_{R1}} + \frac{1}{R_{C2}+R_{AL2}+R_{R2}} \tag{3.12}$$

R_{AL1} and R_{AL2} from Equation (3.11) can be solved relatively easily, since the dimensions of the radii and length of the container are given and the thermal conductivity of aluminum for any temperature given can be easily found in literature.

However, R_{C1}, R_{C2}, R_{R1}, and R_{R2} from Equation (3.11) are more complicated to decipher. Even though the radii and dimension of the container are given, the heat transfer coefficient term, h, for each of the fluid resistance equations needs to be calculated. h can be solved for using the Nusselt Number equation.

iii. Nusselt Number Correlation & Calculation

The Nusselt Number represents the ratio between the convective heat transfer and the conductive heat transfer across the boundary involved, as shown in equation (3.13):

$$Nu = \frac{Convective\ Heat\ Transfer}{Conductive\ Heat\ Transfer} = \frac{hD}{k} \quad . \tag{3.13}$$

In Equation (3.13), D represents the hydraulic diameter. The hydraulic diameter is a characteristic length that is dimensionless, and usually finds a ratio between the wetted perimeter and the surface area involved. In this radial case, this characteristic length calculation involves the radii involved across the boundary.

The conductive heat transfer includes the thermal conductivity term, k, which is the only heat transfer term used in the R_{AL} resistance equations (Eq. 3.11). This is because this is the Aluminum solid is going through solely conductive heat transfer. The heat transfer coefficient, h, helps provide a convective heat transfer term for the fluids involved. The thermal conductivity can be found from literature. To find the Nusselt Number, there are different methodologies used for the refrigerant and the coolant.

a) Nusselt Number Correlation and Calculation for the Refrigerant

Since the refrigerant is flowing in a steady flow, it is said to going through forced convective heat transfer. For this scenario, a correlation between the Nusselt Number and the Reynolds Number can be used, such that the Nusselt Number can be solved as a function of the Reynolds Number and the Prandtl Number:

$$Nu = f(Re,Pr) \tag{3.14}$$

Correlations for this function equation can be found using literature found on turbulent fully developed internal flow. In this case, the 2013 ASHRAE (American Society of Heating, Refrigerating and Air-Conditioning Engineers) Handbook – Fundamentals (SI) was used to provide an equation for the Nusselt Number for this particular scenario [53]:

$$Nu = 0.023\, Re^{\frac{4}{5}} Pr^{0.3} \tag{3.15}$$

For this study, the Nusselt Number of the refrigerant changes Equation (3.15) to

$$Nu_R = 0.023 Re_R^{0.8} Pr_R^{0.3} \tag{3.16}$$

where Re_R is the Reynolds Number of the refrigerant fluid flow and Pr_R is the Prandtl Number of the refrigerant.

As shown in Equation (3.16), the Reynolds Number and Prandtl Number need to be found. The Reynolds Number is a dimensionless number that is used to analytically help predict fluid flow behavior. The general equation for Reynolds Number is

$$Re = \frac{\rho V L}{\mu} \tag{3.17}$$

For this particular case; since the fluid flow of refrigerant is considered, The Reynolds Number for the refrigerant changes Equation (3.17) to become

$$Re_R = \frac{\rho_R V_R L_R}{\mu_R} \quad , \tag{3.18}$$

where ρ_R is the density of the refrigerant, V_R is the velocity of the refrigerant, L_R is the characteristic length of the boundary of which the refrigerant flows through, and μ_R represents the dynamic viscosity. ρ_R and μ_R can be found through the literature. L_R can be

found knowing the dimensions of the boundaries that enclose the refrigerant fluid flow. V_R can be solved for knowing the mass flow rate of the refrigerant and solving for the velocity accordingly.

The general equation for mass flow rate is

$$\dot{m} = \rho V A \quad . \tag{3.19}$$

The equation of the mass flow rate of the refrigerant flowing in and out of the coolant chiller at a steady state changes Equation (3.19) to

$$\dot{m}_R = \rho_R V_R a_R \tag{3.20}$$

where a_R represents the cross sectional area of the refrigerant going through the coolant chiller.

Now that all the variables have either been found or calculated, Re_R can be determined leaving only the Prandtl Number to be found.

The Prandtl Number is a dimensionless number that provides a ratio between momentum diffusivity to thermal diffusivity with the general equation

$$Pr = \frac{C_p \mu}{k} \quad . \tag{3.21}$$

In this study with regards to the refrigerant, Equation (3.21) becomes

$$Pr_R = \frac{C_R \mu_R}{k_R} \quad . \tag{3.22}$$

With the Prandtl Number and Reynolds Number of the refrigerant calculated, Nu_R can be found. With Nu_R, h_r can be found and with h_r, both R_{R1} and R_{R2} can be solved for.

For the total resistance equation for R_{R1}, R_{R2}, R_{AL1}, and R_{AL2} have been solved. The resistance of coolant can be solved similarly to the resistance calculation of refrigerant using a Nusselt Number correlation and calculation.

b) Nusselt Number Correlation and Calculation for the Coolant

The Nusselt Number correlation for the coolant is different from the Nusselt Number correlation for the refrigerant because rather than the Nusselt Number for the coolant is a function of the Rayleigh number rather than a function of the Reynolds Number:

$$Nu = f(Ra) \quad . \quad (3.23)$$

The reason for this difference is because unlike the steady state of fluid flow provided by the refrigerant in the case study, the coolant is stagnant in the coolant chiller reservoir. This means that the coolant is providing free or natural convective heat transfer.

For the refrigerant, literature was used to find the Nusselt Number-Reynolds Number correlation for a fully developed internal flow. However, for a Nusselt Number-Rayleigh Number correlation, literature for this specific model, whether an annular semi-circular pipe for the top coolant or semi-circular pipe for the bottom, was sparse. To gain confidence in a capable Nusselt Number-Rayleigh Number correlation for the coolant, a custom correlation for both the bottom coolant and the top coolant was created by simulating the design through a Computational Fluid Dynamics (CFD) Simulation.

For this simulation, both the bottom and the top parts of the coolant chiller were simulated.

Bottom Coolant: CFD Simulation and Nusselt-Number Correlation

For the bottom part of the coolant the geometry was drawn as shown in Figure 3.8.

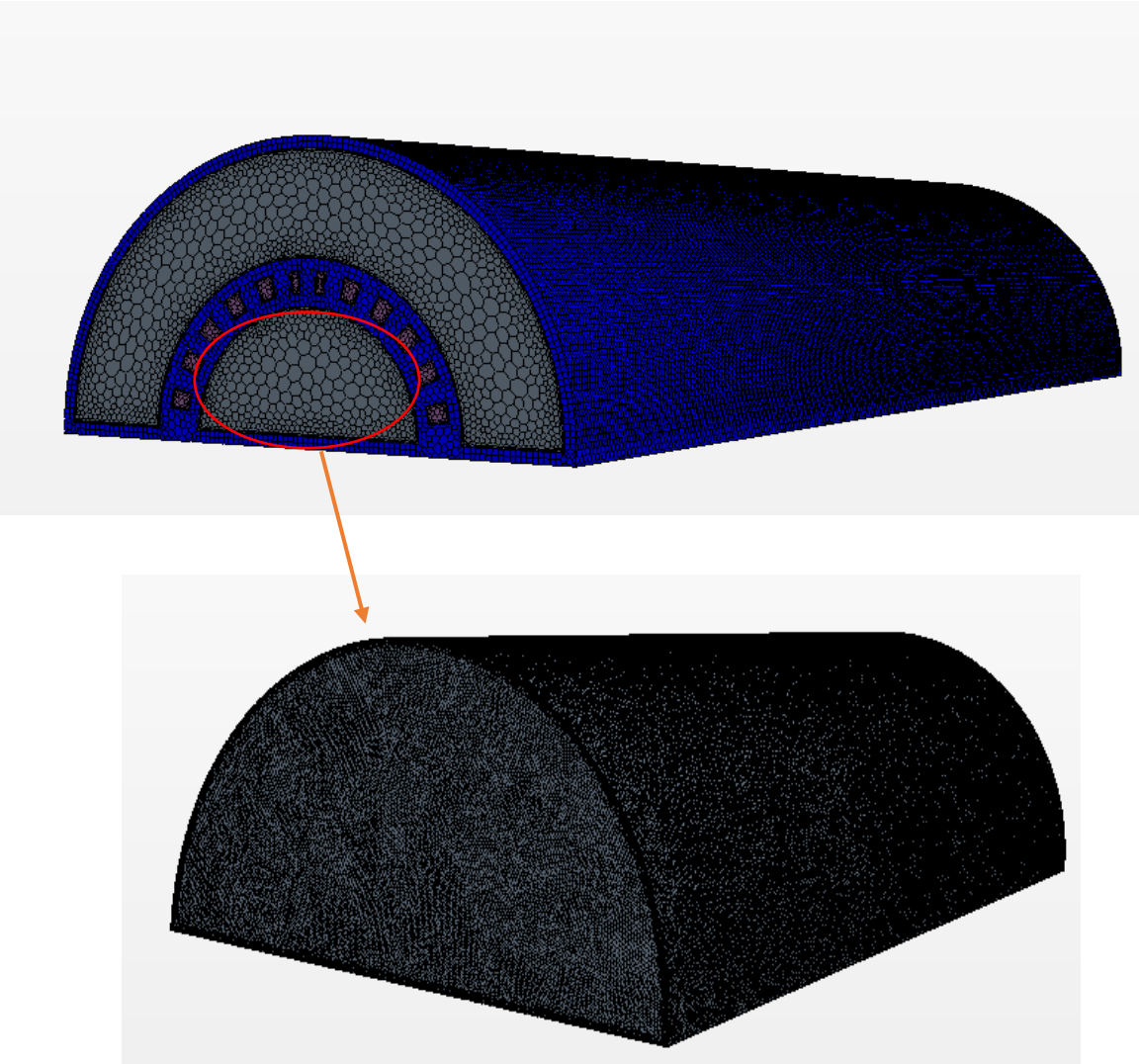

Figure 3.8: Design Geometry of Bottom Coolant

Assumptions and inputs for this CFD simulation of this bottom coolant include

1. Coolant is stagnant with the standard CFD natural convection model. (Bousinessq Model, gravity)

2. Properties of coolant are used, such as density, dynamic viscosity, thermal conductivity and specific heat.
3. Bottom flat surface is adiabatic.
4. Top radial surface has a boundary temperature of $10°C$ to predict the temperature coming from the aluminum in contact with the sub-ambient steady state of the refrigerant.
5. Initial temperature of the coolant was $30°C$, $35°C$, $40°C$, $45°C$, and $50°C$ for different iterations. The reason for this is because for this study, the ambient/outside temperature is predicted to be in the range of $10°C$-$30°C$. The engine coolant is typically $20°C$ more than the ambient air hence the coolant initial temperature is $30°C$-$50°C$.

With these inputs, a CFD simulation was performed for each initial temperature iteration. The reason for the simulation is to provide certain outputs, such as a heat transfer rate coming from the top radial surface, a stabilized volume average temperature (bulk temperature) of the coolant, and corresponding side view temperature and velocity profiles of the coolant after the heat transfer is stabilized.

The heat transfer rate, $\dot{Q}$ and the volume average temperature, T_B are used to solve for the heat transfer coefficient, h, using the heat transfer rate equation similar to Equation (3.5),

$$\dot{Q} = hA(T_B - T_W) \ ,$$

where T_W represents the Wall Temperature from the Top Radial Surface

For this study, the equation becomes

$$\dot{Q}_{BOT} = h_{BOT} A_{BOT} (T_{B_{BOT}} - T_{W_{BOT}}) \quad , \tag{3.24}$$

where “BOT” represents the bottom coolant

Solving for h_{BOT} provides a calculation to solve for the Nusselt Number, similar to Equation (3.13):

$$Nu_{BOT} = \frac{h_{BOT} D_{BOT}}{k_C} \quad . \tag{3.25}$$

Nu_{BOT} is solved for each initial temperature iteration ($30°C$-$50°C$). In parallel with solving for Nu_{BOT}, the Rayleigh Number for the bottom coolant at each temperature iteration also needs to be determined to understand a correlation between the Nusselt Number and the Rayleigh Number.

The Rayleigh Number is a dimensionless number to quantify buoyancy-driven flow that is going through natural convective heat transfer. To solve for the Rayleigh Number, the equation to be used is

$$Ra = \frac{\rho g \beta \Delta T L_C^3}{\alpha \mu}$$

or for this study,

$$Ra_{BOT} = \frac{\rho_C g \beta_C (T_{B_{BOT}} - T_{W_{BOT}}) D_{BOT}}{\alpha_C \mu_C} \quad . \tag{3.26}$$

β_C represents the thermal expansion coefficient of the coolant and α_C represents the thermal diffusivity of the coolant, where

$$\alpha = \frac{k}{\rho c_p}$$

Solving for the Rayleigh Number of the bottom coolant at a specific initial coolant temperature iteration with the calculated Nusselt Number with the same initial coolant temperature iteration provides an individual data point. Solving the Rayleigh Number and Nusselt Number using initial coolant temperature at $30°C$, $35°C$, $40°C$, $45°C$, and $50°C$ results in Figure 3.9.

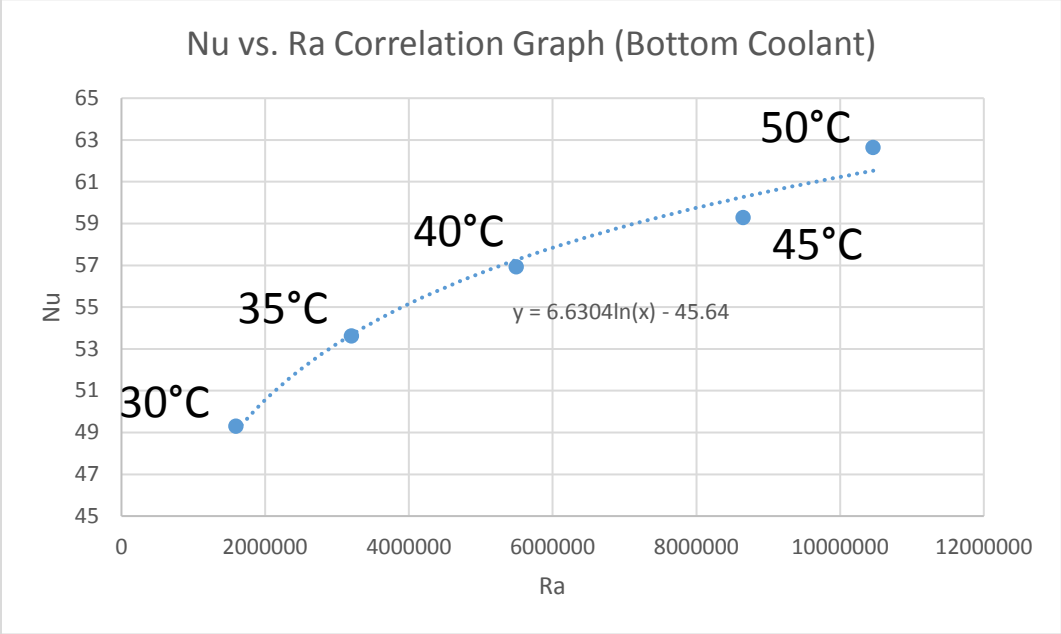

Figure 3.9: Nusselt Number vs. Rayleigh Number for the Bottom Coolant

Figure 3.9 shows that the Nusselt Number-Rayleigh Number correlation follows a logarithmic trend line. These exact data points can be found in Appendix A. This correlation can be used in equation form. However, since this is a logarithmic trend line, logarithmic scales for both the Nusselt Number and the Rayleigh Number to make the correlation

equation look a bit cleaner. Figure 3.10 represents the logarithmic scales for both the Nusselt and Rayleigh Numbers at the initial coolant temperature provided:

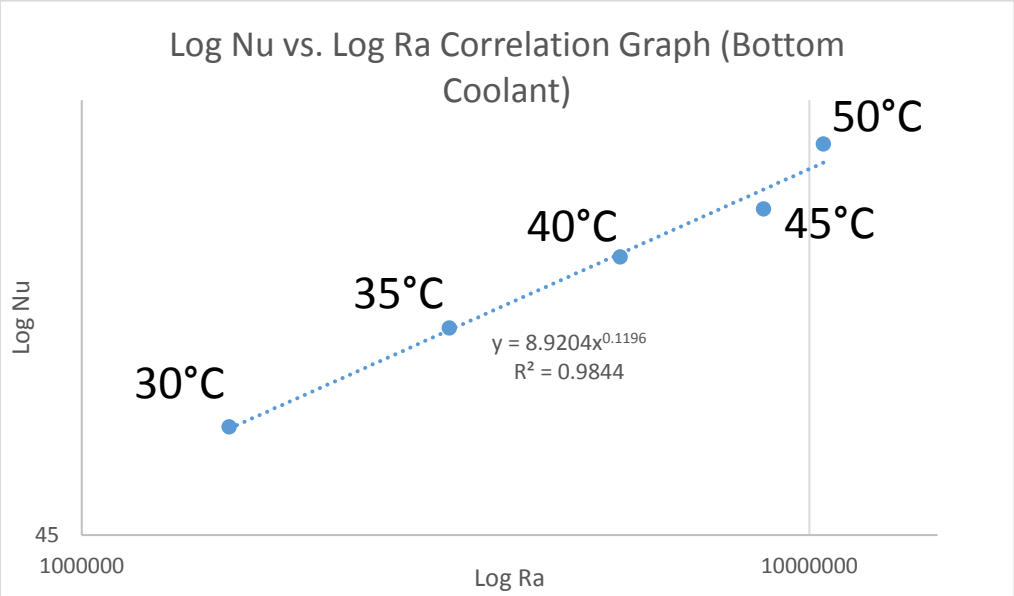

Figure 3.10: Log-scale Nusselt Number vs. Log-scale Rayleigh Number for the Bottom Coolant

Figure 3.10 presents a correlation equation for the Nusselt-Number and the Rayleigh Number for the Bottom Coolant. This equation is:

$$Nu_{BOT} = 8.92(Ra_{BOT}^{0.1196}) \tag{3.27}$$

To validate that this simulation, and therefore determine if this correlation is acceptable, side-view temperature and velocity profiles of the bottom coolant were used to analyze the results. Figure 3.11 shows the temperature and velocity profiles when the initial coolant temperature is set at $40°C$.

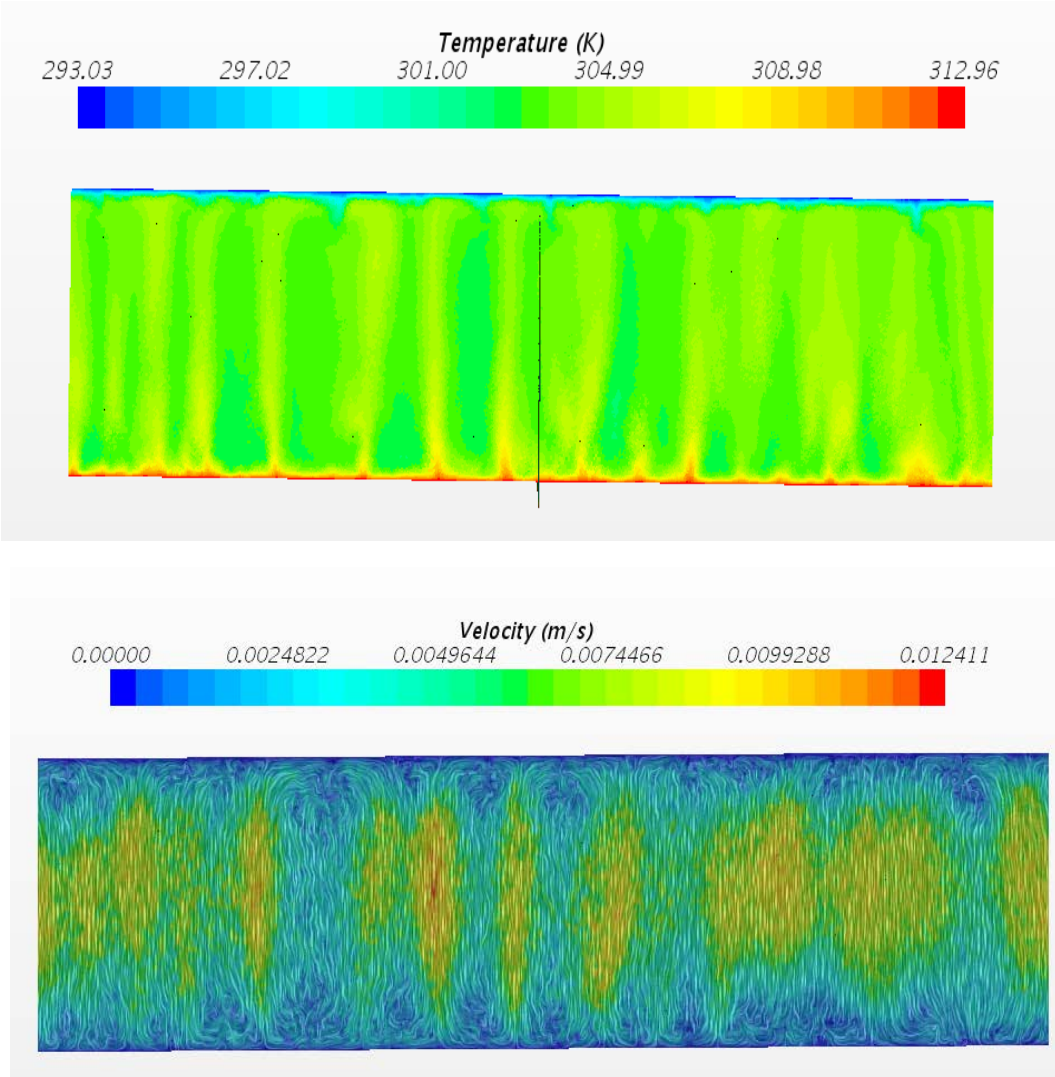

Figure 3.11: Side View of the Temperature and Velocity Profiles of the Bottom Coolant for $40°C$

As can be seen in Figure 3.11, the temperature profile shows streaks of fluid trending upward for heat transfer and the velocity profile confirms that the motion of fluid is elliptical. The reason for this constant motion is because the hot coolant is flowing to the top where the coolant is getting cooled and therefore will drop to the bottom. This motion continually happens, which will help the heat transfer of the coolant. The temperature and velocity

profiles for the initial coolant temperatures are $30°C$, $35°C$, $45°C$, and $50°C$ are very similar in trend and pattern and can be seen in Appendix B. Observing these profiles with an analysis to explain the reason for the motion provides a validation for added confidence in the numbers and data points for the calculations to eventually find the Nusselt Number-Rayleigh Number correlation.

Top Coolant: CFD Simulation and Nusselt-Number Correlation

For the top part of the coolant the geometry was drawn as shown in Figure 3.12.

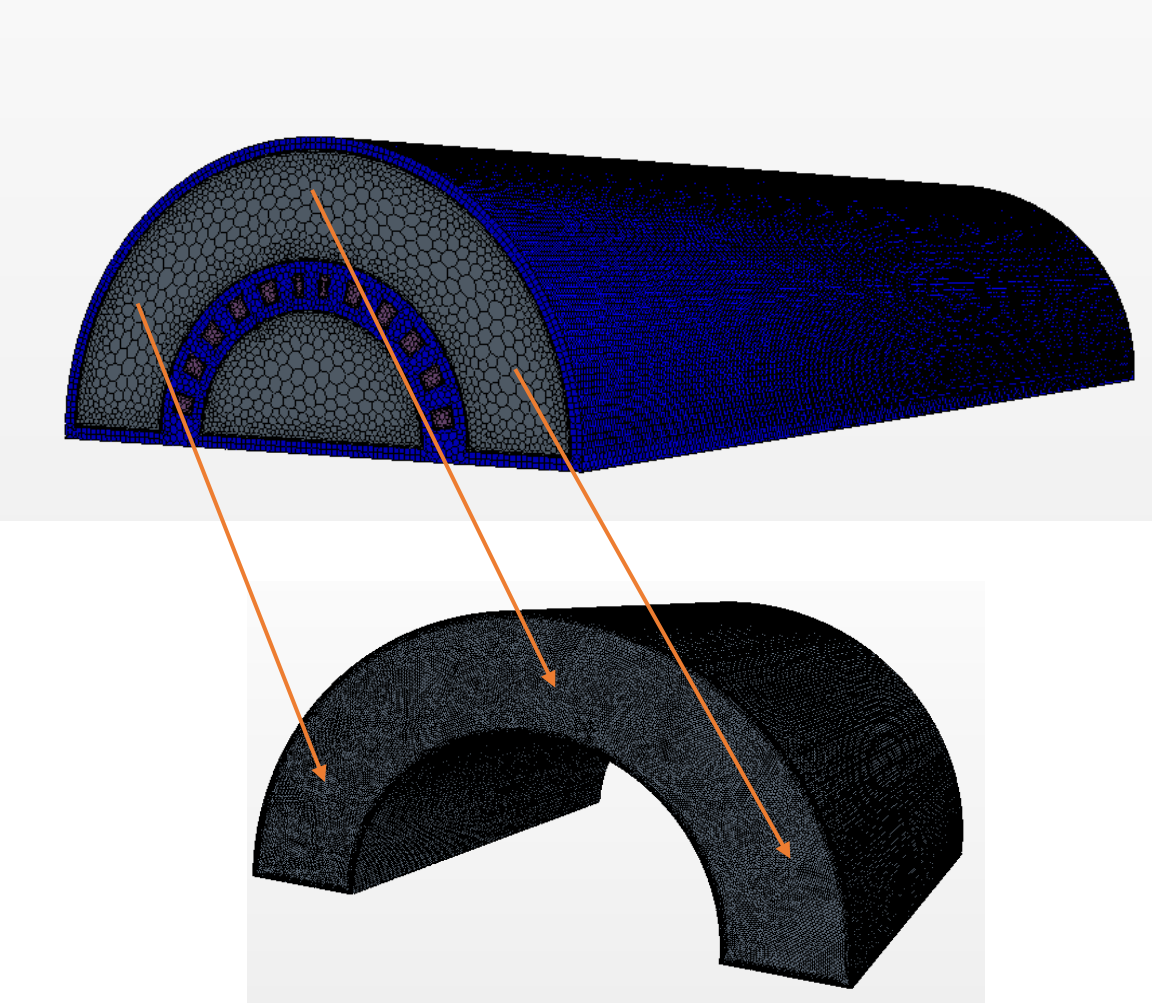

Figure 3.12: Design Geometry of Bottom Coolant

Assumptions and inputs for this CFD simulation of this bottom coolant include the following.

1. Coolant is stagnant with the standard CFD natural convection model (similar to bottom coolant assumption).
2. Properties of the coolant used, such as density, dynamic viscosity, thermal conductivity and specific heat (similar to bottom coolant assumption).
3. The top radial surface is adiabatic.
4. The bottom radial surface has a boundary temperature of $10°C$ to predict the temperature coming from the aluminum in contact with the sub-ambient steady state of refrigerant.
5. The initial temperature of the coolant was $30°C$, $35°C$, $40°C$, $45°C$, and $50°C$ for different iterations. (similar to bottom coolant assumption).

With these inputs, one differing output that the top coolant has from the bottom coolant is that instead of finding the heat transfer rate from the top radial surface for the bottom coolant, the heat transfer rate from the bottom radial surface needs to be found. Similar outputs to the bottom coolant include a stabilized volume average temperature of the coolant, and corresponding side view temperature and velocity profiles of the coolant after the heat transfer is stabilized.

Similar to Equation 2.24,

$$Q_{TOP} = h_{TOP} A_{TOP} (T_{B_{TOP}} - T_{W_{TOP}}) \quad , \tag{3.28}$$

where “TOP” represents the bottom coolant

Solving for h_{TOP} provides a calculation to solve for the Nusselt Number, similar to Equation 3.25:

$$Nu_{TOP} = \frac{h_{TOP} D_{TOP}}{k_C} \quad . \tag{3.29}$$

Nu_{TOP} is solved for each initial temperature iteration ($30°C$-$50°C$). In parallel with solving for Nu_{TOP}, the Rayleigh Number for the bottom coolant at each temperature iteration is solved for similar to Equation 3.26:

$$Ra_{TOP} = \frac{\rho_C g \beta_C (T_{B_{TOP}} - T_{W_{TOP}}) D_{TOP}}{\alpha_C \mu_C} \quad . \tag{3.30}$$

Ra_{TOP} and Nu_{TOP} using initial coolant temperature at $30°C$, $35°C$, $40°C$, $45°C$, and $50°C$ provides Figure 3.13 (similar to Figure 3.9) shown below.

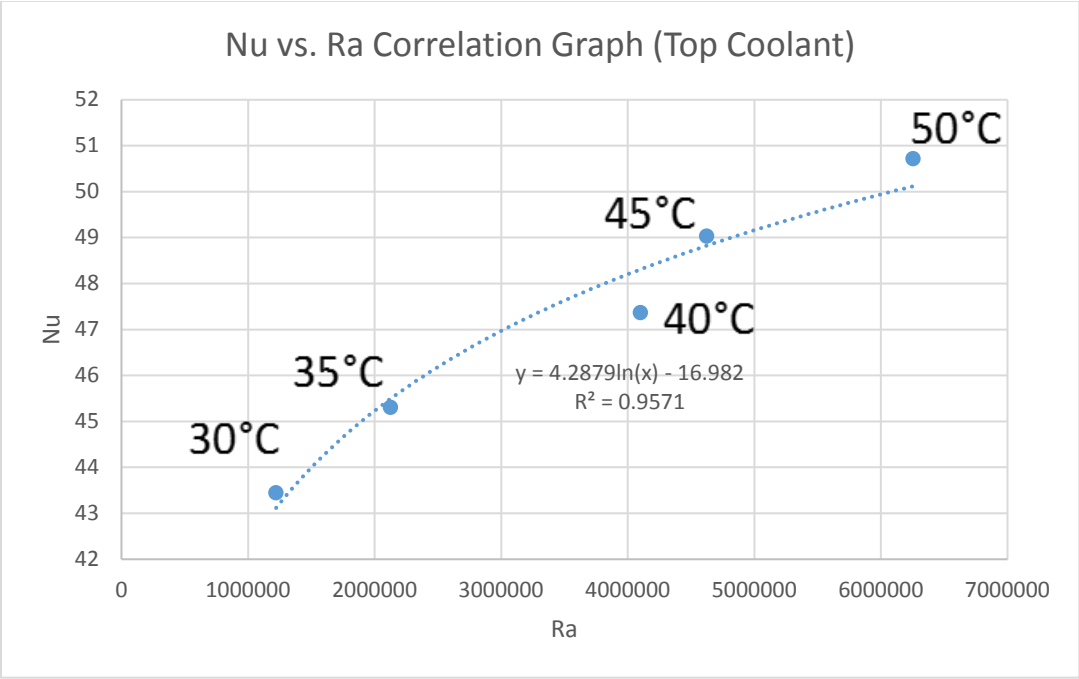

Figure 3.13: Nusselt Number vs. Rayleigh Number Correlation (Top Coolant)

As seen in Figure 3.13 and as similar to the bottom coolant, the Nusselt Number-Rayleigh Number Correlation for the top coolant follows a logarithmic trend line, where exact data points for this study can be found in Appendix C. With similar logic used to find Figure 3.10, Figure 3.14 is produced.

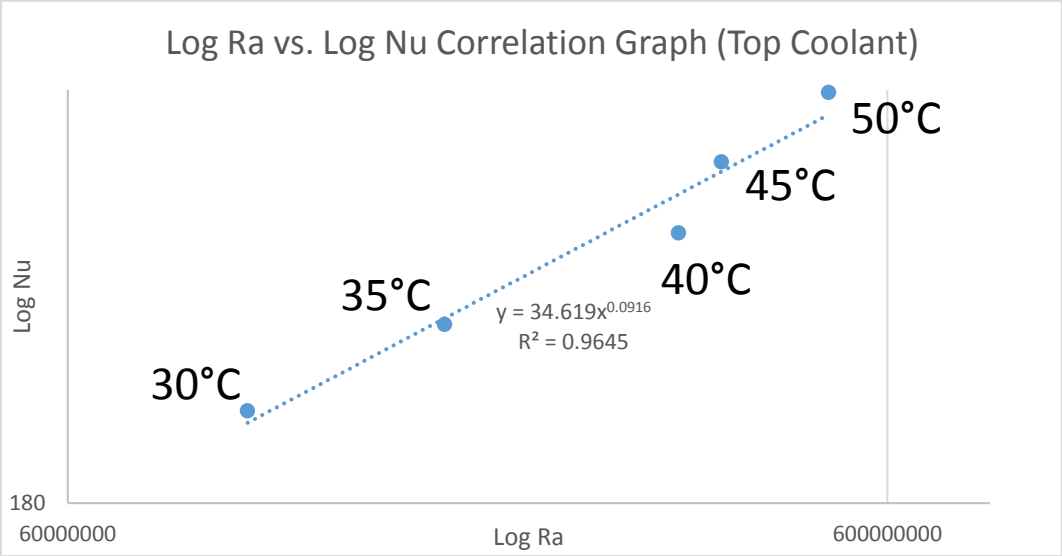

Figure 3.14: Log-scale Nusselt Number vs. Log-scale Rayleigh Number for the Top Coolant

Similar to Equation (3.27), the Nusselt Number-Rayleigh Number Correlation for the top coolant is:

$$Nu_{TOP} = 34.619(Ra_{TOP}^{0.0916}) \tag{3.31}$$

Figure 3.11 provides a side view temperature and velocity profile for the top coolant at $40°C$ to validate the $Nu_{TOP}Ra_{TOP}$ correlation similar to Figure 3.11.

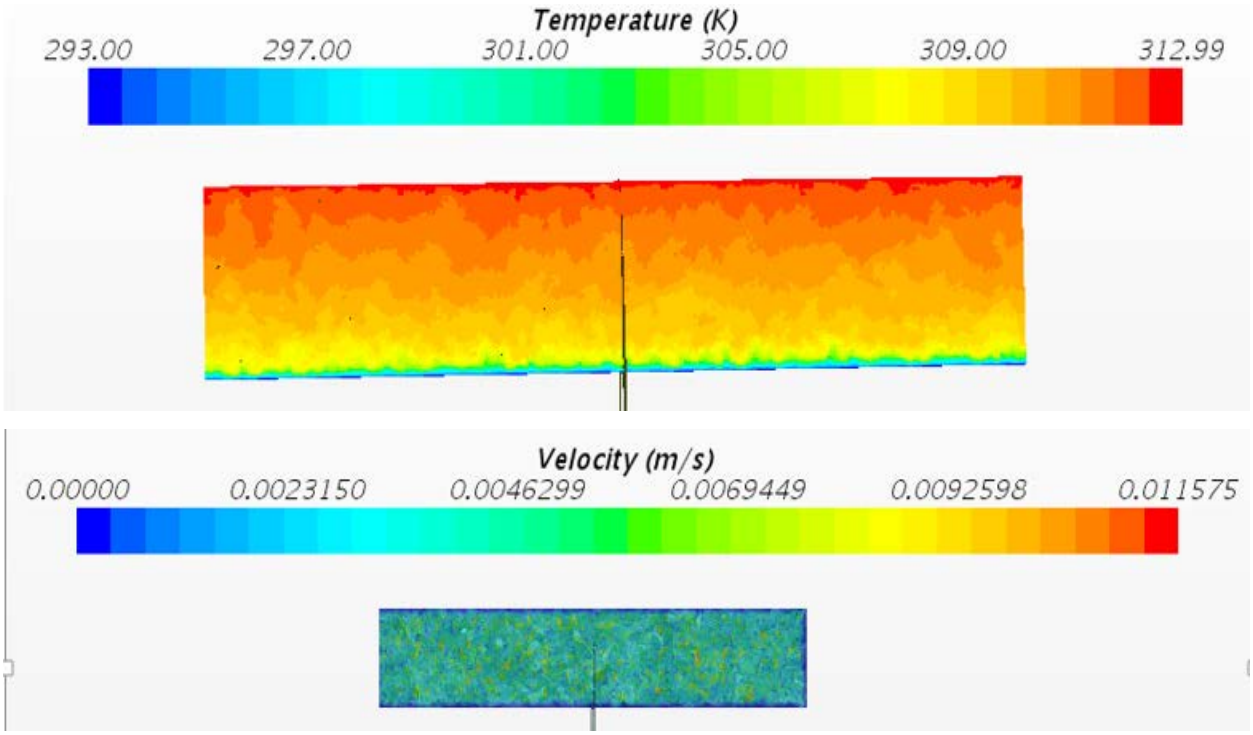

Figure 3.15: Side View of the Temperature and Velocity Profiles of the Top Coolant for $40°C$

The temperature profile in Figure 3.15 shows the stratification of the temperature where the hot coolant stabilizes at the top and cold coolant stabilizes at the bottom. The velocity profile shows that there is not much constant motion different from the bottom coolant velocity profile. The reason for this is because the hot coolant is flowing to the top; however, the coolant is cooled from the bottom therefore the coolant will stratify based on temperature of it. Thus, the lack of motion of the fluid provides relatively poor heat transfer when compared to the bottom coolant. Similar to the bottom coolant, The temperature and velocity profiles for the initial coolant temperatures are $30°C$, $35°C$, $45°C$, and $50°C$ are very

similar in trend and pattern and can be seen in Appendix D that assist in providing the validation and analysis for the $Nu_{TOP}Ra_{TOP}$ correlation equation.

iv. Overall Heat Transfer Coefficient Calculation

Now that the Nusselt Number for both the refrigerant and the coolant is known, the Nusselt Number for the refrigerant can be found using the Prandtl Number and Reynolds Number using Equation (3.16). The heat transfer coefficient for the refrigerant can be solved for using a form of Equation (3.13),

$$Nu_R = \frac{h_R D_R}{k_R} \quad , \tag{3.32}$$

where the thermal conductivity of the refrigerant, k_R, can be found in literature. h_R can then be used to find the resistances of the refrigerant, R_{R1} and R_{R2}, using Equation (3.12).

The Nusselt Number for the upper and bottom coolant can be found using the Rayleigh Number dependent on initial coolant temperature using Equations (3.27) and (3.31). The heat transfer coefficient for the coolant can be solved similar to equation (3.32):

$$Nu_C = \frac{h_C D_C}{k_C} \quad . \tag{3.33}$$

Similar to the refrigerant, k_C can be found in literature and h_C can be used to find the resistances of the coolant, R_{C1} and R_{C2}, using Equation (3.12).

Now that R_{R1}, R_{R2}, R_{C1}, R_{C2}, R_{Al1}, and R_{Al2} can all be calculated, Equation (3.12) can used to determine R_{tot}, which in turn is used to find UA from Equation (3.6). The overall heat transfer coefficient and the area (UA) can be substituted into the heat transfer rate equation, Equation (3.5), where this heat transfer equation can be combined with the

thermodynamic analytical equation, Equation (3.4), to provide the Lumped Capacitance Model.

3.4 Lumped Capacitance Model

Combining Equations (3.4) and (3.5) yields:

$$mc_v \frac{dT_C}{dt} = UA(T_R - T_C) \quad . \tag{3.34}$$

Rearranging and separating the variables and provides.

$$\frac{dT_C}{(T_R - T_C)} = \frac{UA}{mc_v} dt \quad .$$

Integrating dT_C from T_i (initial coolant temperature) to T_v (variable coolant temperature) and integrating dt from 0 (initial time) to t (variable time) results in

$$\int_{T_i}^{T_v} \frac{dT_C}{(T_R - T_C)} = \int_0^t \frac{UA}{mc_v} dt$$

$$= ln\left[\frac{(T_V - T_R)}{(T_i - T_R)}\right] = -\frac{UA}{mc_v} t$$

$$= e^{ln\left[\frac{(T_V - T_R)}{(T_i - T_R)}\right]} = e^{-\frac{UA}{mc_v} t}$$

$$= \frac{(\boldsymbol{T_V - T_R})}{(\boldsymbol{T_i - T_R})} = \boldsymbol{e^{-t/\tau}} \quad , \tag{3.35}$$

where, $\frac{1}{\tau} = \frac{UA}{mc_v}$ due to the units of $U, A, m,$ and c_v, which are

$$U = \frac{w}{m^2 K}, A = m^2, m = kg, c_v = \frac{J*K}{kg}$$

Therefore,

$$\frac{UA}{mc_v} = \frac{1}{s} = \frac{1}{\tau} \tag{3.36}$$

Equation (3.35) provides a Lumped Capacitance Model equation to solve for the variable coolant Temperature, T_V based on time passed, t and the initial coolant temperature, T_i.

3.5 Design Model for Multiple Iterations

The goal of this thesis is to provide a design model to predict the temperature of the coolant after a certain time, t for a certain structural design. Keeping the exterior design constant is one of the parameters for this project due to design restrictions in an LCAC-LTR circuit loop. This means the overall length, height, and width can-not change. However, τ changes if there is a change in the interior design of the chiller.

One way to change the initial design is to change the radii of the aluminum that is holding the refrigerant in the chiller. As shown in Figure 3.16; r_1, r_2, r_3, and r_4 can all change to provide a refrigerant flow at a different radial height.

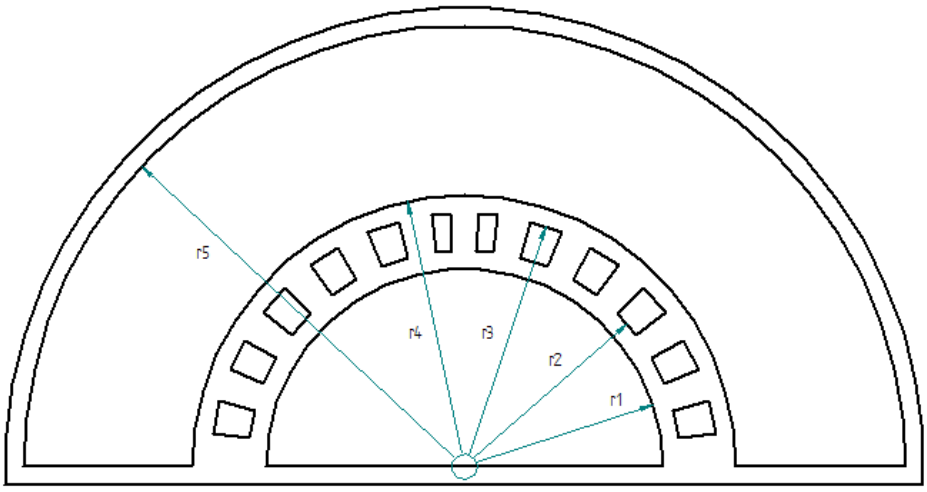

Figure 3.16: Front View of Initial Coolant Chiller Design with Radii designations

The value of r_5 cannot change, since it is part of the exterior design of the heat exchanger. Changing the interior radii dimensions changes the heat transfer and behavior of the coolant and ultimately the temperature of the coolant. The reason this happens is because the resistance equation, Equation (3.11) contains the interior radii as variables. As shown before, the resistance equations is directly correlated to the heat transfer coefficient using Equation (3.6), which in turn directly impacts the Lumped Capacitance Model Equation (3.35) by modifying τ.

Having a design model that can provide different heat transfer calculations for various radii dimensions is just the first step to understanding how and why the coolant behavior acts the way that it does. There is more to add on to this design model to fully understand the capabilities of the heat transfer mechanisms. Such possible modifications include different orientations of the chiller and the addition of extended surfaces/fins.

CHAPTER 4. **RESULTS AND ANALYSIS**

For this section, the knowns and assumptions for the materials and design processes will be laid out, such as the material properties involved and the interior structural design layout of the coolant. With this information, calculations for the Rayleigh/Reynolds Number, Nusselt Number, thermal resistances will be provided to analyze the relationship between the transient coolant temperature and the time passed using the custom Lumped capacitance model equation. Analysis for this comes from the study of the behavior of the coolant that is above the refrigerant and the study of the behavior of the coolant what is below the refrigerant. This analysis ultimately provides a design model to understand how the behavior of the coolant changes based on the changes to the interior design.

4.1 Knowns & Assumptions

i. Material Properties

Three materials are being used in this project: Coolant, Refrigerant, and Aluminum.

Coolant

The coolant being used for this project is 50% Ethylene Glycol mixed with 50% Water by volume. Ethylene Glycol is commonly used as a medium for convective heat transfer in automobile applications specifically in radiators. The reason ethylene glycol is mixed with water is to lower the freezing temperature and to increase the boiling temperature from what water would have alone. A 50-50 mixture of ethylene glycol and water provides the maximum range for temperature change with minimal phase change. The properties of this specific coolant mixture, such as thermal conductivity, specific heat, and dynamic viscosity; were found using a software program called REFPROP [54]. REFPROP is commonly used to find a fluid's thermodynamic and heat transfer properties . For this study, the focus is on the initial coolant temperature being at $40°C$, as given in Table 4.1.

Temperature	Density	Specific Heat	Thermal Conductivity	Prandtl Number	Dynamic Viscosity
[°C]	$\frac{kg}{m^3}$	$\frac{J*K}{kg}$	$\frac{W*K}{m}$		$\frac{kg*s}{m}$
40	1059.62	3427.68	0.402235	19.785	0.00232175

Table 4.1: Properties of Coolant at $40°C$

The properties using this specific software can be found in Appendix E.

To find the Thermal Expansion Coefficient of 50% Ethylene Glycol 50% Water, the book, "FUNDAMENTALS OF HEAT AND MASS TRANSFER, Fifth Edition" by Incropera & Dewitt was

used [55]. Table A.5 in this book states that the thermal expansion coefficient for pure ethylene glycol between 273 K and 373 K is $6.5E^{-04}K^{-1}$. Saturated water varies much more, and a curve-fit can be made from the data from Table A.6. The curve-fit equation is

$$\beta_{Water} = 1.0607E^{-09}(T^3) - 1.81445E^{-07}(T^2) + 1.6845E^{-05}(T) - 6.4277E^{-05}. \quad (4.1)$$

To get the composite 50/50 ethylene glycol thermal expansion coefficient, the surface temperature from Equation (4.1) is used. Then both the water thermal expansion coefficient and the pure ethylene glycol thermal expansion coefficient is mass weighted and added together, such that the mass fraction of the pure ethylene glycol in 50/50 ethylene glycol water mixture by volume is 0.775. This gives the equation to find the Thermal Expansion Coefficient of the 50/50 ethylene glycol water mixture to be

$$\beta_{5050EGW} = 0.775\left(\beta_{pureEG}\right) + (1 - 0.775)\beta_{Water} \quad . \quad (4.2)$$

As an example, using Equations (3.1) and (3.2) at a coolant temperature of $40°C$ result as

$$\beta_{5050EGW} = 8.72E^{-05}\,\frac{1}{K} \quad .$$

The thermal expansion coefficient results at a coolant from $30°C - 50°C$ can be found in Appendix F.

In addition to these coolant properties, the properties of the refrigerant also must be found, since a steady state of the refrigerant is chilling the stagnant coolant.

Refrigerant

The refrigerant being used is 1,1,1,2-Tetrafluoroethane, more commonly known as R-134a. R-134a is widely used in refrigeration, specifically in an automobile's air conditioning system. The R134a for this research is presumed to be flowing at a constant mass flow rate of 70 g/sec with a liquid/gas quality of 0.2 and a constant temperature of $5°C$. Since this research is more inclined to the study of the coolant behavior and heat transfer, the refrigerant is assumed to go through a single phase flow throughout the heat transfer process.

The properties of the refrigerant were found using a Heat Transfer book, "HEAT AND MASS TRANSER: A Practical Approach, Third Edition" by Yunus A. Cengel [56]. At a temperature of $5°C$ with a quality of 0.2, the properties are

Temperature	Density	Specific Heat	Thermal Conductivity	Thermal Expansion Coefficient	Dynamic Viscosity
[°C]	$\frac{kg}{m^3}$	$\frac{J*K}{kg}$	$\frac{W*K}{m}$	$\frac{1}{K}$	$\frac{kg*s}{m}$
5	1278	1358	0.0925	0.00269	0.0002589

Table 4.2: Properties of Refrigerant at $5°C$ with a quality of 0.2

Between the steady state of refrigerant and the stagnant coolant is aluminum. The container and the extended surfaces inside the container is aluminum.

Aluminum

The only property that is needed for aluminum in this project is thermal conductivity, since the heat transfer for the aluminum is mainly conduction. Cengel, Third Edition [56] states that the thermal conductivity of aluminum is 205 $\frac{W*m}{K}$ from $0°C$ to $60°C$.

ii. Dimensions of the Coolant Chiller Container

Using Figure 3.2 (shown below), the original design will have the outer dimensions that are constant.

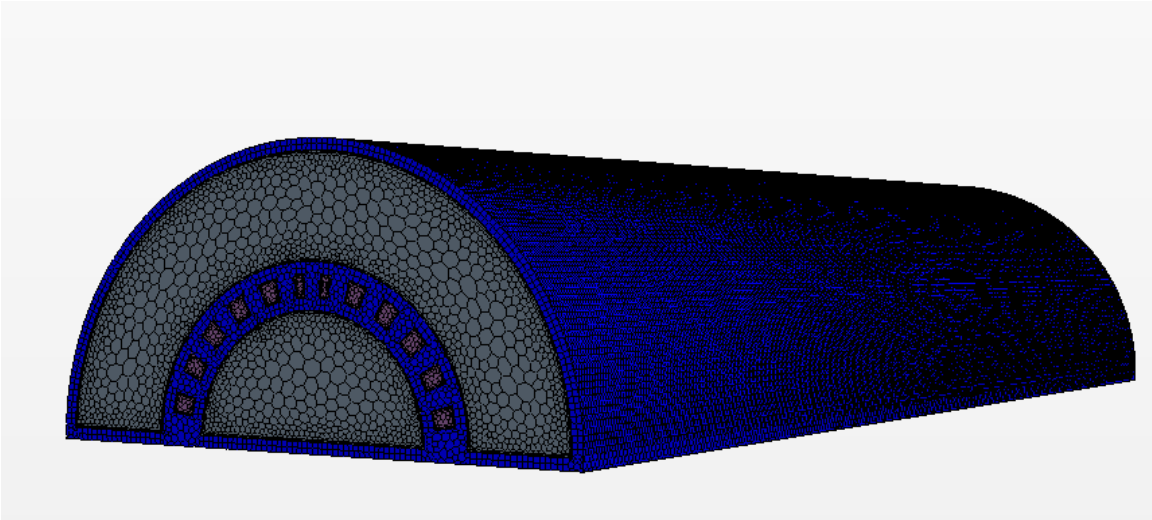

Figure 3.2: Initial Design of the Coolant Chiller

These outer dimensions are the length and outer radius of the coolant. This can be seen in Figure 4.1, which shows a side view of the coolant chiller with a constant length of the container at 440 mm and a constant outer radius of the container at 65 mm.

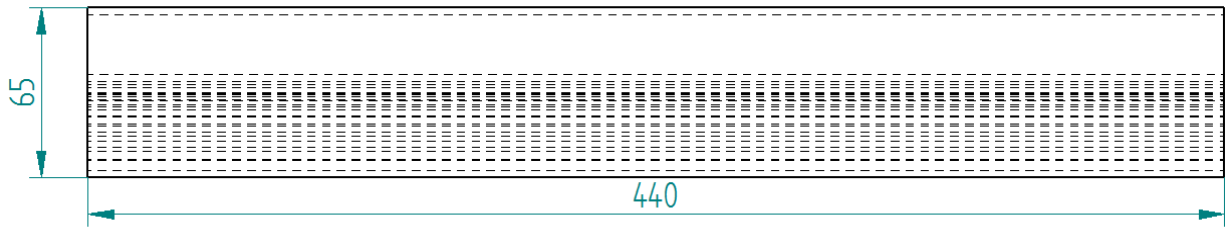

Figure 4.1: Side View of the Coolant Chiller

While the outside dimensions of the container are constant, the inner dimensions are being changed to find how the coolant behavior and heat transfer changes with the inner structural design. For the original structural design, the inner dimensions are

r1: 0.0275 m

r2: 0.03 m

r3: 0.035 m

r4: 0.0375 m

r5: 0.06 m

where r1, r2, r3, r4, and r5 are identified in Figure 3.5 (shown below).

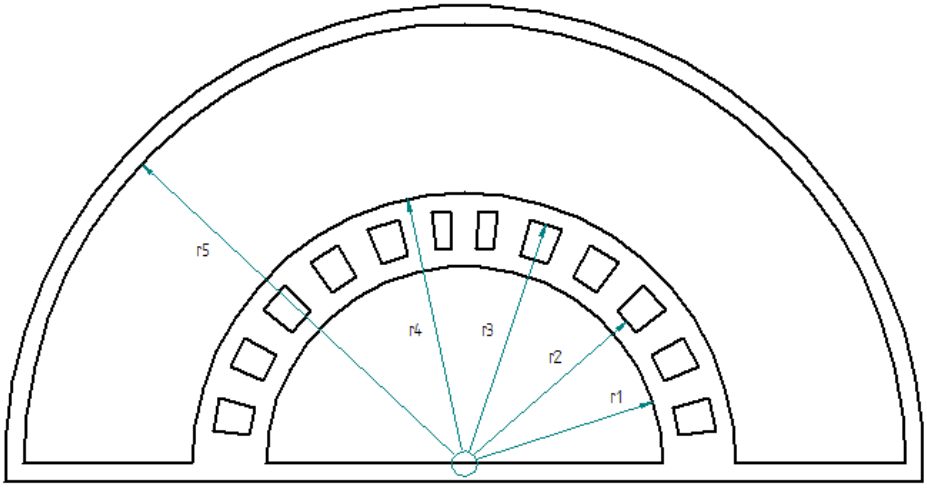

Figure 3.5: Front View of Initial Coolant Chiller Design with Radii designations

4.2 Thermal Resistance Calculations

The properties stated for the aluminum, coolant, and refrigerant and the inner and outer dimensions of the container are all building blocks for developing a relationship between the coolant temperature and the time passed using the custom Lumped Capacitance Model, as outlined in Equation (3.35):

$$\frac{(T_V - T_R)}{(T_i - T_R)} = e^{-t/\tau} \quad , \tag{3.35}$$

where τ can be solved by knowing UA, where U is the Overall Heat Transfer and A is the overall surface area using Equation (3.36):

$$\frac{UA}{mc_v} = \frac{1}{s} = \frac{1}{\tau} \quad . \tag{3.36}$$

UA can be solved for as it is in correlation with the total radial resistance of the coolant chiller, as shown in Equation (3.6):

$$\frac{1}{UA} = R_{total} \quad . \tag{3.6}$$

The total resistance is a parallel summation of the bottom coolant and the top coolant:

$$\frac{1}{R_{tot}} = \frac{1}{R_{Bot}} + \frac{1}{R_{Top}} \quad . \tag{4.3}$$

where R_{Bot} can be represented as:

$$R_{Bot} = R_{C1} + R_{AL1} + R_{R1} \tag{4.4}$$

and R_{Top} can be represented as:

$$R_{Top} = R_{C2} + R_{AL2} + R_{R2} \tag{4.5}$$

From this, the resistances of the three materials: aluminum, coolant, and refrigerant, have to be determined. Each of the materials has a different process of resistance calculation because the aluminum is a solid going through conductive heat transfer, the coolant is a liquid going through natural convective heat transfer due to a stagnant coolant, and the refrigerant is a liquid going through forced convective heat transfer due a steady state of refrigerant fluid flow.

<u>Aluminum</u>

The equation for the aluminum resistance that affects the top coolant and the bottom coolant can be found in Equation (3.11):

$$R_{AL1} = \frac{\ln\left(\frac{r_2}{r_1}\right)}{2\pi k_{Al} L_{Al}} \quad , \tag{3.11b}$$

$$R_{AL2} = \frac{\ln\left(\frac{r_4}{r_3}\right)}{2\pi k_{Al} L_{Al}} \quad , \tag{3.11e}$$

where all the variables to solve for R_{AL} are known. Therefore,

$$R_{AL1} = 6.67E^{-5}\,\frac{m^2}{WK},$$

$$R_{AL2} = 5.29E^{-5}\,\frac{m^2}{WK}.$$

Coolant

The equation for the coolant resistance for both the top and bottom coolant can be found in Equation (3.11) from the "Methodology Section":

$$R_{C1} = \frac{1}{h_C 2\pi r_1 L}, \quad , \qquad (3.11a)$$

$$R_{C2} = \frac{1}{h_C 2\pi r_4 L} \quad , \qquad (3.11d)$$

where all the variables except for the coolant heat transfer coefficient are known.

To find the coolant heat transfer coefficient, Equation (3.13) is used.

$$Nu = \frac{hD}{k} \quad . \qquad (3.13)$$

To find the Nusselt Number of the coolant, the Rayleigh Number must be determined from a Nusselt Number-Rayleigh Number correlation using Equation (3.27) for the bottom coolant,

$$Nu_{BOT} = 8.92(Ra_{BOT}^{0.1196}) \quad , \qquad (3.27)$$

and Equation (3.31) from the "Methodology" Section for the top coolant,

$$Nu_{TOP} = 34.619(Ra_{TOP}^{0.0916}) \quad . \qquad (3.31)$$

The Rayleigh Number can be found using Equations (3.26) and (3.30) for the top and bottom coolant respectively:

$$Ra = \frac{\rho g \beta \Delta T L_C^3}{\alpha \mu} \quad . \tag{3.26}$$

Since all the variables are known; for the bottom coolant at a coolant temperature of $40°C$, the Rayleigh Number is:

$$Ra_{BOT} = 2{,}047{,}000 \quad .$$

For the top coolant at a coolant temperature of $40°C$, the Rayleigh Number is:

$$Ra_{TOP} = 11{,}210{,}000 \quad .$$

The Rayleigh Number results for the bottom and top coolant temperature from $30°C - 50°C$ can be found in Appendix G.

Knowing the Rayleigh Number, Equations (3.27) provides the Nusselt Number for the bottom coolant at a temperature of $40°C$:

$$Nu_{BOT} = 66.667 \quad . \tag{3.27}$$

Similarly, using Equation (3.31) provides the Nusselt Number for the top coolant at a temperature of $40°C$:

$$Nu_{TOP} = 154.449 \quad . \tag{3.31}$$

The Nusselt Number results for the bottom and top coolant temperature from $30°C - 50°C$ can be found in Appendix H.

Using Equation (3.13), the results for the coolant heat transfer coefficient becomes

$$h_{BOT} = 487.6\ \frac{(W)(K)}{m^2} \quad ,$$

$$h_{TOP} = 1381\ \frac{(W)(K)}{m^2} \quad .$$

The coolant heat transfer coefficient for the bottom and top coolant temperature from $30°C - 50°C$ can be found in Appendix I.

Using Equation (3.11), the results for the coolant resistance becomes

$$R_{C1} = 0.0270\ \frac{m^2}{WK}$$

$$R_{C2} = 0.00699\ \frac{m^2}{WK}$$

The coolant resistance for the bottom and top coolant temperature from $30°C - 50°C$ can be found in Appendix J.

Refrigerant

The equation for the refrigerant resistance for both the top and bottom coolant can be found in Equation (3.11):

$$R_{R1} = \frac{1}{h_r 2\pi r_2 L} \quad , \qquad (3.11c)$$

$$R_{R2} = \frac{1}{h_r 2\pi r_3 L} \quad , \qquad (3.11d)$$

where all the variables except for the refrigerant heat transfer coefficient are known.

To find the coolant heat transfer coefficient, Equation (3.13) is used in correlation with the Nusselt Number similar to how the coolant was calculated.

To find the Nusselt Number of the coolant, the Reynolds Number must be solved determined due to a Nusselt Number-Reynolds Number correlation using Equation (3.16) for the refrigerant:

$$Nu_R = 0.023 Re_R^{\frac{4}{5}} Pr_R^{0.3} \quad . \tag{3.16}$$

The Reynolds Number can be found using Equation (3.18) for the refrigerant:

$$Re_R = \frac{\rho_R V_R L_R}{\mu_R} \quad . \tag{3.18}$$

To find the velocity of the refrigerant, Equation (3.20) is used:

$$\dot{m}_R = \rho_R V_R a_R \quad , \tag{3.20}$$

where, $\dot{m}_R$ is given as 70 g/s. Therefore the velocity for the bottom half of the refrigerant is

$$V_{BOT} = 0.0675\ m/s$$

and the velocity for the top half of the refrigerant results to

$$V_{TOP} = 0.0542\ m/s \quad .$$

With the velocities determined, the Reynolds Number can be found. For the bottom half of the refrigerant at a temperature of $5°C$, the Reynolds Number is

$$Re_{BOT} = 2{,}604 \quad .$$

For the top half of the refrigerant at a temperature of $5°C$, the Reynolds Number is

$$Re_{TOP} = 2{,}099 \quad .$$

Knowing the Reynolds Number, Equation (3.16) provides the Nusselt Number for the bottom half of the refrigerant at a temperature of $5°C$:

$$Nu_{BOT} = 17.56 \quad .$$

Similarly, the Nusselt Number for the top half of the refrigerant at a temperature of $5°C$ is

$$Nu_{TOP} = 17.84 \quad .$$

Using Equation (3.13), the results for the refrigerant heat transfer coefficient becomes

$$h_{BOT} = 171.0 \ \frac{(W)(K)}{m^2} \quad ,$$

$$h_{TOP} = 210.2 \ \frac{(W)(K)}{m^2} \quad .$$

Using Equation (3.11), the results for the refrigerant resistance becomes

$$R_{R1} = \ 0.07053 \ \frac{m^2}{WK} \quad ,$$

$$R_{R2} = 0.04918 \ \frac{m^2}{WK} \quad .$$

To validate the accuracy of the resistances of the refrigerant, a CFD simulation was designed using the properties of the refrigerant and the knowns of this particular study, such as the mass flow rate of the steady flow of refrigerant and the temperature of the refrigerant held constant at $5°C$. The geometry of a partial block of refrigerant can be seen in Figure 4.2, where the blue represents the refrigerant and the brown represents the aluminum.

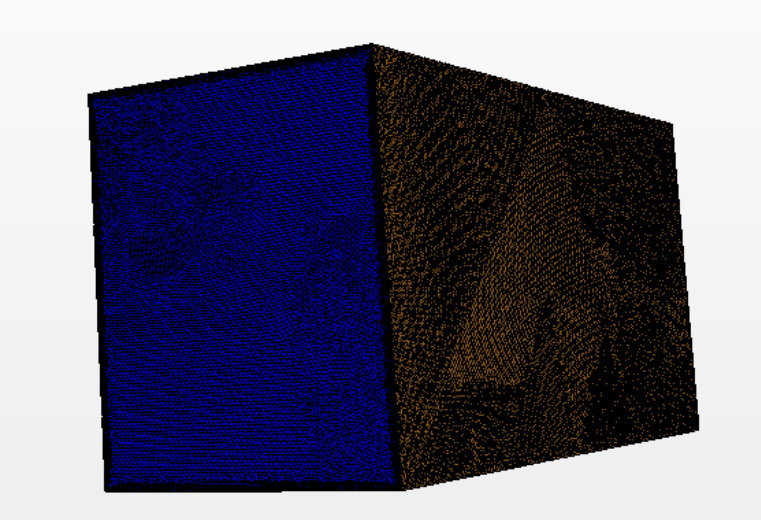

Figure 4.2: CFD Geometry of Partial Block of Refrigerant

Simulating this geometry provides the temperature and velocity profiles as shown in Figure 4.3.

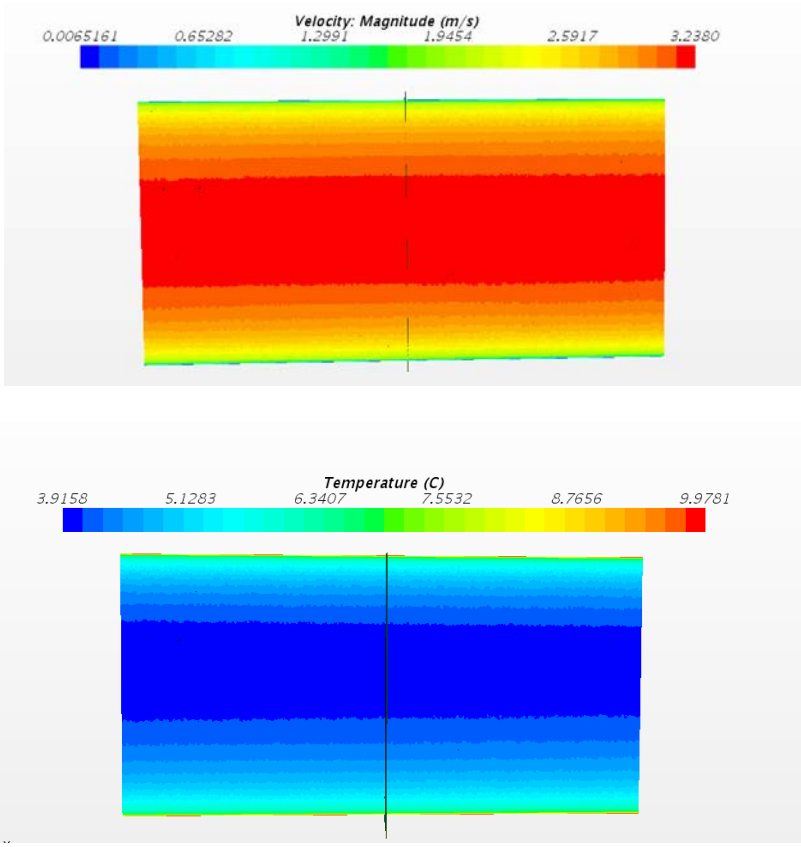

Figure 4.3: Side View of the Temperature and Velocity Profiles of the Refrigerant for $5°C$

Using this simulation, there are several quantities that can be determined, such as heat transfer rate being 2.3 W, the surface area as $1.84E^{-4}\ m^2$, and the heat transfer coefficient as 2510$\frac{W}{m^2K}$. From these results, the resistance of the CFD simulated refrigerant is calculated to be 0.0529 $\frac{K}{W}$. Since the CFD simulated calculation is within the same order of magnitude as the analytical calculation of the refrigerant resistance, this can be seen as a validation of the analytical calculation, making it appropriate to continue this study.

4.3 Results & Analysis

With the individual resistances being calculated for the aluminum, coolant, and refrigerant; the total resistance can now be calculated for the bottom coolant, top coolant, and the overall coolant.

Bottom Coolant

Using Equation (4.4) at a temperature of $40°C$, the resistance for the bottom coolant becomes

$$R_{Bot} = R_{C1} + R_{AL1} + R_{R1} = 0.026991\ \frac{m^2}{WK} + 6.67E^{-5}\frac{m^2}{WK} + 0.07053\ \frac{m^2}{WK} = 0.0976\frac{m^2}{WK} \quad .$$

Using Equation (3.6), the product of the area and the overall heat transfer coefficient of the bottom coolant is

$$UA = \frac{1}{R_{Bot}} = 10.245\frac{WK}{m^2} \quad .$$

This results in τ in Equation (3.36) to become

$$\tau = \frac{mc_v}{UA} = 370.13s^{-1} \quad .$$

The resistance, UA, and τ results for the bottom coolant temperature from $30°C - 50°C$ can be found in Appendix K.

With τ, the custom Lumped capacitance model (Equation (3.35)) can be used to calculate the temperature at various times. Figures 4.4a, 4.4b, and 4.4c provide what the bottom coolant through 20, 200, and 2,400 seconds.

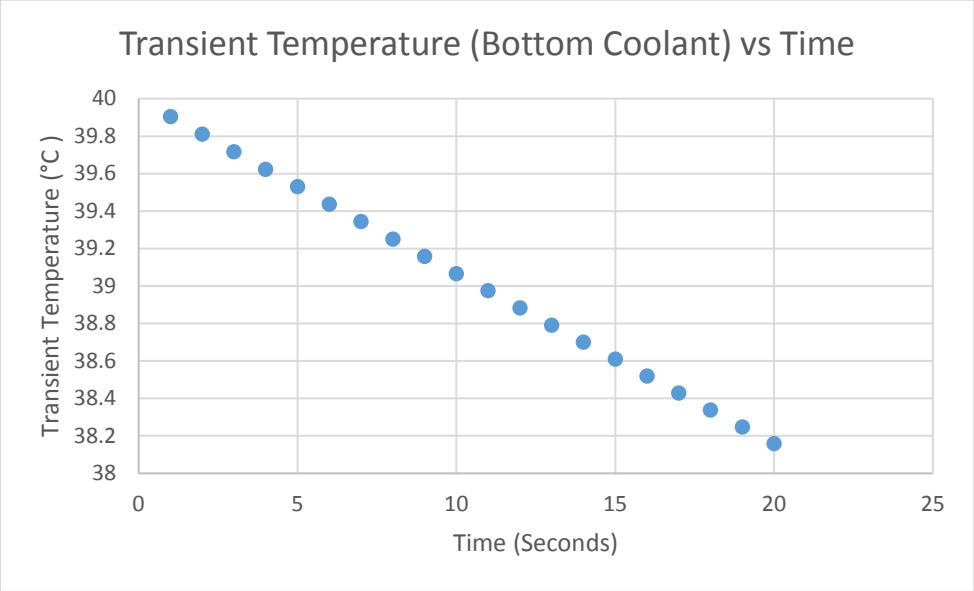

Figure 4.4a: Transient Temperature of the Bottom Coolant vs. Time through 20 seconds

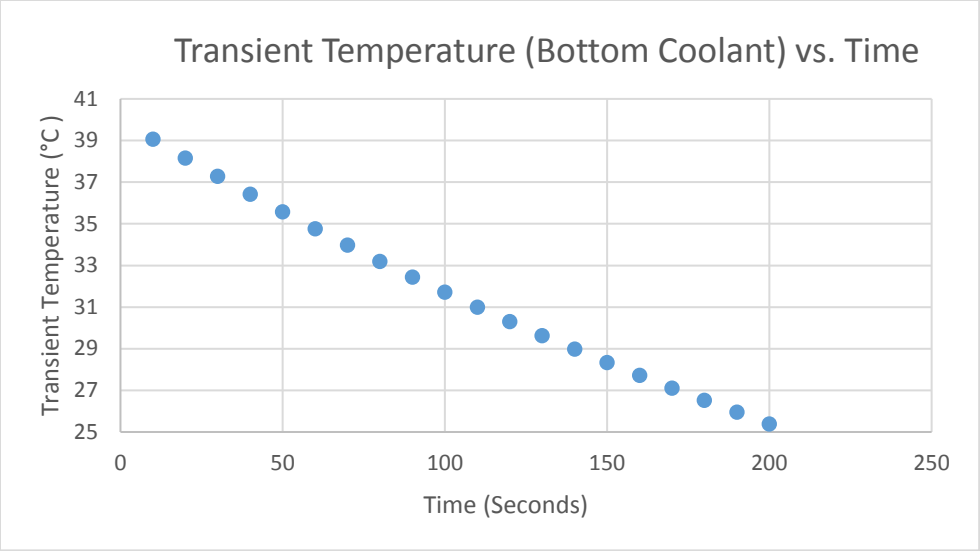

Figure 4.4b: Transient Temperature of the Bottom Coolant vs. Time through 200 seconds

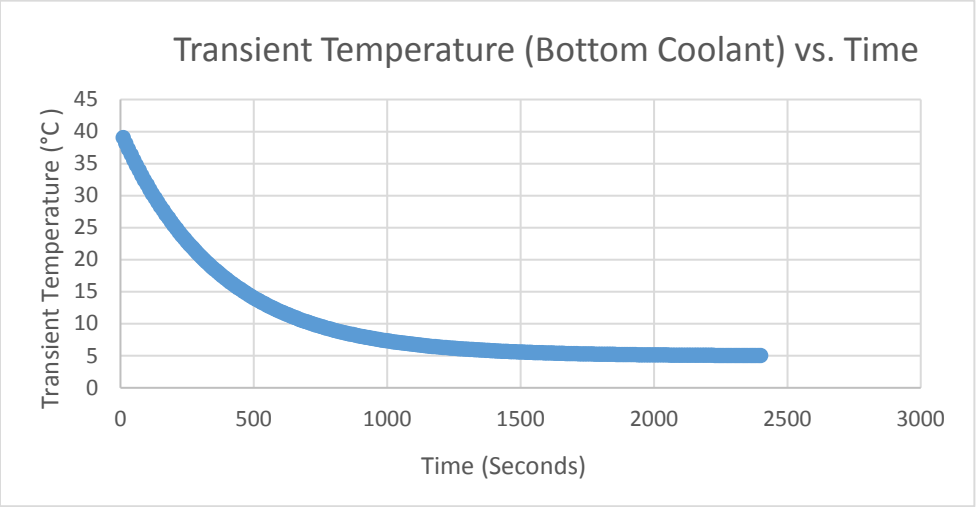

Figure 4.4c: Transient Temperature of the Bottom Coolant vs. Time through 2,400 seconds

Figure 4.4a shows that the bottom coolant temperature does change at what appears to be a linear rate, but as Figures 4.4b and 4.4c show, the rate changes over time to asymptotically approach a minimum temperature of $5°C$, which is the same temperature as the refrigerant. Similar trends can be seen for the bottom coolant lower limit temperature at $30°C$ and the bottom coolant upper limit temperature at $50°C$ in Appendix L.

However, the optimal way to analyze this cooling rate is to compare the bottom coolant to the upper coolant. The reason for this is because the bottom coolant is in constant motion, since the coolant is being cooled from the top and the top coolant is stratified, since the coolant is being cooled from the bottom.

Upper Coolant

Using Equation (4.4) at a temperature of $40°C$, the resistance for the upper coolant becomes

$$R_{Top} = R_{C2} + R_{AL2} + R_{R2} = 0.00699 \frac{m^2}{WK} + 5.29E^{-5} \frac{m^2}{WK} + 0.04918 \frac{m^2}{WK} = 0.0562 \frac{m^2}{WK}$$

Using Equation (3.6), the product of the area and the overall heat transfer coefficient of the bottom coolant becomes

$$UA = \frac{1}{R_{Top}} = 17.79 \frac{WK}{m^2} \quad .$$

This results in τ in Equation (3.36) to be

$$\tau = \frac{mc_v}{UA} = 618.58 s^{-1} \quad .$$

The resistance, UA, and τ results for the top coolant temperature from $30°C - 50°C$ can be found in Appendix M.

With τ, the custom Lumped capacitance model can be used to calculate for temperature given a certain time. Figures 4.5a, 4.5b, and 4.5c provide what the upper coolant temperature would be through 20, 200, and 2,400 seconds.

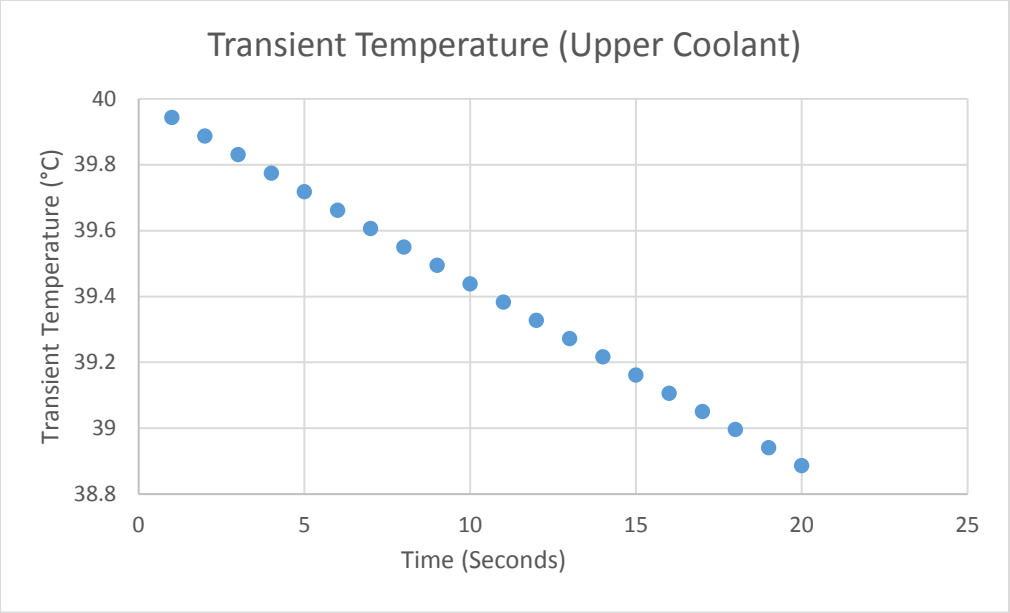

Figure 4.5a: Transient Temperature of the Top Coolant vs. Time through 20 seconds

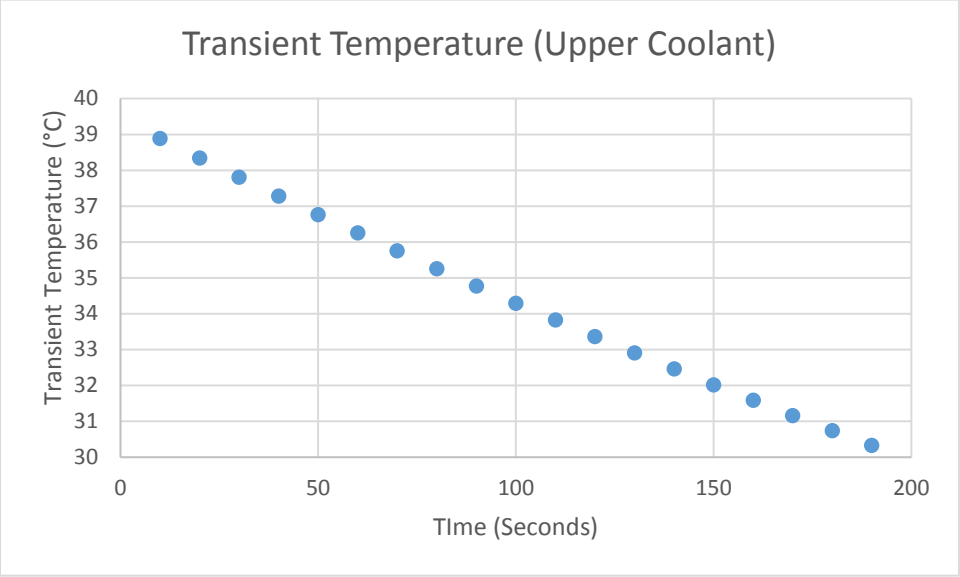

Figure 4.5b: Transient Temperature of the Top Coolant vs. Time through 200 seconds

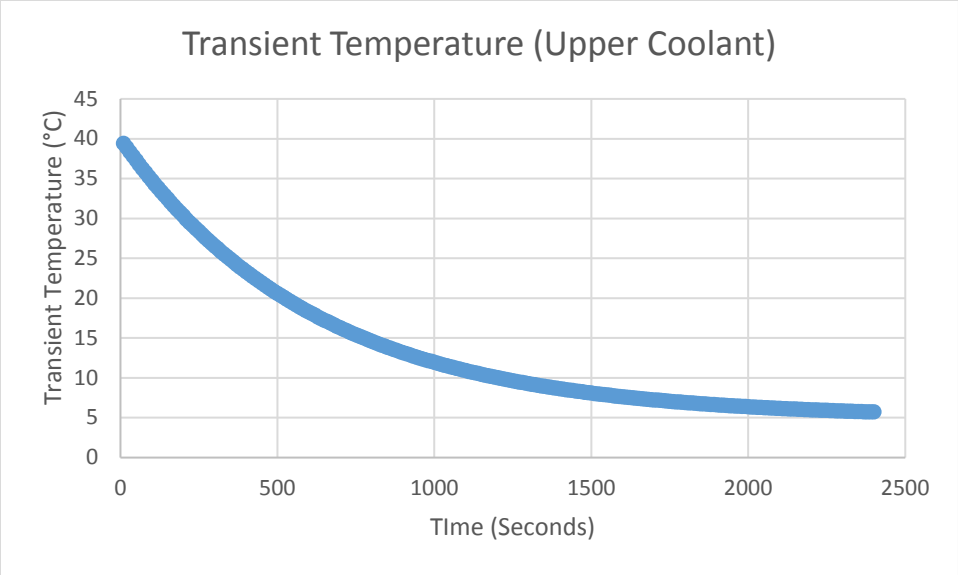

Figure 4.5c: Transient Temperature of the Top Coolant vs. Time through 2,400 seconds

Similar to the bottom coolant; Figure 4.5a shows that the coolant does cool, Figure 4.5b shows that it is not linear, and Figure 4.5c shows the trend line as asymptotic with the minimum temperature being $5°C$. Similar trends can be seen for the top coolant lower limit temperature at $30°C$ and the top coolant upper limit temperature at $50°C$ in Appendix N.

Compared to the bottom coolant, the top coolant transient temperature has a higher temperature after 20 and 200 seconds because it takes longer to cool the top coolant than it takes for the bottom coolant. This occurs because of two reasons:

1. the top coolant has a greater volume of fluid that needs cooling; and
2. the top coolant is stratified, since the cooling is happening from the bottom. That means the colder coolant will closer to the bottom and the hotter coolant will trend to the top. On the other hand, the bottom coolant will be in constant motion because the hotter coolant will always rise just to be cooled from the refrigerant and aluminum from the top causing a circular/elliptical motion.

Overall Coolant

Using Equation (4.3) at a temperature of $40°C$, the resistance for the overall coolant becomes

$$\frac{1}{R_{tot}} = \frac{1}{R_{Bot}} + \frac{1}{R_{Top}} = \frac{1}{0.0976} + \frac{1}{0.0562} \Rightarrow R_{tot} = 0.0357 \frac{m^2}{WK}$$

Using Equation (3.6), the area and the overall heat transfer coefficient of the bottom coolant becomes

$$UA = \frac{1}{R_{Tot}} = 28.03 \frac{WK}{m^2} \quad .$$

This results in τ in Equation (3.36) to become

$$\tau = \frac{mc_v}{UA} = 527.8 s^{-1} \quad .$$

The resistance, UA, and τ results for the overall coolant temperature from $30°C - 50°C$ can be found in Appendix O.

Similar to the top and bottom coolant calculations; with τ, the custom Lumped capacitance model can be used can be found to calculate for temperature given a certain time. Figures 4.6a, 4.6b, and 4.6c provide what the overall coolant temperature would be through 20, 200, and 2,400 seconds.

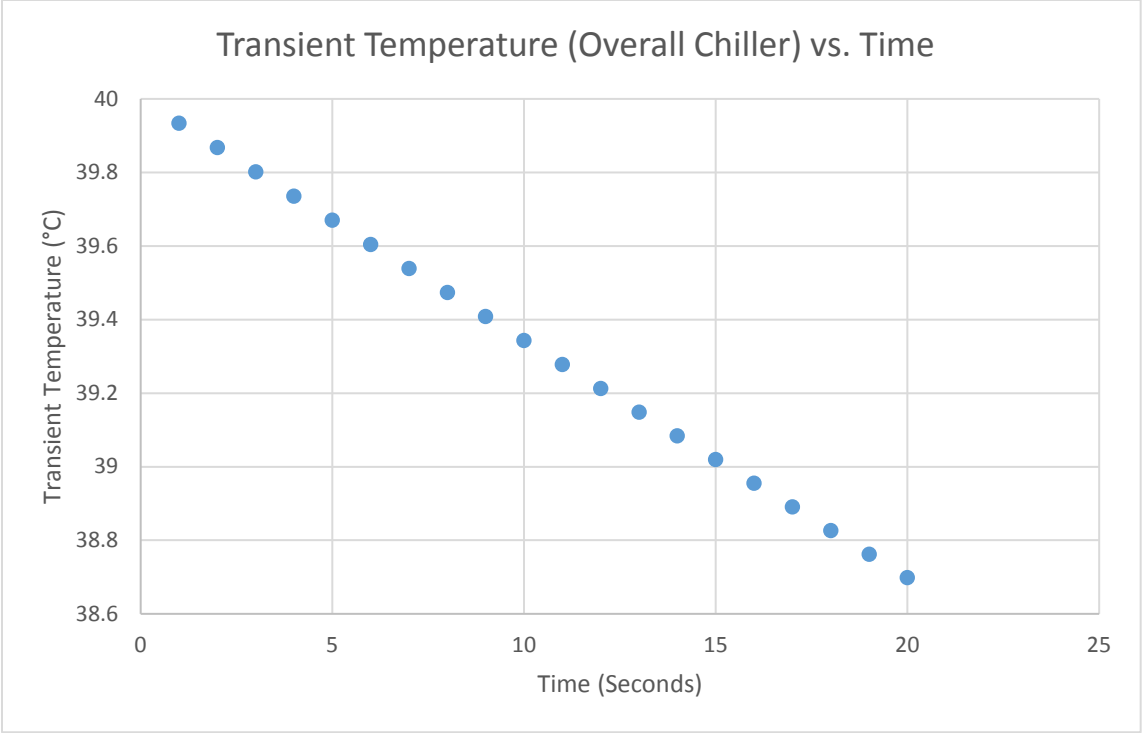

Figure 4.6a: Transient Temperature of the Overall Coolant vs. Time through 20 seconds

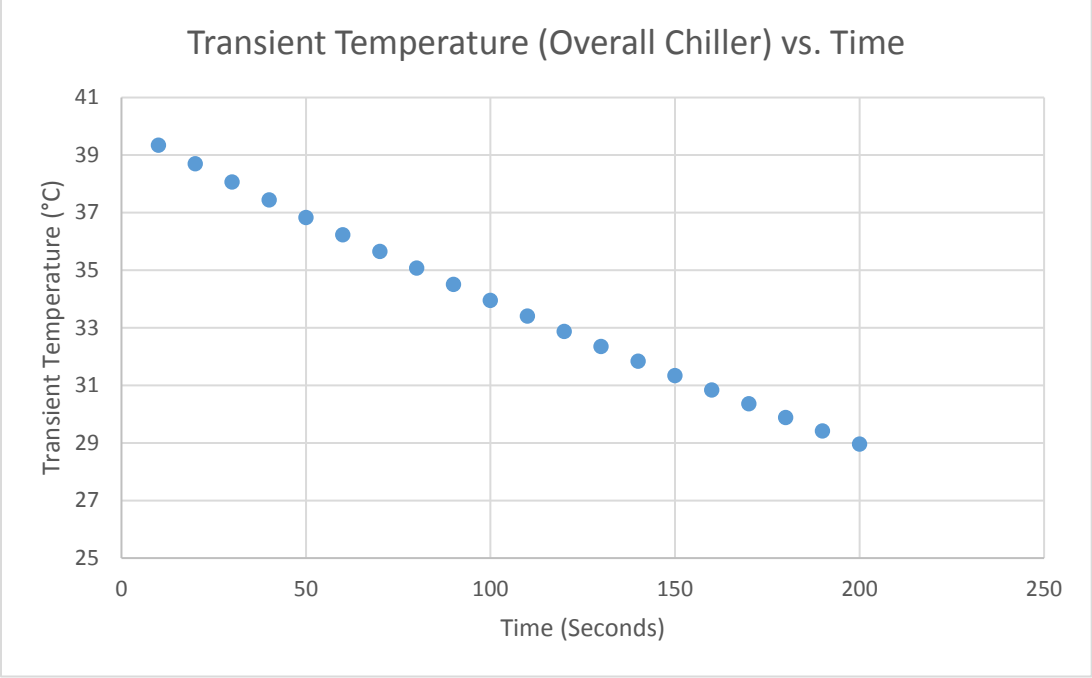

Figure 4.6b: Transient Temperature of the Overall Coolant vs. Time through 200 seconds

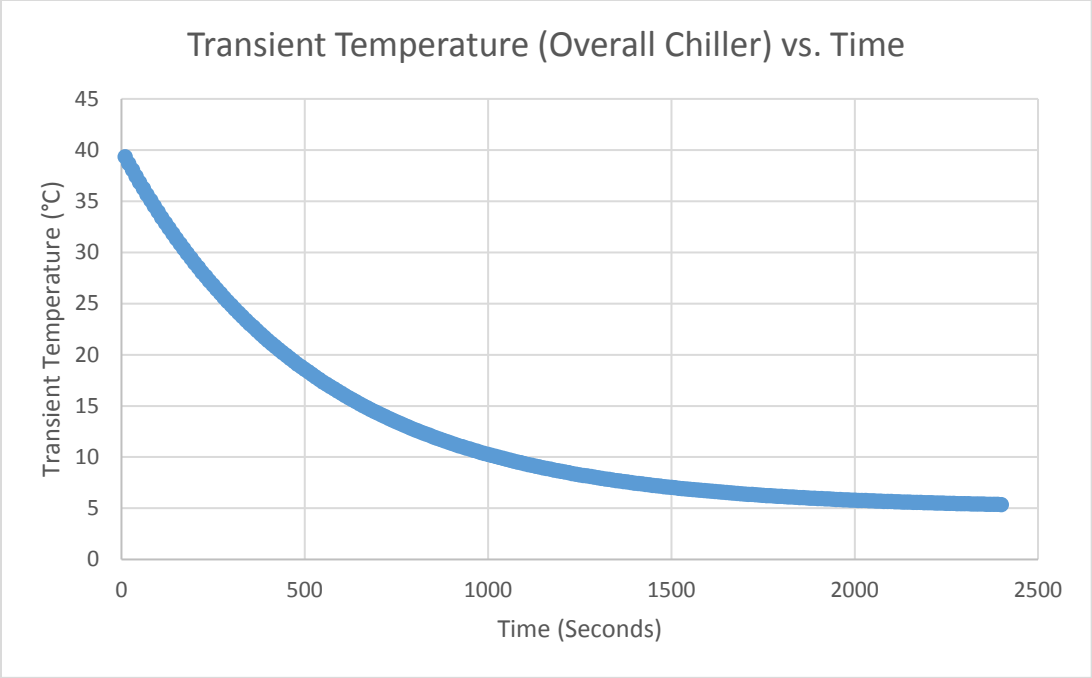

Figure 4.6c: Transient Temperature of the Overall Coolant vs. Time through 2,400 seconds

Similar to the bottom coolant and top coolant; Figure 4.6a shows that the overall coolant does cool, Figure 4.6b shows that it is not linear, and Figure 4.6c shows the trend line as asymptotic with the minimum temperature being $5°C$. Similar trends can be seen for the overall coolant lower limit temperature at $30°C$ and the overall coolant upper limit temperature at $50°C$ in Appendix P.

Predictably, the overall coolant transient temperature is between the top coolant and the bottom coolant, since it is a combination of both. This validates that the top coolant and the bottom coolant thermal resistance circuits are indeed in parallel instead of in series. This can be seen in Figures 4.7a and 4.7b that show the comparison of the transient temperature between the bottom, top, and overall coolant after 10 and 100 seconds.

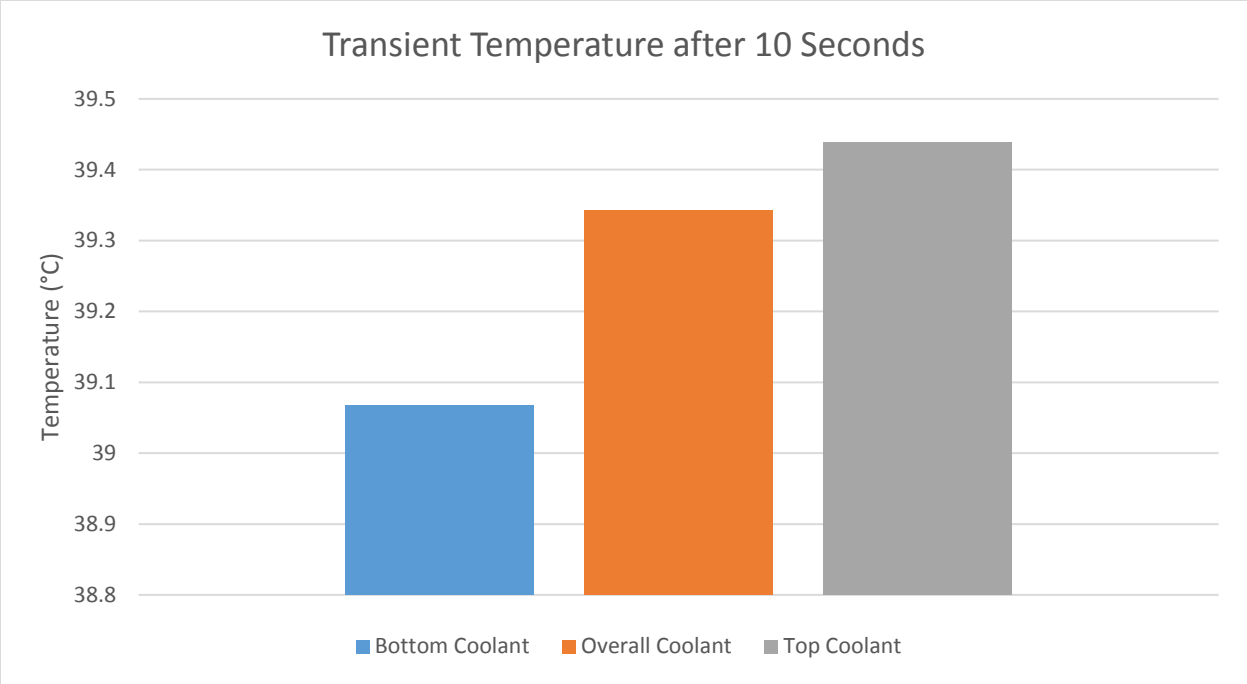

Figure 4.7a: Transient Temperature of the Bottom, Top, and Overall Coolant after 10 seconds

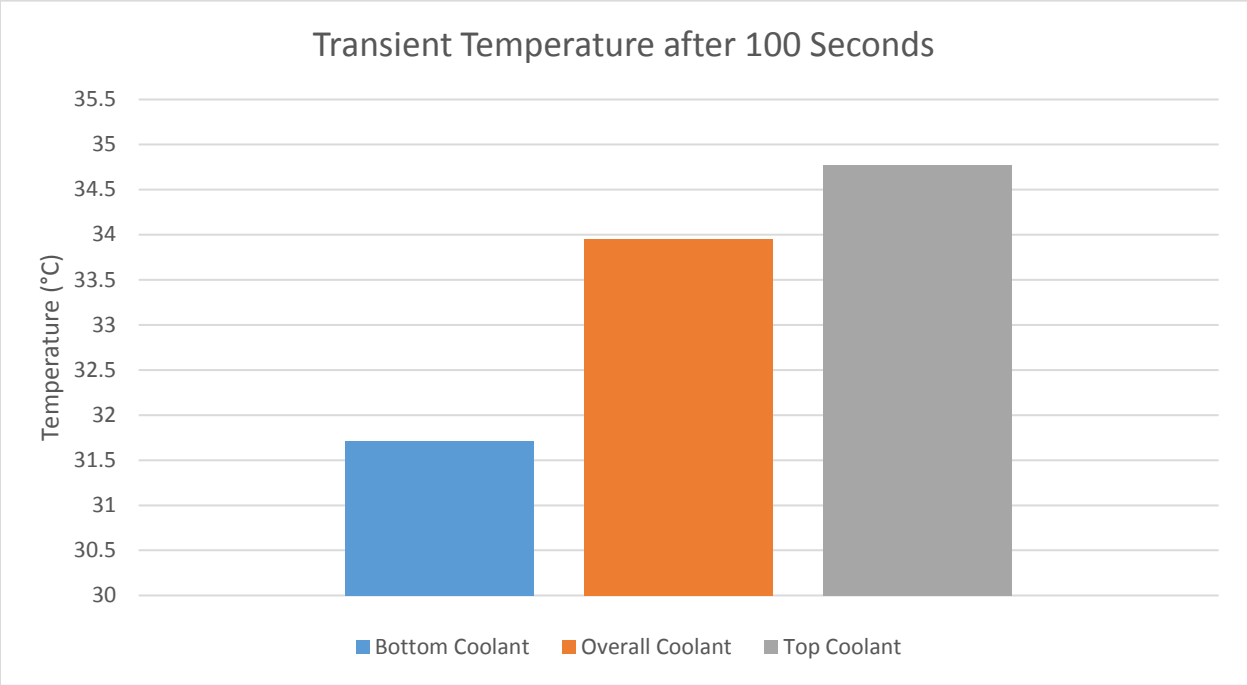

Figure 4.7b: Transient Temperature of the Bottom, Top, and Overall Coolant after 100 seconds

This provides a logical basis to change the interior design orientation of the chiller to understand how the coolant behavior and temperature changes based on a different design iterations.

4.4 Design Iterations

With the coolant behavior and temperature for above and below the steady state of refrigerant being calculated a function of time given, an analytical model was developed to determine how this coolant temperature would change based on changes to the interior design. The basis for the interior design to change is the idea that the refrigerant dimension changes with the corresponding aluminum that is surrounded by the coolant, while the outer dimensions of the aluminum surrounding the coolant remains the same throughout. This can be seen in Figure 2.16 from the "Methodology" Section, where r4 can change and r1, r2, and r3 will always change with r4, such that r1 always has a radius 10 mm less than r4, r2 always has a radius 7.5 mm less than r4, and r3 always has a radius 2.5 mm less than r4.

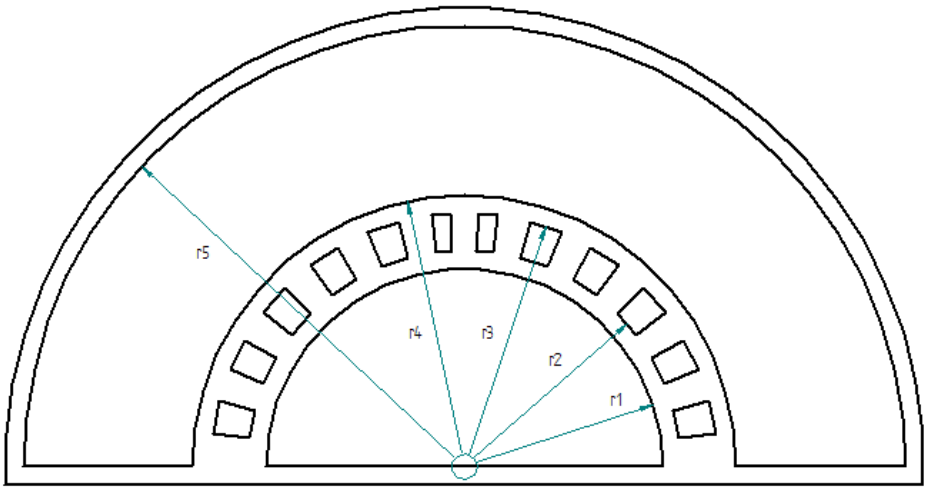

Figure 3.16: Front View of Initial Coolant Chiller Design with Radii designations

With r4,r3,r2, and r1 changing in unison, the coolant temperature given a specific time also changes. The design model provided to calculate the original design can also be used to study the bottom coolant, top coolant, and the overall coolant at different design iterations.

Bottom Coolant

For the bottom coolant; Figures 4.8a, 4.8b, and 4.8c provide what the bottom coolant temperature would be based on changing the interior radii, specifically r1 at an initial coolant temperature of $40°C$.

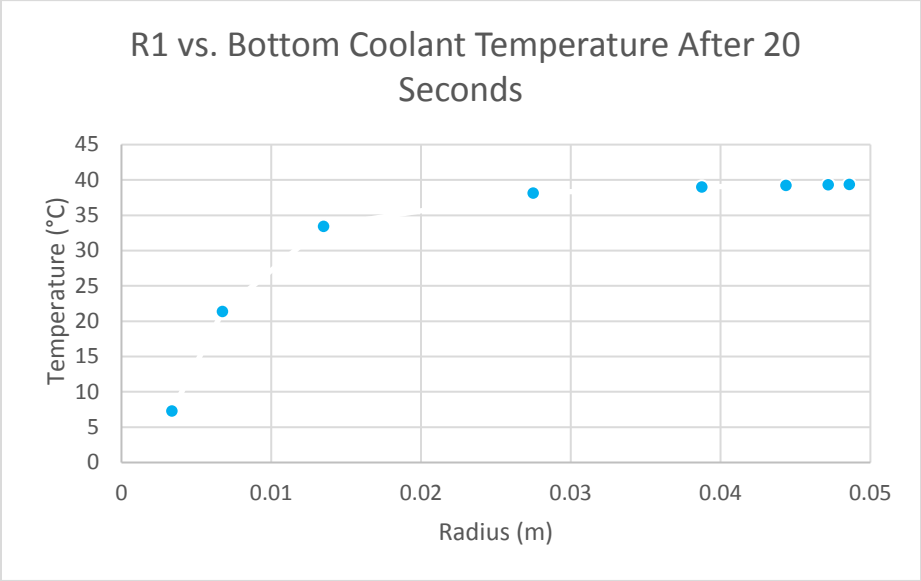

Figure 4.8a: Transient Temperature of the Bottom Coolant based on different iterations of r1 after 20 seconds

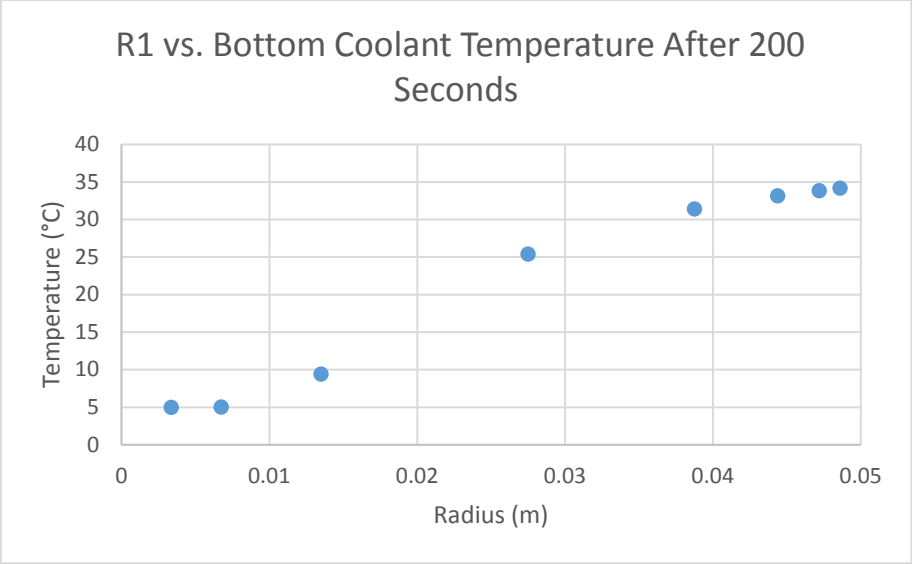

Figure 4.8b: Transient Temperature of the Bottom Coolant based on different iterations of r1 after 200 seconds

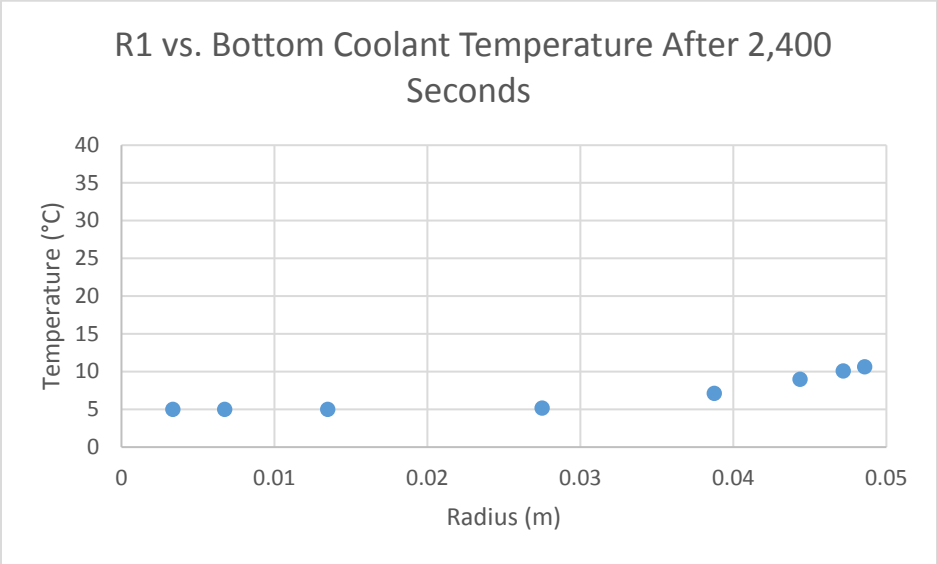

Figure 4.8c: Transient Temperature of the Bottom Coolant based on different iterations of r1 after 2,400 seconds

The general trend from Figures 4.8 a-c is that the smaller the interior radii, the quicker the bottom coolant temperature reaches to the minimum temperature of $5°C$. Similar trends can

be seen for the bottom coolant lower limit temperature at $30°C$ and the bottom coolant upper limit temperature at $50°C$ in Appendix Q.

The reason for this is because as r1 is reduced, the volume of the bottom coolant gets smaller. With a smaller volume, the bottom coolant temperature will decrease considerably, since the refrigerant provides the cooling heat transfer to a smaller mass of coolant.

From 20 seconds to 200 to 2,400 seconds, the trend shows that regardless of where the size of r1, the bottom coolant temperature will eventually reach the minimum temperature of $5°C$.

Top Coolant

For the top coolant; Figures 4.9a, 4.9b, and 4.9c provide what the top coolant temperature would be based on changing the interior radii, specifically r1 at an initial coolant temperature of $40°C$.

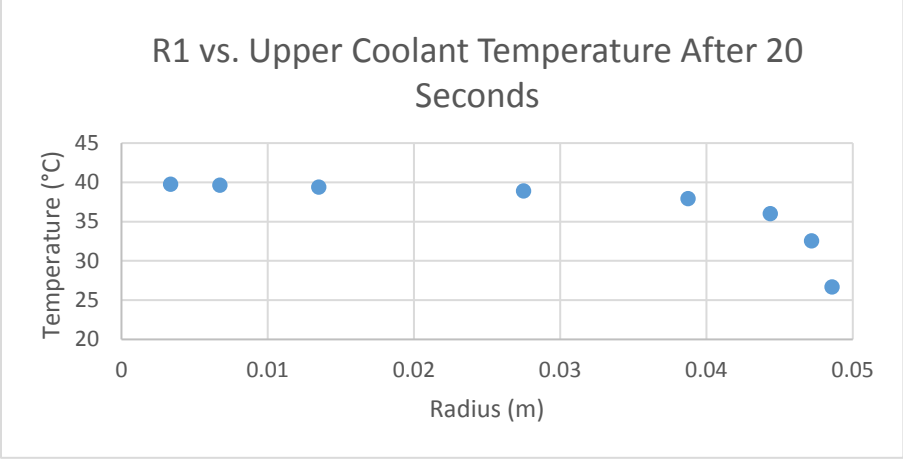

Figure 4.9a: Transient Temperature of the Upper Coolant based on different iterations of r1 after 20 seconds

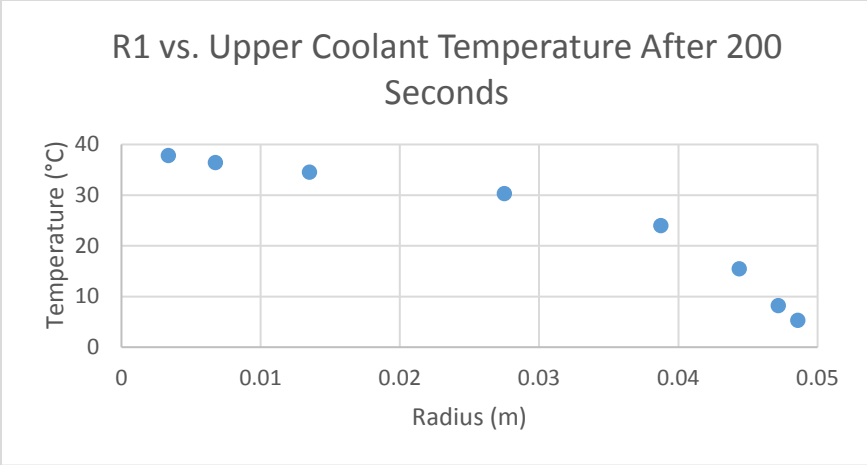

Figure 4.9b: Transient Temperature of the Upper Coolant based on different iterations of r1 after 200 seconds

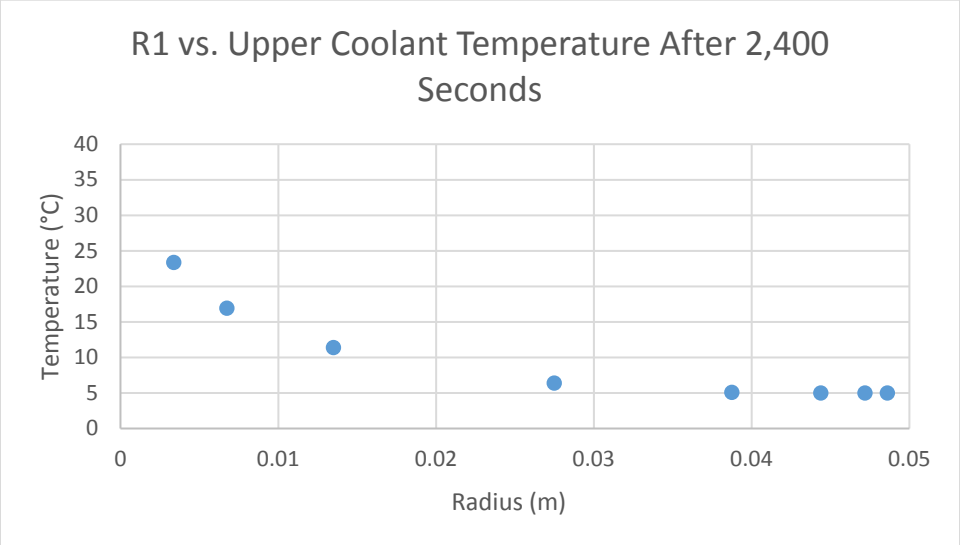

Figure 4.9c: Transient Temperature of the Upper Coolant based on different iterations of r1 after 2,400 seconds

The general trend observed from Figures 4.9 a-c is that the smaller the interior radii, the more time that is needed for the top coolant temperature to reach the minimum temperature of $5°C$. Similar trends can be seen for the top coolant lower limit temperature at $30°C$ and the top

coolant upper limit temperature at $50°C$ in Appendix R. The reason for this is because as r1 is reduced, the volume of the top coolant increases. With a larger volume, the top coolant temperature will drop slowly, since the refrigerant provides the cooling heat transfer to a bigger mass of coolant.

Similar to the bottom coolant; from 20 seconds to 200 to 2,400 seconds, the trend shows that regardless of the length of r1, the bottom coolant temperature will eventually reach the minimum temperature of $5°C$.

Overall Coolant

For the overall coolant; Figures 4.10a, 4.10b, and 4.10c provide what the overall coolant temperature would be based on changing the interior radii, specifically r1 at an initial coolant temperature of $40°C$.

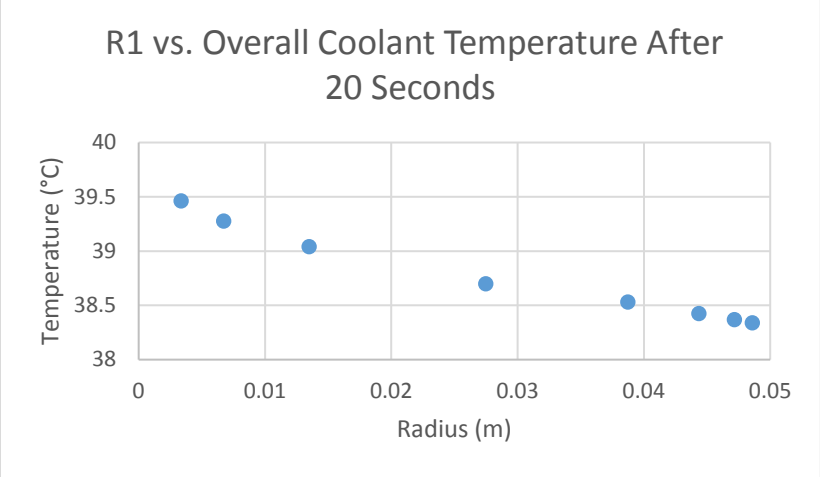

Figure 4.10a: Transient Temperature of the Overall Coolant based on different iterations of r1 after 20 seconds

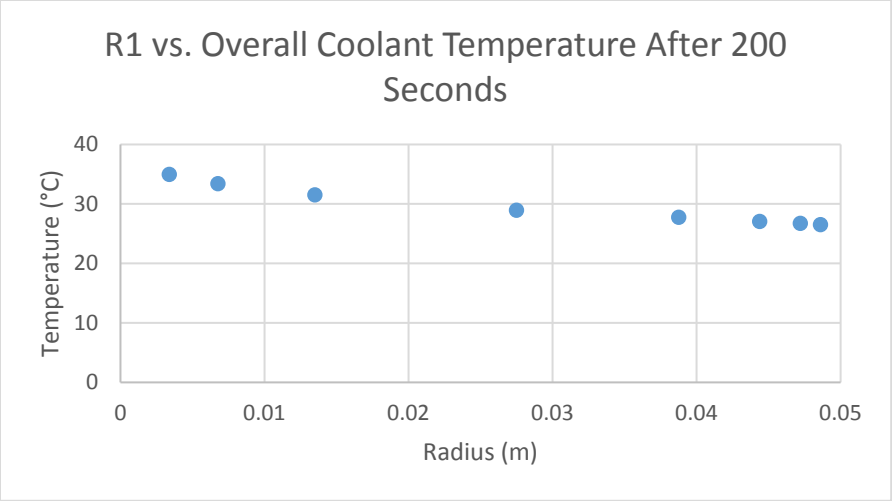

Figure 4.10b: Transient Temperature of the Overall Coolant based on different iterations of r1 after 200 seconds

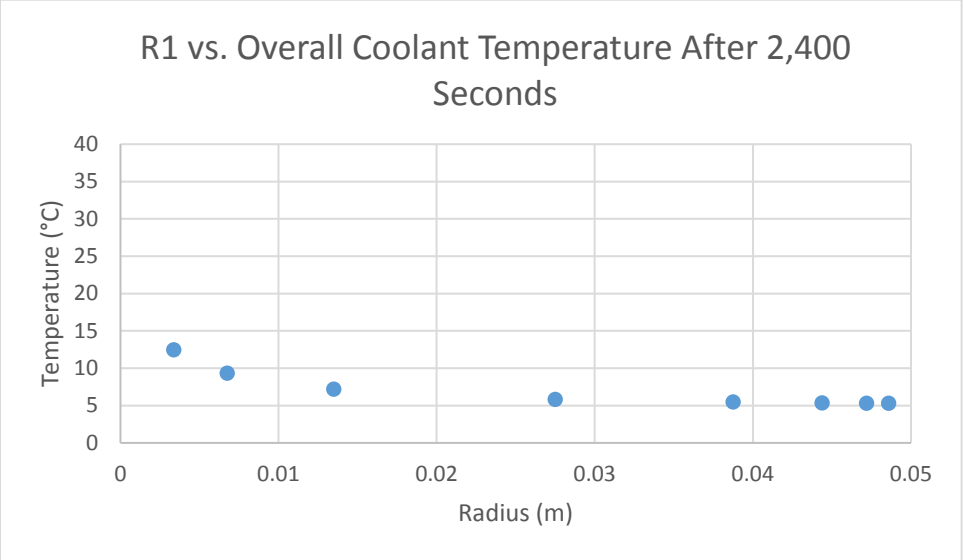

Figure 4.10c: Transient Temperature of the Overall Coolant based on different iterations of r1 after 2,400 seconds

The general trend observed from Figures 4.10 a-c is that the smaller the interior radii, the slower the overall coolant temperature reaches to the minimum temperature of $5°C$. Similar

trends can be seen for the overall coolant lower limit temperature at $30°C$ and the overall coolant upper limit temperature at $50°C$ in Appendix S. The reason for this is because the heat transfer rate is better in the bottom coolant than the top coolant. Therefore, the larger the interior radii, the more bottom coolant volume, therefore the lower the overall coolant temperature would be. The reason the heat transfer rate is better in the bottom coolant than the top coolant is because the bottom coolant is in constant motion with the refrigerant cooling from the top causing the cold coolant to be at the top of the bottom coolant, where the warmer coolant coming from the bottom will naturally want to rise causing a constant cyclical motion resulting in better heat transfer. Comparatively, the top coolant is stratified because the refrigerant will cool the bottom of the top coolant and the warmer coolant from the top will stay there causing a lack of motion and eventual stratification.

Similar to the bottom coolant and top coolant; from 20 seconds to 200 to 2,400 seconds, the trend shows that regardless of the size of r1, the bottom coolant temperature will eventually reach the minimum temperature of $5°C$.

Being able to change just the r1 to provide the coolant temperatures for the bottom, top, and overall coolant is an efficient design tool that effectively provides the transient temperature based on time and the refrigerant orientation in a timely fashion.

4.5 Summary

Using the knowns and assumptions for the materials and design processes, a 1-D thermodynamic analysis was studied in relation to a thermal resistance circuit of the heat exchanger to provide a custom Lumped capacitance model equation to find a relationship

between the transient coolant temperature and the time involved. To get to this, calculations for the Rayleigh, Number, Reynolds Number, and Nusselt Number were calculated to provide an analysis of the coolant behavior for the coolant above the refrigerant, coolant below the refrigerant, and the overall coolant. With this information, a design model that changes the interior design of the heat exchanger was created to further understand of the effects of the chilling coolant at various iterations.

CHAPTER 5: Conclusions and Future Work

5.1 Conclusions

The need for high performance in a vehicle will always be vital. A high performance vehicle engine loop usually contains a supercharger, charge air cooler, and an engine. The supercharger pressurizes the ambient air, also causing the air to rise in temperature. A charge air cooler cools this pressurized air on its way to the engine to increase the density, mass flow rate of the air going into the engine to allow the engine to operate at a higher performance. Since liquid coolant is being used in heat transfer with the air, the liquid charge air cooler involved is in a loop with the low temperature radiator.

For this thesis, the focus of study is the addition of a separate heat exchanger that is independent of the low temperature radiator loop. This is used as a reservoir to hold sub-ambient coolant that is held stagnant until the vehicle provides a signal to use this specific sub-ambient coolant, instead of the regular coolant coming from the LTR. This will deliver a temporarily higher mass flow rate to the internal combustion engine for a transient high

performance boost. The way this unique heat exchanger achieves a stagnant coolant at a sub-ambient temperature is through heat transfer with a steady state of refrigerant provided by the A/C equipment in the car.

This thesis provides a comprehensive study of the coolant behavior that goes through a heat transfer cooling transition. The way this study was conducted was through the thermodynamic analysis of the energy of the system and the calculations of the heat transfer rate and coefficients involved. The combination of the thermodynamic and heat transfer analysis provides a custom Lumped capacitance model equation that shows the relationship between the transient coolant temperature and the time.

Studying and analyzing this relationship provides the emergence of an analytical design model that can be manipulated to provide the changes in the coolant behavior for a certain time. For this thesis, the design model focuses on the internal design of the heat exchanger to determine the coolant temperature and behavior.

The lessons learned from this study include the appropriateness of the parallel vs. series thermal circuit, the behavior of coolant that is being chilled above and below it, and the derivation of the Lumped capacitance model needed to provide the relationship between coolant temperature and time.

1. Originally, the thermal resistance circuit in series was used to calculate the summation of the thermal resistance to eventually solve for the variable coolant temperature. The reason for this thinking is seeing the circuit using the frontal view of the heat exchanger and starting from the bottom to the top. This is not correct since the upper and lower

coolant should have the same initial temperature. The thermal resistance circuit in series does not allow for the initial temperature of both the upper and lower coolant to be the same. Starting from the refrigerant to the bottom coolant and the top coolant in parallel to get a uniform overall transient temperature of the coolant is accurately shown through a thermal resistance circuit in parallel.

2. The heat transfer rate is greater when the coolant is being cooled from the top compared to the coolant being cooled from the bottom. The reason for this is because the coolant being cooled from the bottom results in stratification of the coolant. This is due to the warm coolant continuing to rise while the chilled coolant stays at the bottom resulting in a lack of activity to provide for a good heat transfer compared to the coolant being cooled from the top. The simulations performed using CFD validated this analysis as it shows there was far more activity when the coolant was being cooled from the top due to hot coolant rising only to be cooled and fall again causing a constant cyclical motion of the coolant.

3. The relationship between the coolant temperature based on time is provided by a custom Lumped capacitance model. This Lumped capacitance model is a combination of the first law of Thermodynamics and the heat transfer rate equation. This combination involves the use of the overall heat transfer coefficient affecting the temperature and time. To get this relationship between temperature and time, fundamental

thermodynamic and heat transfer principles are derived to provide a custom Lumped capacitance model equation.

A thorough and comprehensive study shows the development of this analytical design tool. While this thesis proceeds to answer some questions, such as understanding the stratification and constant motion of stagnant coolant going through heat transfer, this thesis also provides more opportunities for further study to understand how different structural designs and fluid properties can continue to affect the stagnant coolant going through heat transfer cooling.

With this in mind, potential design improvements for this heat exchanger based on the conclusions that have been stated include the emphasis of the coolant being cooled from the top over the coolant being cooled from the bottom and the relevance of the surface area provided by the aluminum for better heat transfer.

1. Due to better heat transfer provided by the coolant being cooled from the top, the bottom coolant should have more of an emphasis on future designs due to an improved heat transfer rate. More emphasis should mean that the bottom coolant should be expanded and be more impactful than the top coolant.

2. However, the overall coolant should not be uniformly cooled from the top. The reason for this is because one benefit that the top coolant does have is that it provides more surface area in contact with aluminum to provide better overall heat transfer for the heat exchanger. The understanding of the balance between how minimal the top

coolant heat transfer should be is vital to learning the optimal design for better overall heat transfer.

5.2 Future Work

The opportunities and questions that can be formed to further understand the coolant behavior from this thesis are listed below.

i. The addition of heat transfer fins and extended surfaces

In the interior design of the heat exchanger, heat transfer fins and extended surfaces can assist with improved heat transfer through the addition of thermal conductive properties coming from the aluminum. Figure 5.1 shows just an example of how a fin could look like.

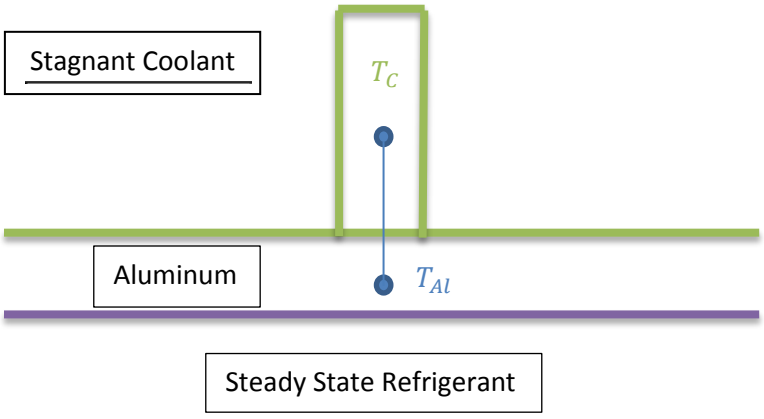

Figure 5.1: The Addition of a Heat Transfer Fin

With the addition of fins, the Resistance equation [3.12] for the coolant is

$$R_C = \frac{1}{\eta_f h_C A_C} \tag{5.1}$$

where $\eta_f =$ efficiency of the fin:

$$\eta_f = \frac{\tanh \chi}{\chi} \text{ (Rectangular)}$$

$$\eta_f = \frac{\tanh \sqrt{2}\chi}{\sqrt{2}\chi} \text{ (Pin)}$$

$$\text{where } \chi = \frac{h_C P_f L_f^2}{k_C A_f} \quad ,$$

L_f = Length of fin, A_f = Surface Area of Fin, P_f = Perimeter of fin

Not only adding fins, but understanding the quantity, dimensions, and shape adds another dimension to understanding the relationship between the time and the transient cooling temperature and ways to improve the heat transfer rate.

ii. Various orientations of the heat exchanger

For this thesis, one of the main assumptions was that the heat exchanger was horizontal. However, to continue study the heat transfer rate and heat transfer rate extensively; another aspect of this study involves the heat exchanger at different orientations, including vertical orientation, as shown in Figure 5.2.

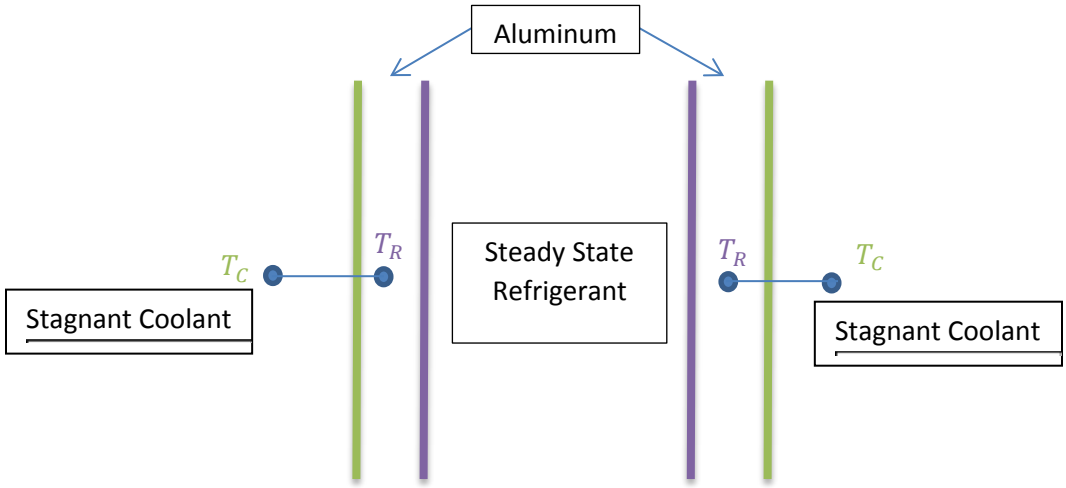

Figure 5.2: Vertical Orientation of the Coolant Chiller with Corresponding thermal resistance circuit

Regardless of whether the stagnant coolant is to left or right of the vertical aluminum metal that is in direct contact with the refrigerant coolant, the heat transfer coefficient remains the same due to the equation to solve the Nusselt Number at a vertical wall [1]:

$$Nu_C = 0.68 + \frac{0.67Ra^{1/4}}{\left[1+(0.492/Pr)^{9/16}\right]^{4/9}} \qquad Ra \leq 10^9 \tag{5.2}$$

Further analysis can be done using this information to delve more deeply into understanding how the coolant cools in a vertical orientation and compare it to the horizontal orientation.

iii. Multiphase flow of refrigerant

This thesis mainly involves the study of the coolant with the assumption that the refrigerant is always in liquid state while cooling the coolant. However, there needs to be a deeper study into understanding the behavior of the refrigerant and determining whether the refrigerant truly stays in the liquid state or does it become a multi-phase problem. Multi-phase refrigerant will add complications and require a more in depth understanding of the heat transfer rate coming from the refrigerant to the coolant.

iv. The mixture of nanofluids with the coolant

Ethylene glycol mixed with water based on volume was used as the coolant for this project. However, recent literature has shown that heat transfer coefficients and the overall heat

transfer can be improved with the addition of nanofluids [57]. Therefore, there should be additional studies understanding the effects of the coolant with these nanofluids in the design of future heat exchangers.

REFERENCES

1. Cotter, M. & Charles, M. (1992). Transient cooling of petroleum by natural convection in cylindrical storage tanks—I. Development and testing of a numerical simulator. *Int. J. Heat Mass Transfer.* 2165-2174.
2. Belmdany, M., Belgacem, A., and Rebiai, R. (2008). Analysis of Natural convection in liquid nitrogen under storage conditions. *Journal of Applied Science 8,* 2544-2552.
3. Prasanth Kumar, S., Prasad, B., Venkatarathnam, G., Ramamurthi, K., & Srinivasa Murthy, S. (2007). Influence of surface evaporation on stratification in liquid hydrogen tanks of different aspect ratios. *International Journal of Hydrogen Energy,* 1954-1960.
4. Khelifi-Touhami, M.S., Benbric, A., Lemonnier, D., & Blay, D. (2001). Laminar natural convection flow in a cylindrical cavity application to the storage of LNG. *J. of Petroleum science and Engineering,* 126-132.
5. Roh, S. & Son, G. (2012). Numerical study of natural convection in a liquefied natural gas tank. *Journal of Mechanical Science and Technology,* 3133-3140.
6. Nakamoto, H., Aya, N., Kurita, H., & Yoshizawa, A. (1984). Simulation of Natural Convection in a High Pressure CZ Furnace. *Journal of the Faculty of Engineering. University of Tokyo. Series A,* 50-51.
7. Shulman, G. & Whitelaw, R. (1995). Geothermal Heat-Mining by Controlled Natural Convection Water Flow in Hot Dry Rock for Electric Power Generation. *Bulletin 0160-7782.* 182-185.
8. Zeng, H., Diao, N., & Fang, Z. (2003). Heat transfer analysis of boreholes in vertical ground heat exchangers. *International Journal of Heat and Mass Transfer 46.* 4467-4481.

9. Gehlin, S. & Hellstrom, G. (2000). Analytical studies of the influence of regional groundwater flow on the performance of borehole heat exchangers. *Terrastock 8th International Conference on Thermal Energy Storage.*
10. Gustafsson, A., Westerlund, L. & Hellstrom, G. (2009). CFD-modelling of natural convection in a groundwater-filled borehole heat exchanger. *Applied Thermal Engineering.* 683-691.
11. Sparrow, E. & Abraham, J. (2003). A new buoyancy model replacing standard pseudo-desnity difference for internal natural convection gases. *International Journal of Heat and Mass Transfer 46,* 3583-3591.
12. Mistry, H., Dey, S., Bishnoi, P. & Castillo, J. (2006). Modeling of transient natural convection heat transfer in ovens. *Applied Thermal Engineering 26,* 2448-2456.
13. Fujii, T., Honda, H. & Morioka, I. (1973). A Theoretical Study of Natural Convection Heat Transfer from Downward Facing Horizontal Surfaces with Uniform Heat Flux. *Int. J. Heat Mass Transfer,* 16, 3, 611.
14. Wright, J. & Douglas, R. (1986). Natural Convection in the Narrow Gap Spherical Annuli. *Int. J. Heat Mass Transfer,* 29, 725.
15. Kwak, C.E. & Song, T.H. (2000). Natural Convection Around Horizontal Downward-Facing Plate with Rectangular Grooves: Experiments and Numerical Simulations. *Int. J. Heat Mass Transfer,* 43, 825.
16. Lee, J.R., Ha, M.Y., Balachandar, S., Yoon, H. S. & Lee, S. S. (2004). Natural Convection in a Horizontal Layer of Fluid with a Periodic Array of Square Cylinders in the Interior. *Phys. Fluids.* 16, 4, 1097.

17. Liaqat, A. & Baytas, A. C. (2001). Cooling of Molten Core Material Within a Pressurized Water Reactor Vessel Lower Head: Interaction of Surface Radiation and Wall Conduction with Free Convection. *Int. J. Eng. Science,* 39, 2089.
18. Lin, W. & Armfield, S.W. (1999). Direct simulation of natural convection cooling in a vertical circular cylinder. *International Journal of Heat and Mass Transfer 42,* 4117-4130.
19. Sharma, A. K., Das, S. K. & Harvey, J. (2008). Experimental and Numerical Analysis of Natural Convection in Geometrically Modeled Core Catcher of the Liquid-Metal-Cooled Fast Reactor. *Indhira Gandhi Center for Atomic Research,* 43-52.
20. Behnia, M., Dehghan, A. A., Mishima, H. & Nakayama, W. (1998). Convection Cooling of a Heated Obstacle in a Channel. *Int. J. Heat Mass Transfer 41.* 3131-3148.
21. Ramon, L. F. & Berbakow, O. (2002). Natural Convection in Cubical Enclosures with Thermal Sources on Adjacent. *Numerical Heat Transfer, Part A 4*, 334-340.
22. Bhowmic, H. & Tou, K. (2005). Experimental Study of Transient Natural Convection Heat Transfer from Simulated Electronic Chips. *Exp. Thermal Fluid Sci. 29,* 485-492.
23. Lahmer, K. & Bessaih, R. (2014). Numerical simulation of cooling electronic components mounted in a vertical wall by natural convection. *Mechanics & Industry 15,* 89-98.
24. Batchelor, G. K. (1954). Heat transfer by free convection across a closed cavity between vertical boundaries at different temperature. *Q. J. Appl Maths, 12*, 209-233.
25. Barakat, H. Z. & Clark, J. A. (1966). Analytical and experimental study of the transient laminar natural convection flows in partially filled containers. *Trans. Am. Soc. Mech. Engrs 88,* 152-162.

26. Catton, I. (1978). Natural convection in enclosures. *6th Intl Heat Transfer Conf. Toronto, vol. 6,* 13-43.

27. Han, S.M. (1984). A transient numerical analysis of high Rayleigh number convection in a differentially heated square cavity. *ASME Paper 84-HT-57.*

28. Kublbeck, K., Merker, G. P. & Straub J. (1980). Advanced numerical calculation of two-dimensional time-dependent free convection in cavities. *Int. J. Heat Mass Transfer 23,* 203-212.

29. Vasseur, P. & Robillard L. (1982). Natural Convection in a rectangular cavity with wall temperature decreasing at a uniform rate. *Warme-u. Stoffubertr. 16,* 199-207.

30. Nicolette, V.F. & Yang, K.T. (1985). Transient cooling by natural convection in a two-dimensional square enclosure. *Int. J. Heat Mass Transfer 28,* 1721-1732.

31. Jischke, M.C. & Doty, R.T. (1975). Linearized buoyant motion in a closed container. *J. Fluid Mech. 71,* 729-754.

32. Kwak, H.S., Kuwahara, K. & Hyun, J.M. (1998). Convective cool-down of a contained fluid through its maximum density temperature. *Int. J. Heat Mass Transfer* 41, 323-333.

33. Zeitoun, O. & Ali, M. (2006). Numerical Investigation of Natural Convection Around Isothermal Horizontal Rectangular Ducts, *Numer. Heat Transfer A, vol. 50.* 189-204.

34. Mahfouz, F.M. & Kocabiyik, S. (2003). Transient Numerical Simulation of Buoyancy Driven Flow Adjacent to an Elliptic Tube, *Int. J. Heat Fluid Flow, vol 24,* 864-873.

35. De, A. K. & Dalal, A. (2006). A Numerical Study of Natural Convection Around a Square, Horizontal, Heated Cylinder Placed in an Enclosure, *Int. J. Heat Mass Transfer, vol. 49,* 4608-4623.

36. Khodary, K. & T.K. Battacharyya, (2006). Optimum Natural Convection from Square Cylinder in Vertical Channel, *Int. J. Heat Fluid Flow, vol. 27,* 167-180.

37. Gori, F., Serrano, M. G., & Wang, Y. (2006). Natural Convection Along a Vertical Thin Cylinder with Uniform and Constant Wall Heat Flux. *Int. J. Thermophysics, vol. 27,* 1527-1538.

38. Alipoura, M., Hosseini, R., & Rezania, A. (2013). Radius Ratio Effects on Natural Heat Transfer in Concentric Annulus. *Exp. Therm. Fluid Sci., vol. 49*, 135-140.

39. Al-Arabi, M. & Khamis, M. (1982). Natural Convection Heat Transfer from Inclined Cylinder. *Int. J. Heat Mass Transfer, vol. 25,* 325-329.

40. Inaba, Y., Zhang, Y., Takeda, T. & Shiina, Y. (2005). Natural Convection Heat Transfer of High Temperature Gas in an Annulus Between Two Vertical Concentric Cylinders, *Heat Transfer Asian Res., vol. 34, no. 5,* 293-308.

41. Amine, Z., Daverat, C., Xin, S., Giroux-Julien, S., Pabiou, H. & Menezo, C. (2013). Natural Convection in a Vertical Open-Ended Channel: Comparison between Experimental and Numerical Results. *J. Energy Power Eng., vol. 7,* 1265-1276.

42. Husain, S. & Siddiqui, M. (2016). Experimental and numerical analyses of natural convection flow in a partially heated vertical annulus. *Numerical Heat Transfer, Part A, vol. 70, no. 7,* 763-775.

43. Lin, W. & Armfield, S.W. (2001). Natural Convection Cooling of Rectangular and Cylindrical Containers. *Int. J. Heat Fluid Flow.* 22, 72.

44. Lin, W. & Armfield, S.W. (2001). Long-term behavior of cooling fluid in a vertical cylinder. *International Journal of Heat and Mass Transfer 48,* 53-66.

45. Oliveski, R. D. C., Krezinger, A. & Vielmo, H. (2003). Cooling of cylindrical vertical tanks submitted to natural internal convection, *International Journal of Heat and Mass Transfer 46*, 2015-2026.

46. Rodriguez, I., Castro, J., Perez-Segarra, C. D. & Oliva A. (2008). *International Journal of Thermal Sciences,* 708-721.

47. Davis, G.D.V. (1983). Natural convection in a square cavity: a comparison exercise. *Int. J. Numer. Meth. Fluids 3,* 227-248.

48. Schmidt, W., Giel, P.W., Phillipst, R.E., & Wang, D.F. (1986). A comparison of experimental and predicted results for laminar natural convection in an enclosure. *Int. J. Heat Fluid Flow 7,* 183-190.

49. Hiroyuki, O., Akira, M. & Masura, O. (1985). Numerical calculations of laminar and turbulent natural convection in water in rectangular channels heated and cooled isothermally on the opposing vertical walls. *Int. J. Heat Mass Transf. 28,* 125-138.

50. Fusegi, T. & Hyun, J.M. (1994). Laminar and transitional natural convection in an enclosure with complex and realistic conditions. *Int. J. Heat Fluid Flow 15,* 258-268.

51. Turan, O., Poole, R.J. & Chakraborty, N. (2012). Influences of boundary conditions on laminar natural convection in rectangular enclosures with differentially heated sidewalls. *Int. J. Heat Fluid Flow 33*. 131-146.

52. Mahdavi, M., Sharifpur, M., Ghodsinezhad, H., & Meyer, J.P. (2016). Experimental and numerical study of the thermal and hydrodynamic characteristics of laminar natural convective flow inside a rectangular cavity with water, ethylene glycol-water and air. *Experimental Thermal and Fluid Science,* 50-64.

53. (2009). *ASHRAE Handbook: Fundamentals, American Society of Heating, Refrigerating and Air-Conditioning Engineers,* 4.1-4.20.

54. Lemmon, E.W., Bell, I.H., Huber, M.L. & McLinden, M.O. (2018). NIST Standard Reference Database 23: Reference Fluid Thermodynamic and Transport Properties-REFPROP. *National Institute of Standards and Technology, Standard Reference Data Program*.

55. Incropera, F.P. & Dewitt, D.P. (2001). *Fundamentals of Heat And Mass Transfer, Fifth Edition.*

56. Cengel, Y. (2006). *Heat and Mass Transfer: A Practical Approach, Third Edition.*

57. Li, H., Yurong, He., Hu, Y., Jiang, B. & Huang, Y. (2015). Thermophysical and natural convection characteristics of ethylene glycol and water mixture based ZnO nanofluids. *International Journal of Heat and Mass Transfer,* 385-389.

APPENDIX A: **DATA POINTS FROM CFD SIMULATION FOR BOTTOM COOLANT**

		¼ Length
	Length (m)	0.11
	A (m^2)	0.00933
	T_S (K)	293
Initial Coolant Temp @ 40 C	Q (W)	39.28
	T_B (K)	302.927
	h (W/m^2/K)	424.1034579
	Nu	56.93583783
	Ra	5496443.161
Initial Coolant Temp @ 30 C	Q (W)	15.97
	T_B (K)	297.737
	h (W/m^2/K)	361.3432011
	Nu	49.30781636
	Ra	1595129.86
Initial Coolant Temp @ 35 C	Q (W)	26.96
	T_B (K)	300.294
	h (W/m^2/K)	396.1616986
	Nu	53.61828786
	Ra	3202601.108
Initial Coolant Temp @ 45 C	Q (W)	52.77
	T_B (K)	305.7031
	h (W/m^2/K)	445.2415987
	Nu	59.29410077
	Ra	8650576.443
Initial Coolant Temp @ 50 C	Q (W)	67.41971
	T_B (K)	308.3622
	h (W/m^2/K)	470.3832208
	Nu	62.64228269
	Ra	10461374.42

Figure A1: Data Points from CFD Simulation For Bottom Coolant

APPENDIX B: **TEMPERATURE AND VELOCITY PROFILES FOR BOTTOM COOLANT**

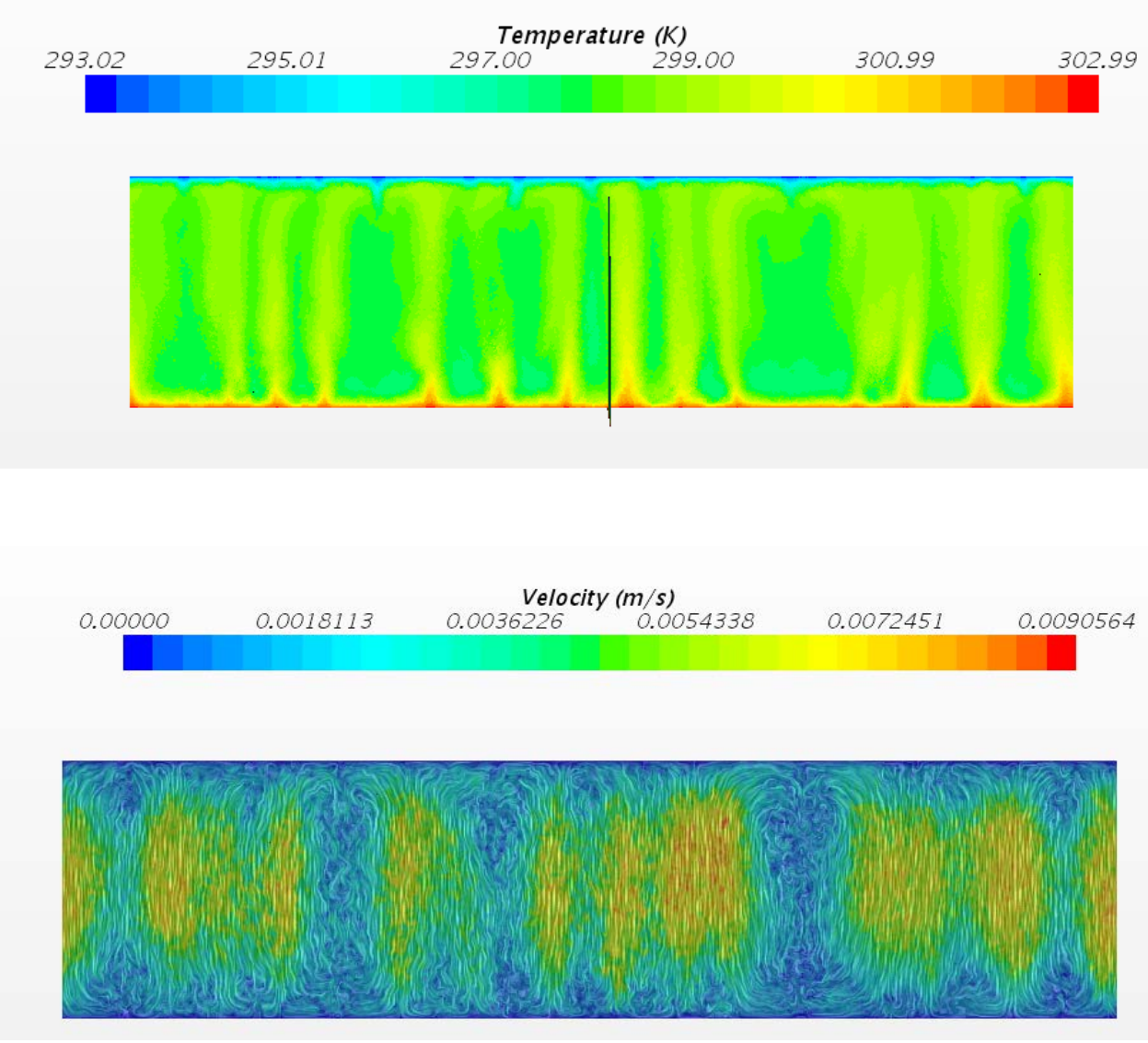

Figure B1: Side View of the Temperature and Velocity Profiles of the Bottom Coolant for $30°C$

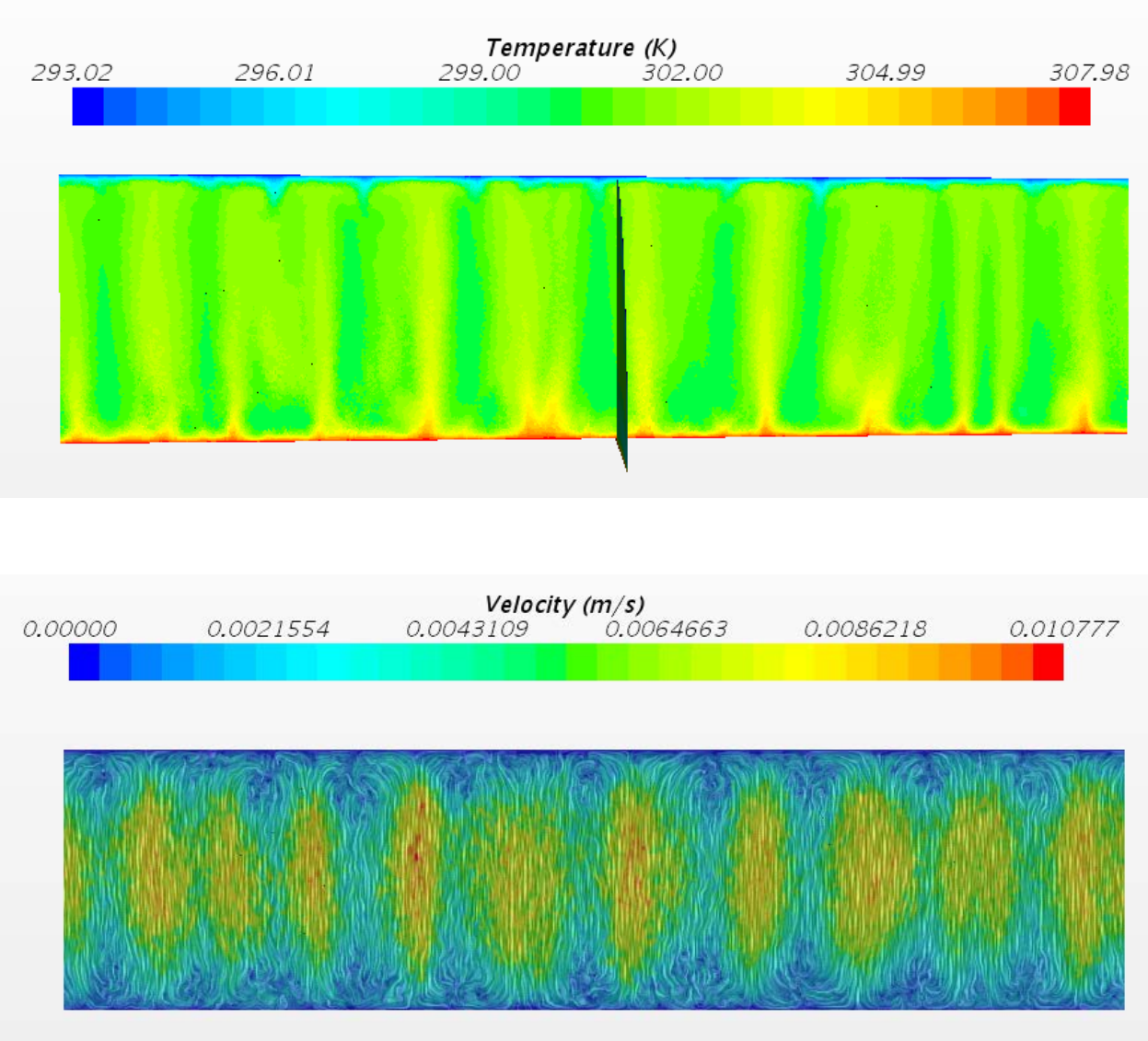

Figure B2: Side View of the Temperature and Velocity Profiles of the Bottom Coolant for $35°C$

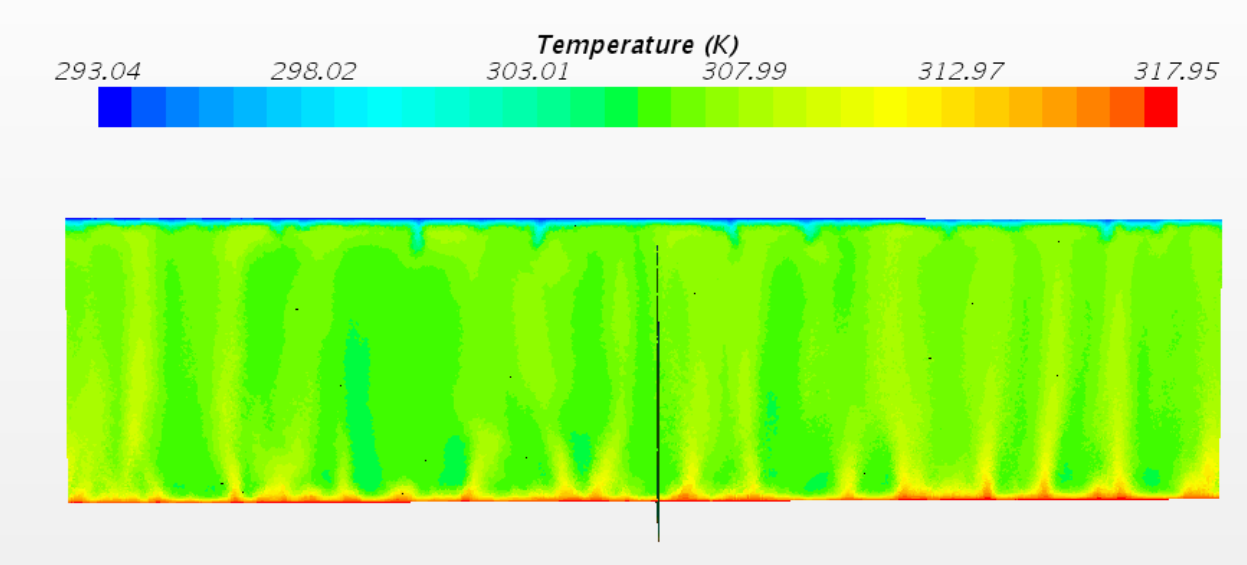

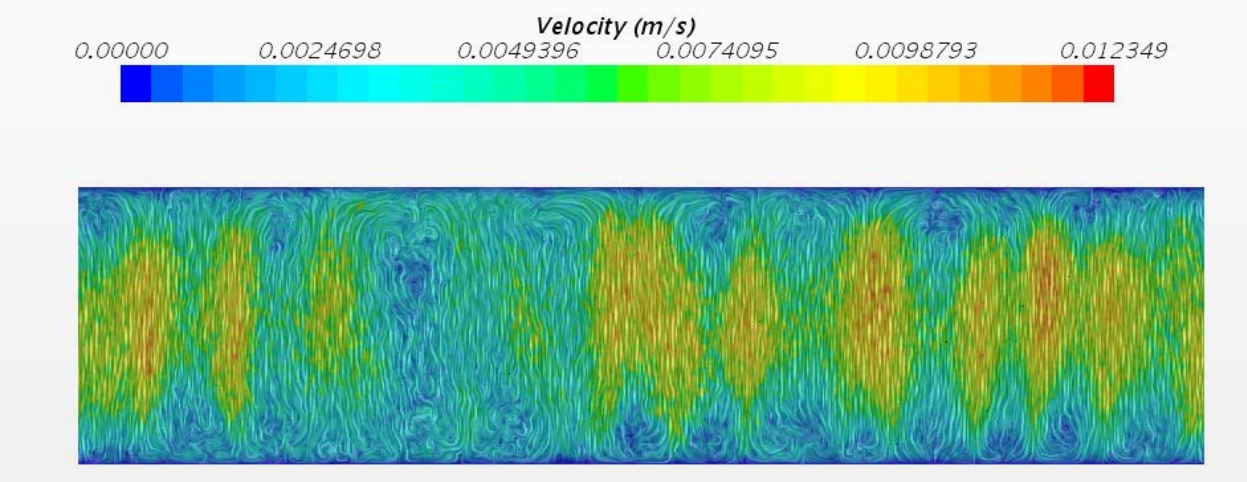

Figure B3: Side View of the Temperature and Velocity Profiles of the Bottom Coolant for $45°C$

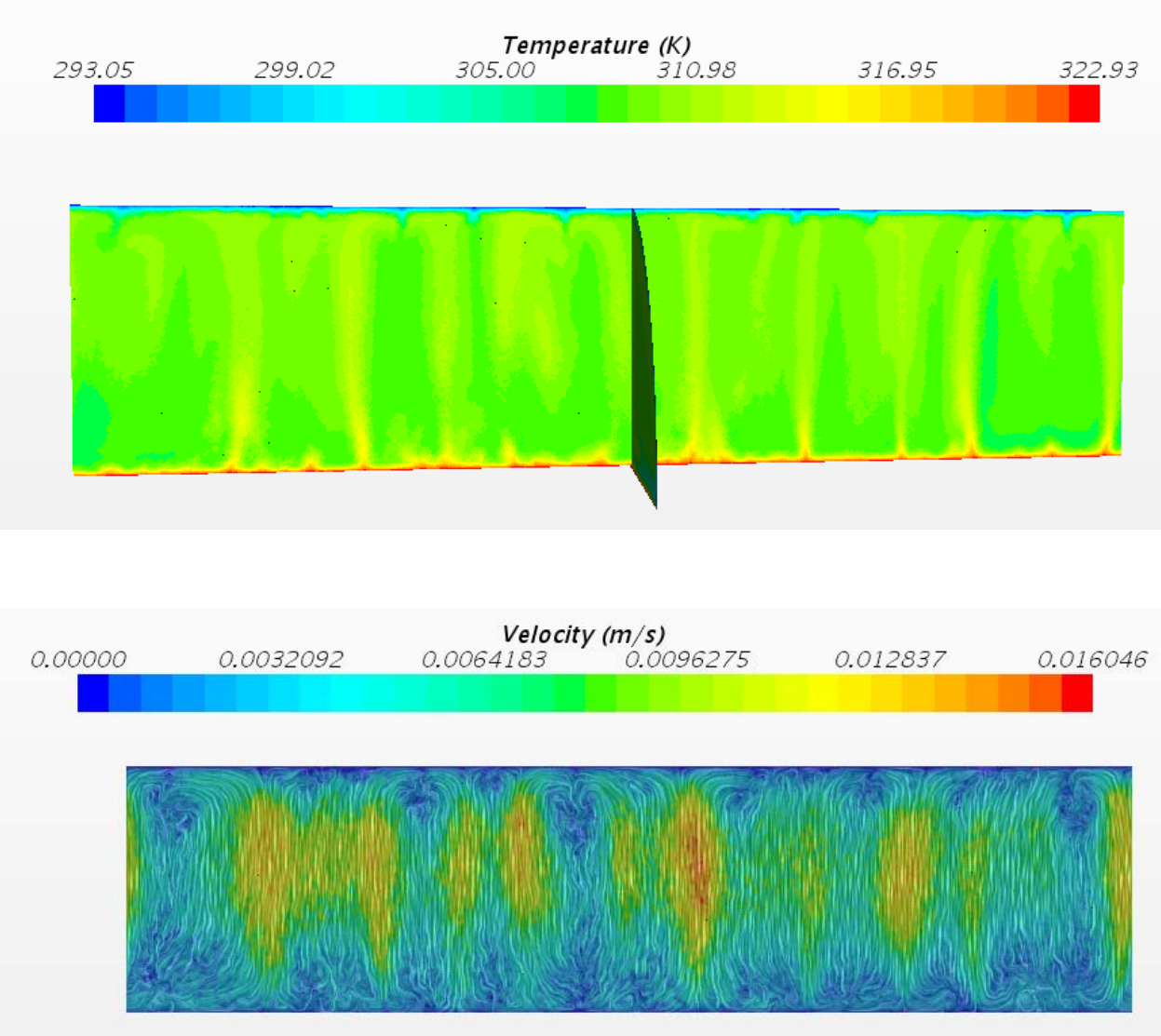

Figure B4: Side View of the Temperature and Velocity Profiles of the Bottom Coolant for $50°C$

APPENDIX C: **DATA POINTS FROM CFD SIMULATION FOR TOP COOLANT**

		¼ Length
	Length (m)	0.11
	A (m^2)	0.00933
	T_S (K)	293
Initial Coolant Temp @ 40 C	Q (W)	50.56
	T_B (K)	305.8
	h (W/m^2/K)	423.3654877
	Nu	47.36397117
	Ra	4101379.449
Initial Coolant Temp @ 30 C	Q (W)	22.35
	T_B (K)	299.27
	h (W/m^2/K)	382.0571599
	Nu	43.44531787
	Ra	1221845.976
Initial Coolant Temp @ 35 C	Q (W)	35.67392
	T_B (K)	302.5183
	h (W/m^2/K)	401.7073716
	Nu	45.30738661
	Ra	2125948.384
Initial Coolant Temp @ 45 C	Q (W)	66.82535
	T_B (K)	309.2117
	h (W/m^2/K)	441.8054204
	Nu	49.03041254
	Ra	4624439.512
Initial Coolant Temp @ 50 C	Q (W)	84.41117
	T_B (K)	312.6402
	h (W/m^2/K)	460.6513733
	Nu	50.71502932
	Ra	6254910.459

Figure C1: Data Points from CFD Simulation For Top Coolant

APPENDIX D: **TEMPERATURE AND VELOCITY PROFILES FOR BOTTOM COOLANT**

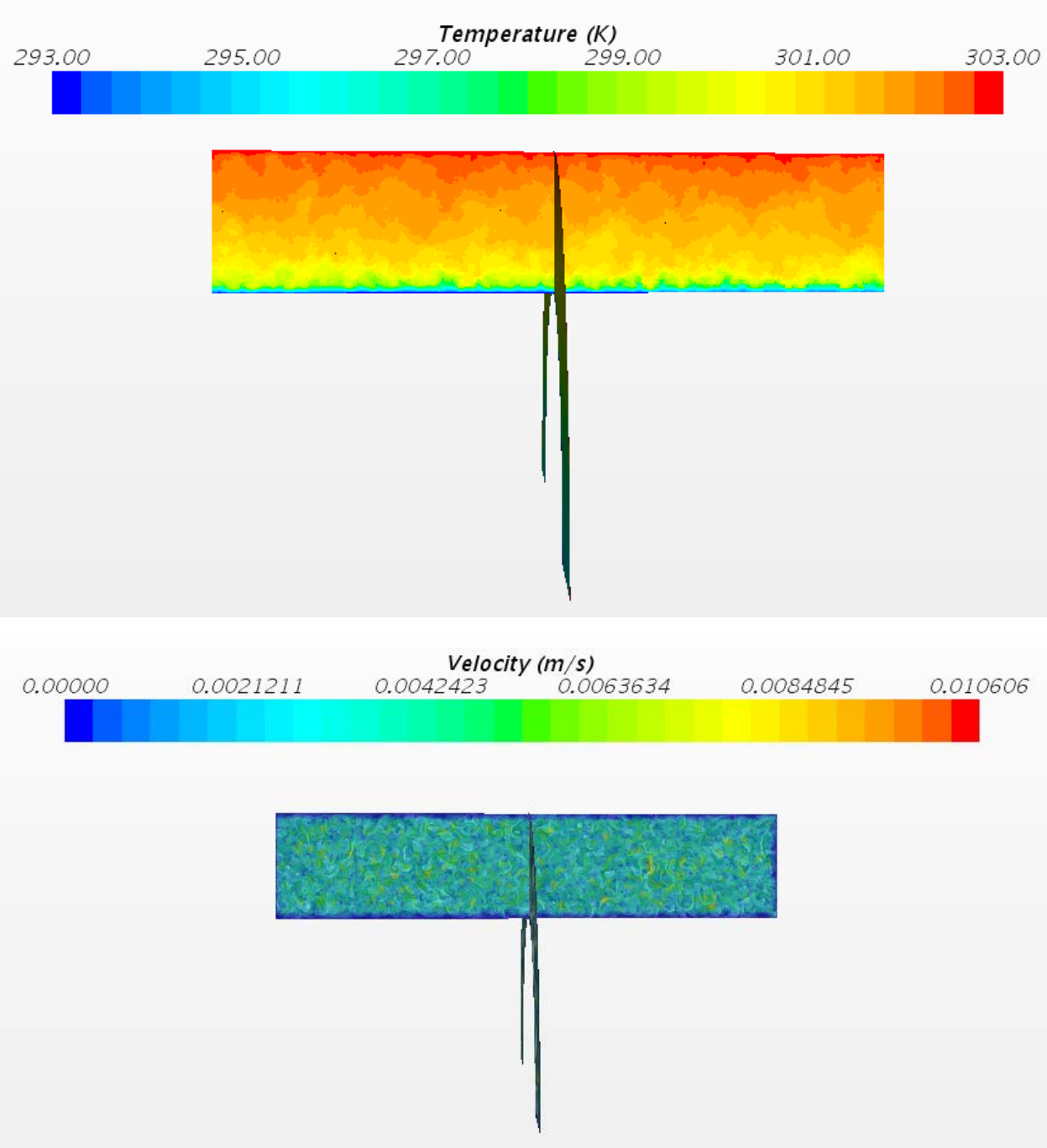

Figure D1: Side View of the Temperature and Velocity Profiles of the Top Coolant for $30°C$

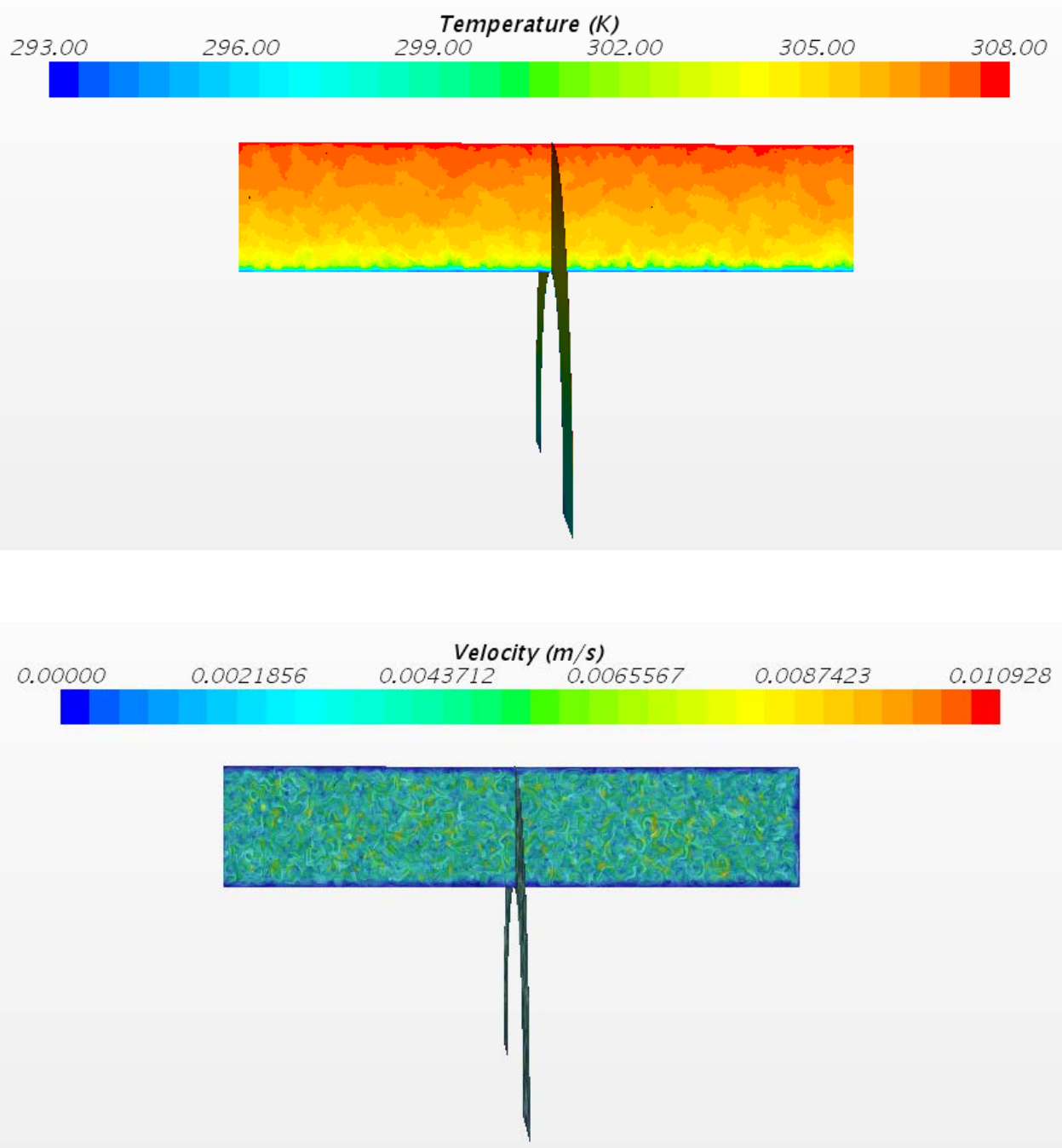

Figure D2: Side View of the Temperature and Velocity Profiles of the Top Coolant for $35°C$

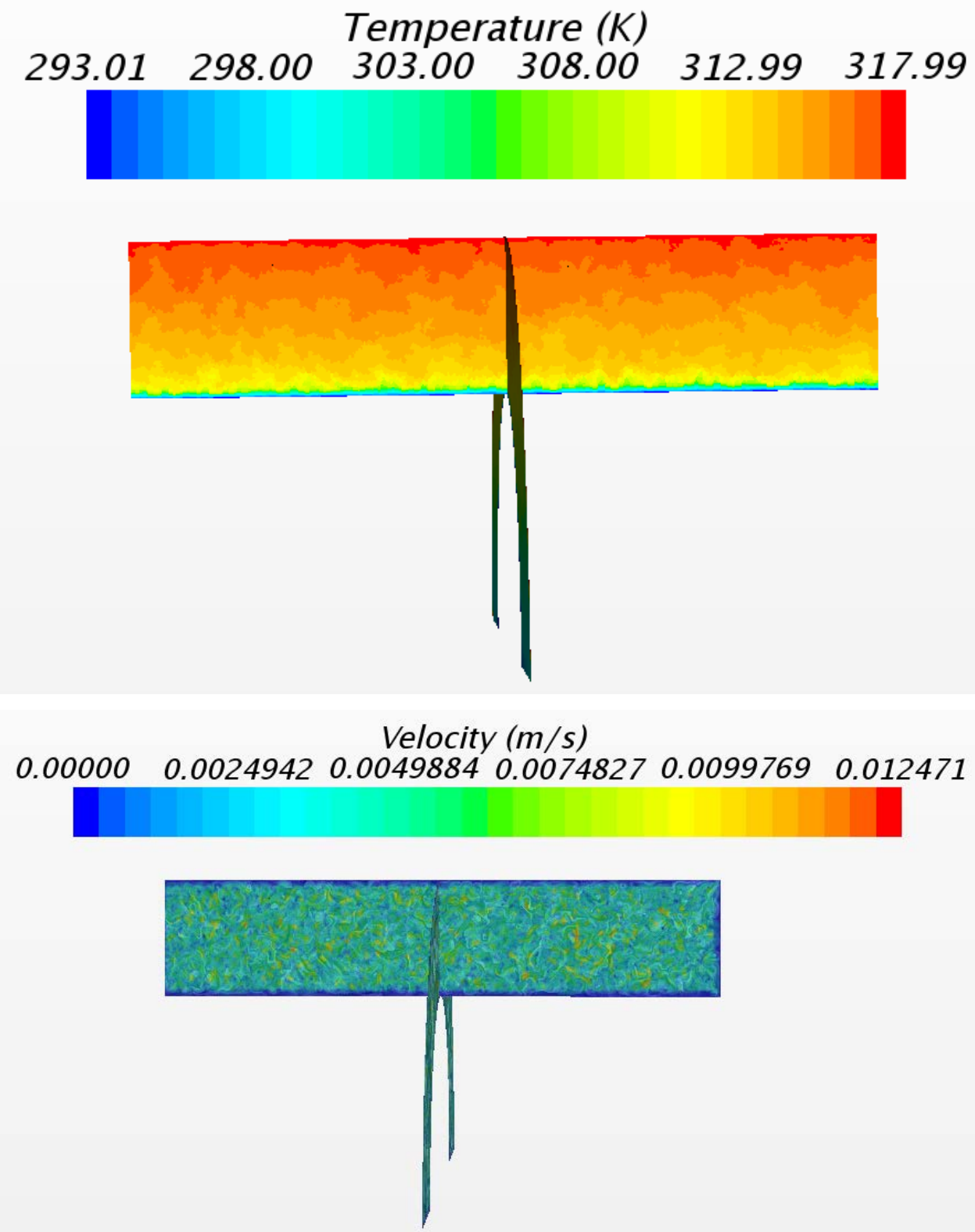

Figure D3: Side View of the Temperature and Velocity Profiles of the Top Coolant for $45°C$

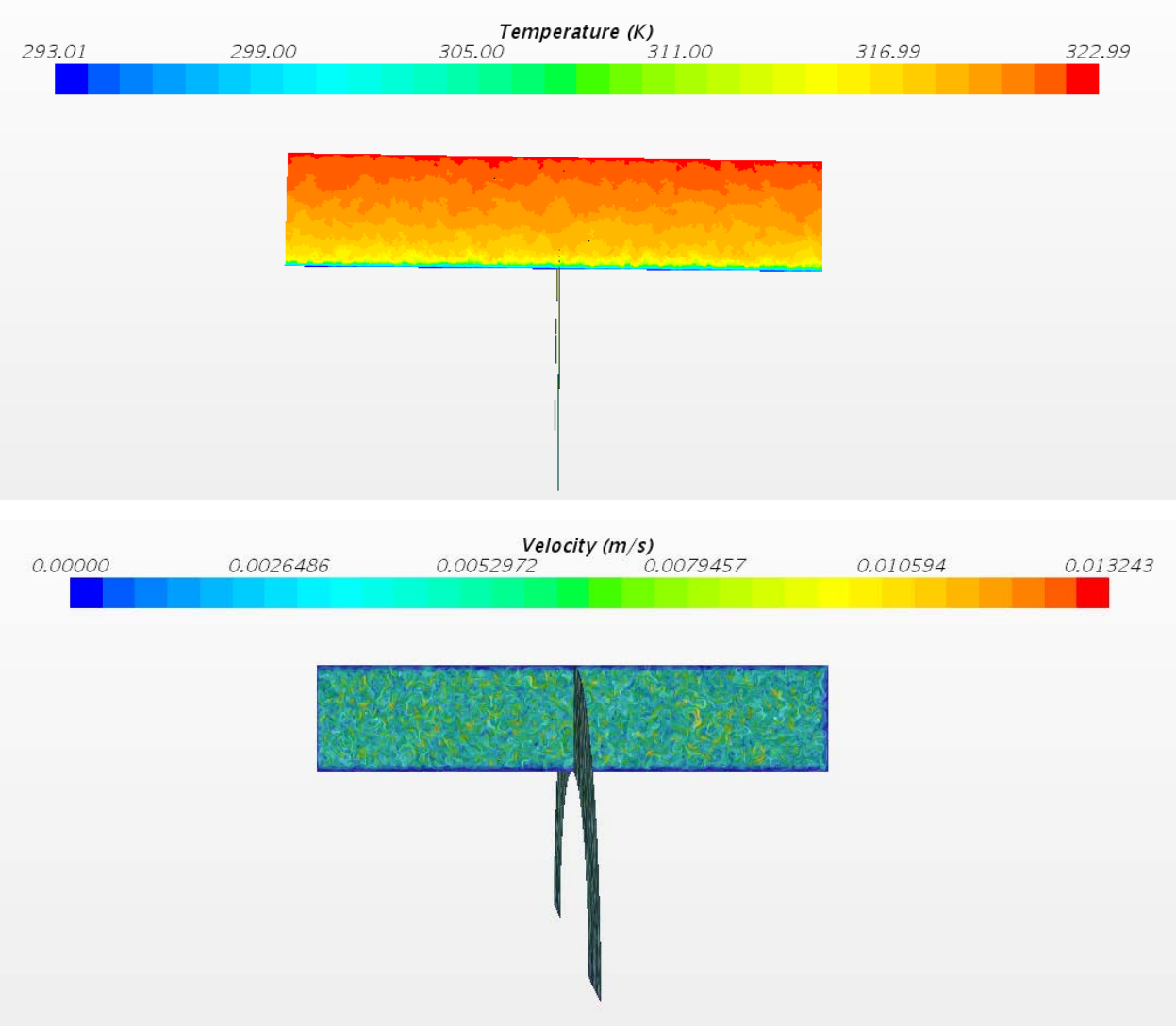

Figure D4: Side View of the Temperature and Velocity Profiles of the Top Coolant for $50°C$

APPENDIX E: **MODINE CUSTOM PROPERTIES FOR 50% ETHYLENE GLYCOL MIXED WITH 50% WATER (BY VOLUME)**

Temp. [°C]	Density [kg/m³]	Cp [J/kg/K]	Th. Cond [W/m/K]	Dyn Visco [kg/m/s]	Kin Visco [m²/s]	Prandtl No.	rho*Cp [J/m³/K]
30	1065.37	3390.25	0.395729	0.00307327	2.88E-06	26.329	3.61E+06
31	1064.73	3393.99	0.396379	0.00298287	2.80E-06	25.5407	3.61E+06
32	1064.09	3397.73	0.39703	0.00289637	2.72E-06	24.7867	3.62E+06
33	1063.45	3401.48	0.397681	0.00281355	2.65E-06	24.0651	3.62E+06
34	1062.81	3405.22	0.398331	0.00273423	2.57E-06	23.3741	3.62E+06
35	1062.18	3408.97	0.398982	0.0026582	2.50E-06	22.7121	3.62E+06
36	1061.54	3412.71	0.399632	0.00258529	2.44E-06	22.0774	3.62E+06
37	1060.9	3416.45	0.400283	0.00251534	2.37E-06	21.4687	3.62E+06
38	1060.26	3420.2	0.400934	0.0024482	2.31E-06	20.8845	3.63E+06
39	1059.62	3423.94	0.401584	0.00238371	2.25E-06	20.3237	3.63E+06
40	1058.98	3427.68	0.402235	0.00232175	2.19E-06	19.785	3.63E+06
41	1058.34	3431.43	0.402886	0.00226219	2.14E-06	19.2674	3.63E+06
42	1057.7	3435.17	0.403536	0.0022049	2.08E-06	18.7696	3.63E+06
43	1057.06	3438.92	0.404187	0.00214978	2.03E-06	18.2909	3.64E+06
44	1056.42	3442.66	0.404838	0.00209672	1.98E-06	17.8301	3.64E+06
45	1055.79	3446.4	0.405488	0.00204563	1.94E-06	17.3866	3.64E+06
46	1055.15	3450.15	0.406139	0.0019964	1.89E-06	16.9594	3.64E+06
47	1054.51	3453.89	0.406789	0.00194895	1.85E-06	16.5477	3.64E+06
48	1053.87	3457.64	0.40744	0.00190319	1.81E-06	16.1509	3.64E+06
49	1053.23	3461.38	0.408091	0.00185906	1.77E-06	15.7683	3.65E+06
50	1052.59	3465.12	0.408741	0.00181647	1.73E-06	15.3992	3.65E+06

Figure E1: Modine Custom Properties For 50% Ethylene Glycol Mixed with 50% Water (By Volume)

APPENDIX F: **THERMAL EXPANSION COEFFICIENT RESULTS FOR 50% ETHYLENE GLYCOL MIXED WITH 50% WATER (BY VOLUME)**

Temp.	Sat. Water Thermal Expansion Coefficient (β_satH2O)	50/50 EGW Thermal Expansion Coefficient (β_5050EGW)
[°C]	1/K	1/K
30	0.000306582	6.89686E-05
31	0.000315336	7.09381E-05
32	0.000323927	7.28706E-05
33	0.000332359	7.47675E-05
34	0.00034064	7.66304E-05
35	0.000348776	7.84605E-05
36	0.000356772	8.02595E-05
37	0.000364637	8.20286E-05
38	0.000372375	8.37694E-05
39	0.000379994	8.54833E-05
40	0.000387499	8.71718E-05
41	0.000394898	8.88362E-05
42	0.000402196	9.0478E-05
43	0.0004094	9.20987E-05
44	0.000416517	9.36996E-05
45	0.000423552	9.52823E-05
46	0.000430513	9.68482E-05
47	0.000437405	9.83987E-05
48	0.000444235	9.99352E-05
49	0.00045101	0.000101459
50	0.000457736	0.000102972

Figure F1: Thermal Expansion Coefficient Results For 50% Ethylene Glycol Mixed with 50% Water (By Volume)

APPENDIX G: **RAYLEIGH NUMBER RESULTS FOR TOP AND BOTTOM COOLANT**

Temp. [°C]	Rayleigh Number – Top Coolant	Rayleigh Number – Bottom Coolant
30	4871794.162	8894866.982
31	5359951.795	9786139.698
32	5878246.004	10732435.43
33	6427575.933	11735395.84
34	7008737.346	12796473.81
35	7622801.437	13917625.12
36	8270356.847	15099924.5
37	8952394.618	16345181.39
38	9669848.529	17655100.68
39	10423670.08	19031419.58
40	11214709.43	20475690.33
41	12043987.45	21989776.81
42	12912500.8	23575498.72
43	13821192.67	25234578.11
44	14771061.73	26968838.36
45	15763461.29	28780750.3
46	16798985.9	30671399.49
47	17878953.62	32643192.42
48	19004592.9	34698371.94
49	20176837.82	36838643.53
50	21397170.92	39066713.98

Figure G1: Rayleigh Number Results For Top and Bottom Coolant

APPENDIX H: **NUSSELT NUMBER RESULTS FOR TOP AND BOTTOM COOLANT**

Temp. [°C]	Nusselt Number - Top Coolant	Nusselt Number – Bottom Coolant
30	143.0924735	60.34000643
31	144.3496123	61.03309557
32	145.5752617	61.71060267
33	146.7714585	62.37351271
34	147.9398211	63.02259394
35	149.0823338	63.65883156
36	150.1999216	64.28263287
37	151.2941435	64.89476834
38	152.3663018	65.49587502
39	153.4175973	66.0865418
40	154.4489883	66.66722895
41	155.461568	67.23847938
42	156.4562922	67.80076518
43	157.4339727	68.3544826
44	158.3954119	68.90002776
45	159.341672	69.43794916
46	160.2730175	69.96834648
47	161.1903436	70.4916816
48	162.0943697	71.00832055
49	162.9855225	71.51846541
50	163.8645943	72.0225305

Figure H1: Nusselt Number Results for Top and Bottom Coolant

APPENDIX I: **COOLANT HEAT TRANSFER COEFFICIENT RESULTS FOR TOP AND BOTTOM COOLANT**

Temp. [°C]	h – Top Coolant	h – Bottom Coolant
30	1258.352	434.1507346
31	1271.492	439.8588616
32	1284.394	445.4720105
33	1297.072	450.9956528
34	1309.534	456.4336885
35	1321.804	461.7950534
36	1333.882	467.079948
37	1345.788	472.2958646
38	1357.53	477.4458756
39	1369.112	482.5326873
40	1380.551	487.5616879
41	1391.851	492.5353092
42	1403.017	497.4554469
43	1414.061	502.3271502
44	1424.988	507.151808
45	1435.803	511.9319114
46	1446.514	516.6704413
47	1457.121	521.3680121
48	1467.638	526.0296386
49	1478.065	530.6553103
50	1488.404	535.2465661

Figure I1: Coolant Heat Transfer Coefficient Results for Top and Bottom Coolant

APPENDIX J: **COOLANT RESISTANCE RESULTS FOR TOP AND BOTTOM COOLANT**

Temp. [°C]	R – Top Coolant	R – Bottom Coolant
30	0.007669	0.030312
31	0.00759	0.029919
32	0.007514	0.029542
33	0.00744	0.02918
34	0.00737	0.028832
35	0.007301	0.028497
36	0.007235	0.028175
37	0.007171	0.027864
38	0.007109	0.027563
39	0.007049	0.027273
40	0.00699	0.026991
41	0.006934	0.026719
42	0.006878	0.026455
43	0.006825	0.026198
44	0.006772	0.025949
45	0.006721	0.025706
46	0.006672	0.025471
47	0.006623	0.025241
48	0.006576	0.025018
49	0.006529	0.024799
50	0.006484	0.024587

Figure J1: Coolant Resistance Results for Top And Bottom Coolant

APPENDIX K: **RESISTANCE, UA, and τ RESULTS FOR BOTTOM COOLANT**

Coolant Temperature	R_Bot	UA	τ
Celsius	m^2/WK	WK/m^2	1/s
30	0.100914	9.909467	380.8286614
31	0.10052	9.948245	379.5345242
32	0.100143	9.985695	378.3002578
33	0.099781	10.0219	377.1225202
34	0.099434	10.05694	375.9953613
35	0.099099	10.09091	374.9198985
36	0.098777	10.12385	373.884585
37	0.098465	10.15585	372.8903066
38	0.098165	10.18694	371.935634
39	0.097874	10.21718	371.0161187
40	0.097593	10.24663	370.1301668
41	0.09732	10.27533	369.2769569
42	0.097056	10.30331	368.4526614
43	0.0968	10.33062	367.6572324
44	0.09655	10.35728	366.8871818
45	0.096308	10.38334	366.1455688
46	0.096072	10.40882	365.4250241
47	0.095843	10.43375	364.7259327
48	0.095619	10.45815	364.0486959
49	0.095401	10.48206	363.3904856
50	0.095188	10.50549	362.7514001

Figure K1: Resistance, UA, and τ results for Bottom Coolant

APPENDIX L: **TRANSIENT TEMPERATURE OF THE BOTTOM COOLANT VS. TIME**

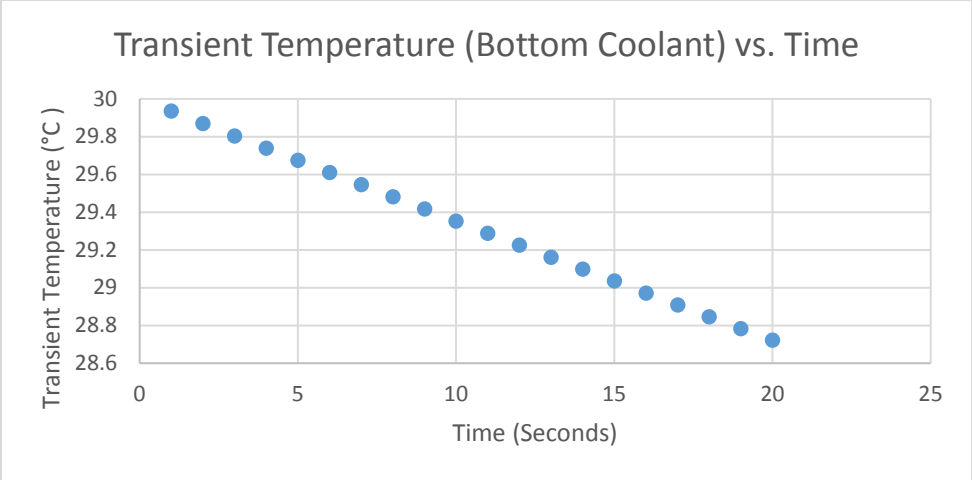

Figure L1: Transient Temperature of the Bottom Coolant vs. Time after 20 seconds starting at $30°C$

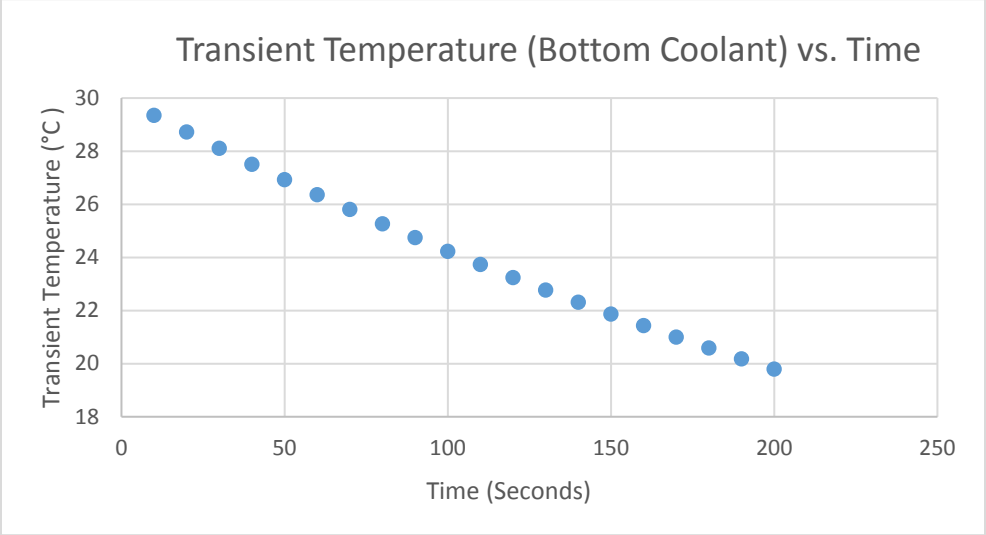

Figure L2: Transient Temperature of the Bottom Coolant vs. Time after 200 seconds starting at $30°C$

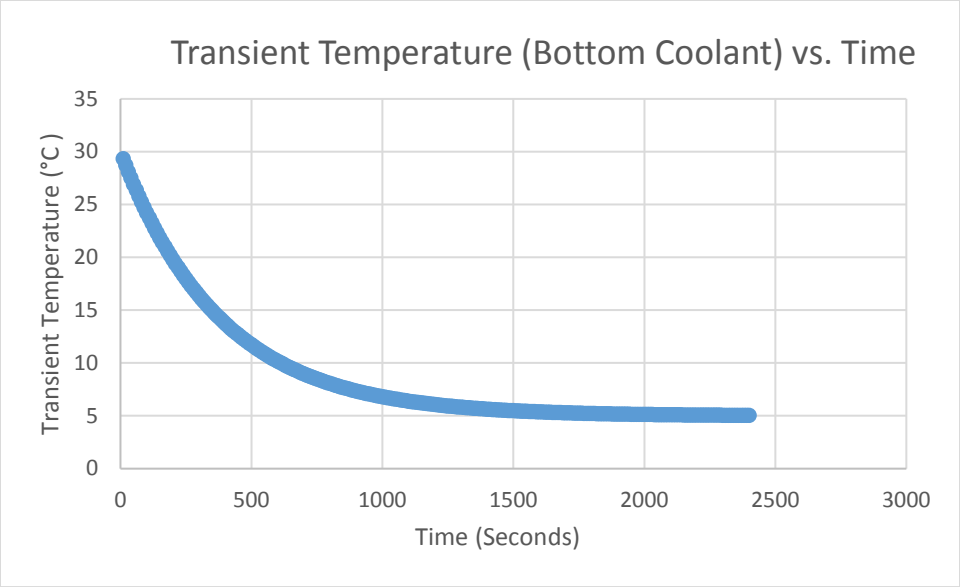

Figure L3: Transient Temperature of the Bottom Coolant vs. Time after 2,400 seconds starting at $30°C$

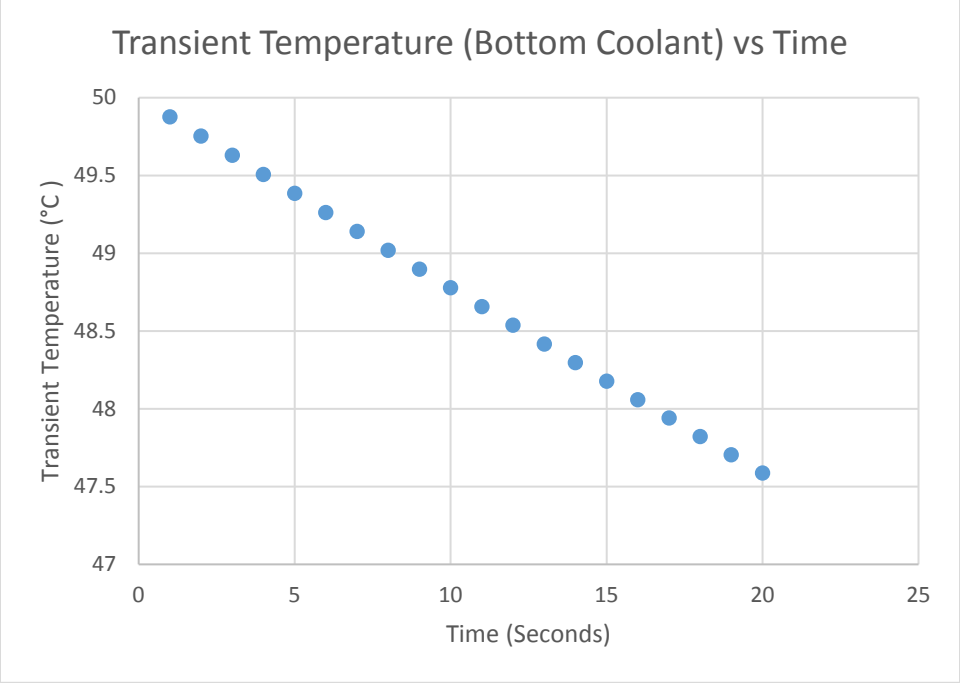

Figure L4: Transient Temperature of the Bottom Coolant vs. Time after 20 seconds starting at $50°C$

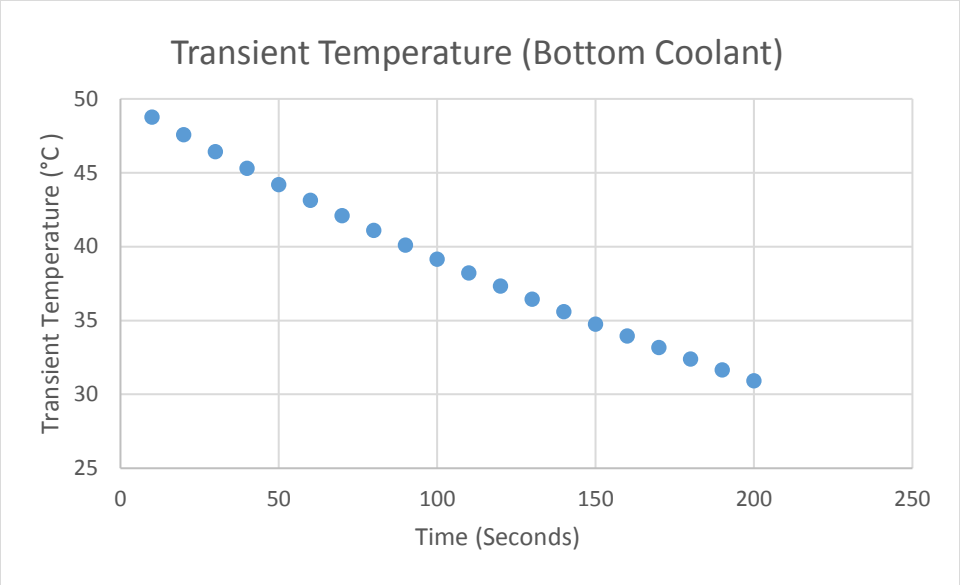

Figure L5: Transient Temperature of the Bottom Coolant vs. Time after 200 seconds starting at $50°C$

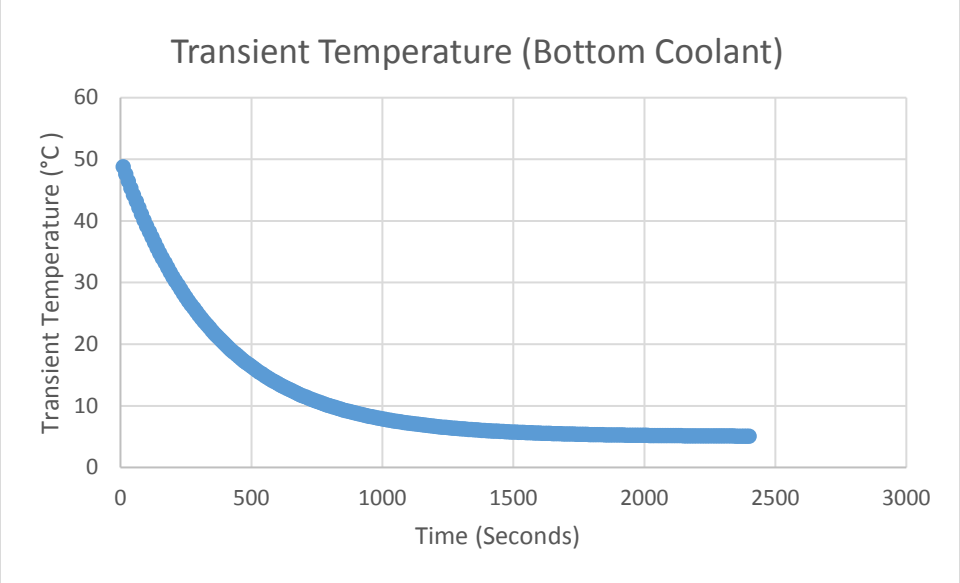

Figure L6: Transient Temperature of the Bottom Coolant vs. Time after 2,400 seconds starting at $50°C$

APPENDIX M: **RESISTANCE, UA, and τ RESULTS FOR TOP COOLANT**

Coolant Temperature	R_tot	UA	τ
Celsius	m^2/WK	WK/m^2	1/s
30	0.056905	17.57317	622.9476599
31	0.056826	17.59768	622.3921455
32	0.056749	17.62132	621.867977
33	0.056676	17.64415	621.3747408
34	0.056605	17.66623	620.9069177
35	0.056537	17.6876	620.4714594
36	0.056471	17.70831	620.052001
37	0.056407	17.7284	619.6541206
38	0.056345	17.74792	619.2783709
39	0.056284	17.76688	618.9199946
40	0.056226	17.78534	618.5792844
41	0.056169	17.80331	618.2570975
42	0.056114	17.82082	617.9490013
43	0.05606	17.83789	617.6573251
44	0.056008	17.85456	617.3778178
45	0.055957	17.87084	617.1173801
46	0.055907	17.88675	616.8652279
47	0.055859	17.9023	616.6232122
48	0.055811	17.91752	616.3938805
49	0.055765	17.93243	616.1733402
50	0.05572	17.94702	615.9629078

Figure M1: Resistance, UA, and τ results for Top Coolant

APPENDIX N: **TRANSIENT TEMPERATURE OF THE TOP COOLANT VS. TIME**

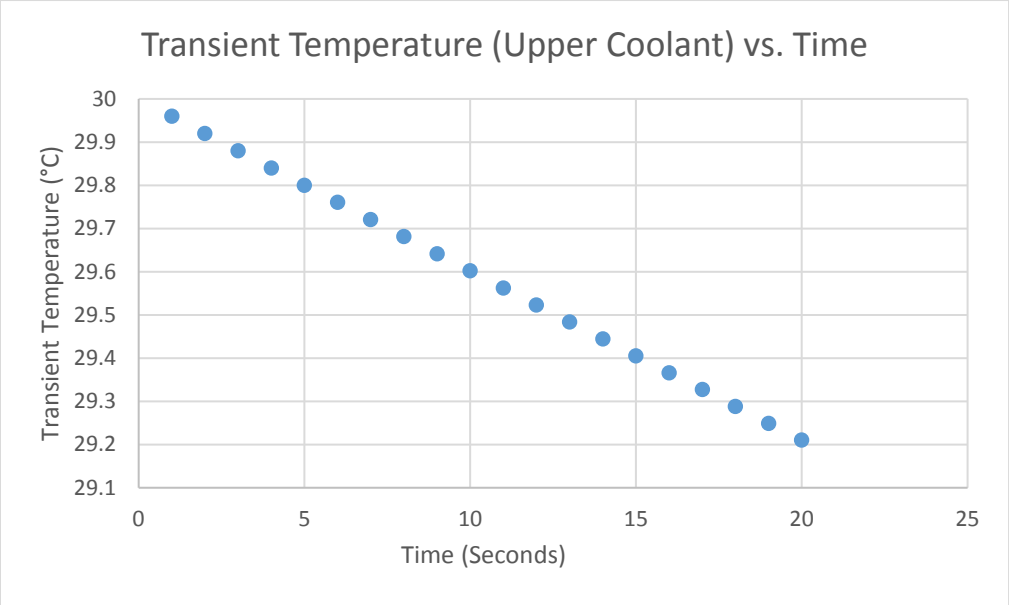

Figure N1: Transient Temperature of the Top Coolant vs. Time after 20 seconds starting at $30°C$

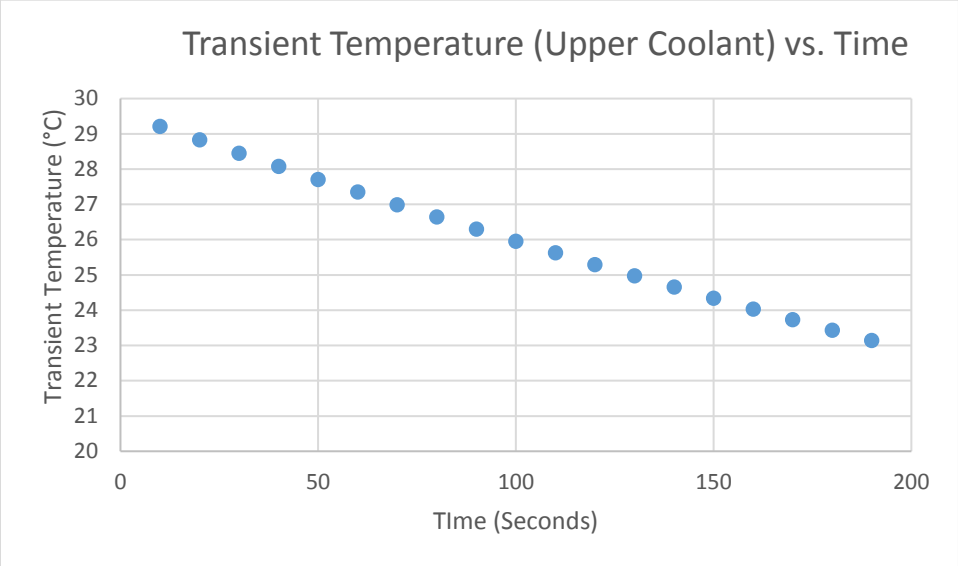

Figure N2: Transient Temperature of the Top Coolant vs. Time after 200 seconds starting at $30°C$

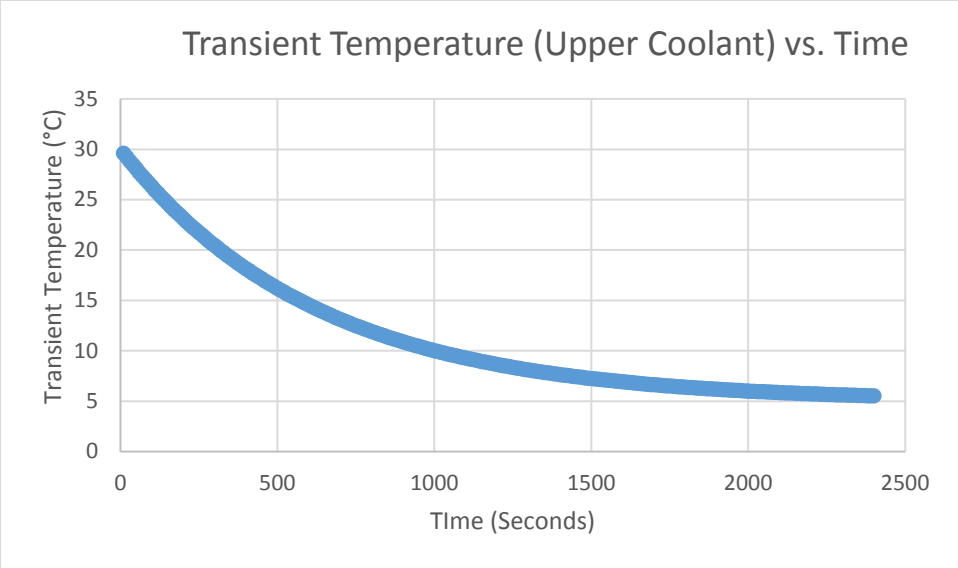

Figure N3: Transient Temperature of the Top Coolant vs. Time after 2,400 seconds starting at $30°C$

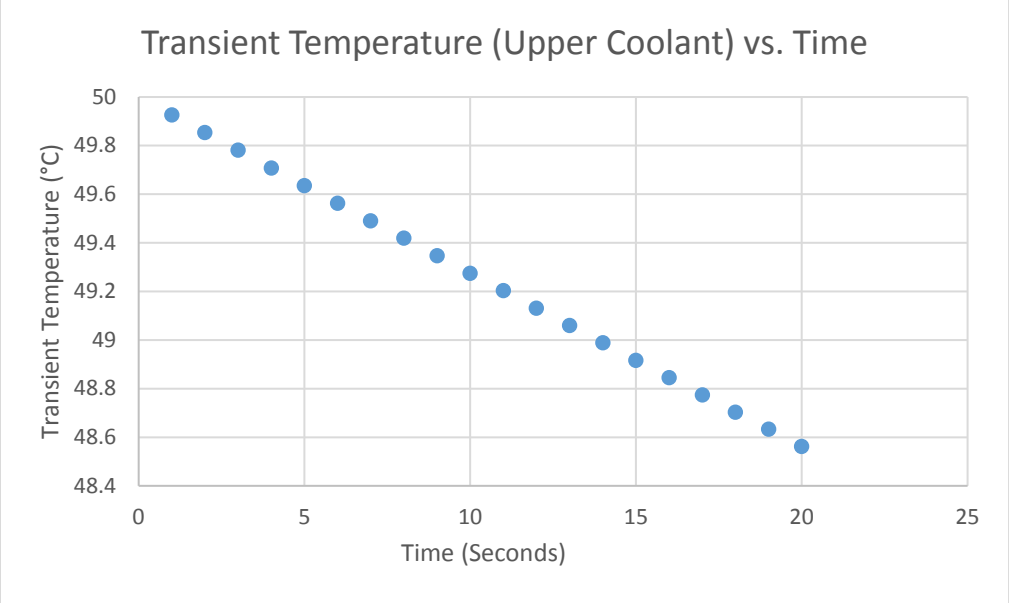

Figure N4: Transient Temperature of the Top Coolant vs. Time after 20 seconds starting at $50°C$

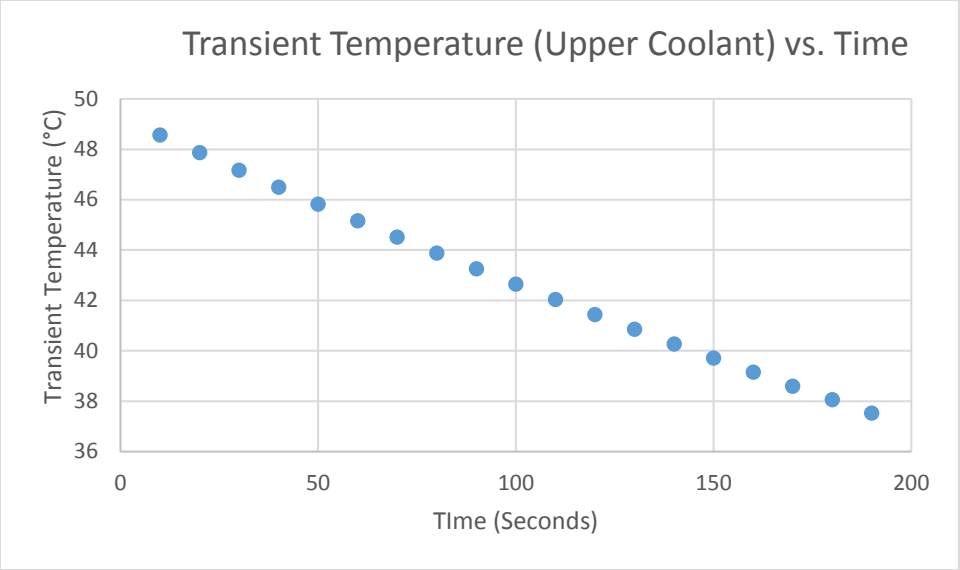

Figure N5: Transient Temperature of the Top Coolant vs. Time after 200 seconds starting at $50°C$

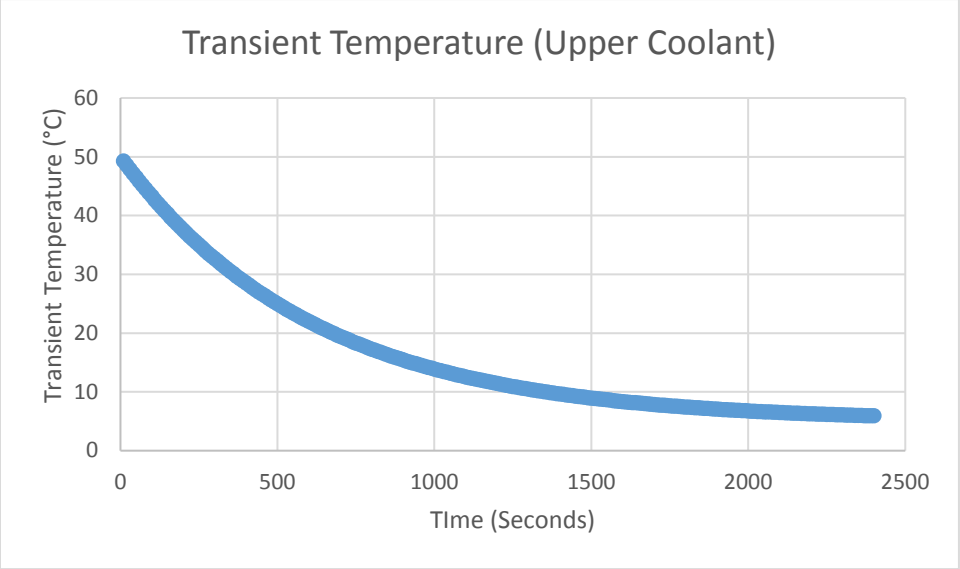

Figure N6: Transient Temperature of the Top Coolant vs. Time after 2,400 seconds starting at $50°C$

APPENDIX O: **RESISTANCE, UA, and τ RESULTS FOR OVERALL COOLANT**

Coolant Temperature	R_tot	UA	τ
Celsius	m^2/WK	WK/m^2	1/s
30	0.036386612	27.48263558	535.6463493
31	0.036303011	27.54592457	534.6838124
32	0.036222674	27.60701728	533.7674424
33	0.036145372	27.66605894	532.8954842
34	0.036070912	27.72316943	532.0620323
35	0.035999043	27.77851598	531.2715981
36	0.035929654	27.83216372	530.5094429
37	0.035862538	27.8842505	529.779176
38	0.035797566	27.93485982	529.080462
39	0.03573462	27.9840671	528.4085054
40	0.035673551	28.03197247	527.7627221
41	0.035614261	28.07863976	527.1432259
42	0.035556662	28.1241247	526.5456925
43	0.035500633	28.16851199	525.9714205
44	0.035446103	28.21184623	525.4163469
45	0.035392994	28.25417945	524.8858526
46	0.035341223	28.29556899	524.3703046
47	0.03529074	28.33604479	523.870948
48	0.03524145	28.37567675	523.3894063
49	0.035193316	28.41448681	522.922134
50	0.035146286	28.45250854	522.4699261

Figure O1: Resistance, UA, and τ results for Overall Coolant

APPENDIX P: **TRANSIENT TEMPERATURE OF THE OVERALL COOLANT VS. TIME**

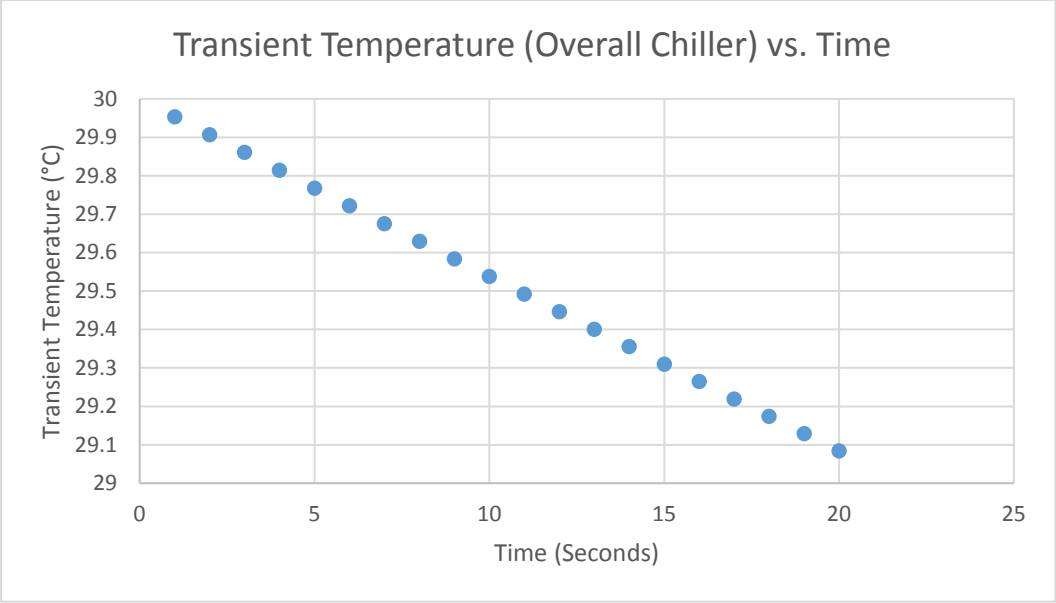

Figure P1: Transient Temperature of the Overall Coolant vs. Time after 20 seconds starting at $30°C$

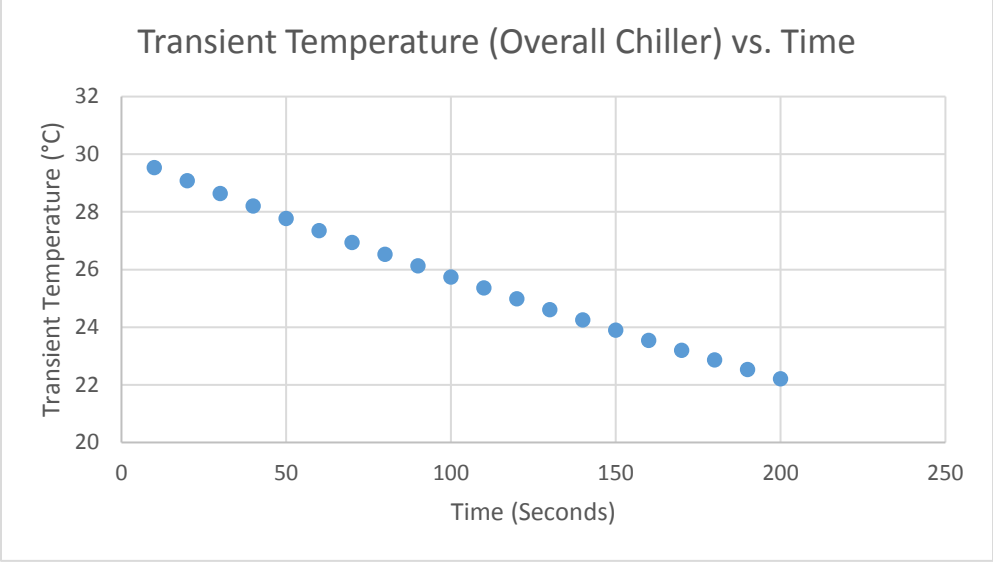

Figure P2: Transient Temperature of the Overall Coolant vs. Time after 200 seconds starting at $30°C$

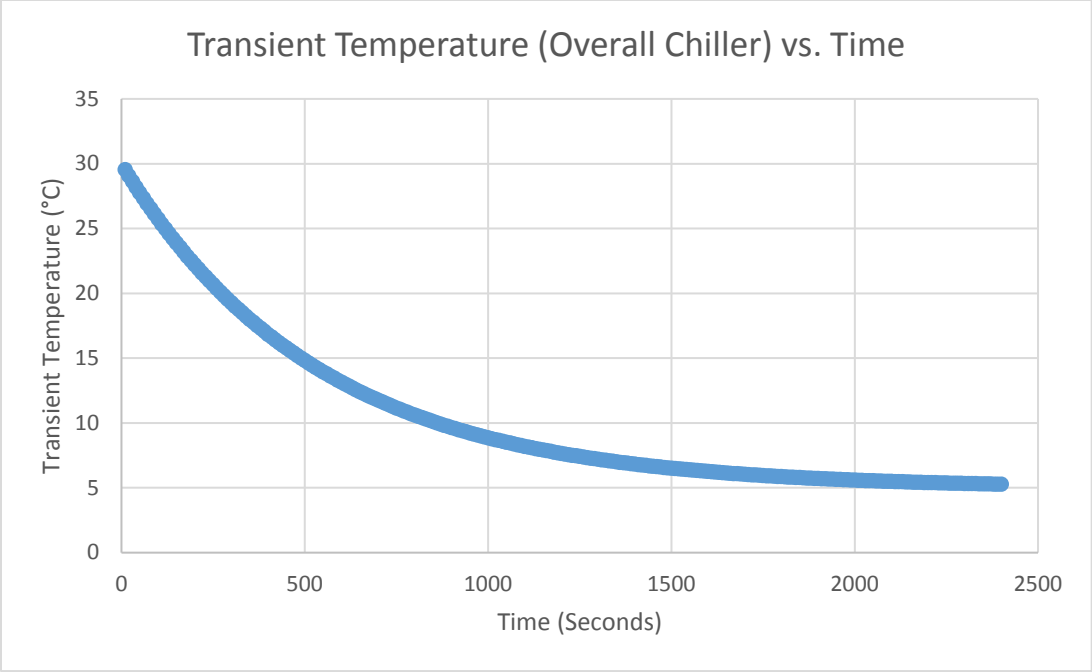

Figure P3: Transient Temperature of the Overall Coolant vs. Time after 2,400 seconds starting at $30°C$

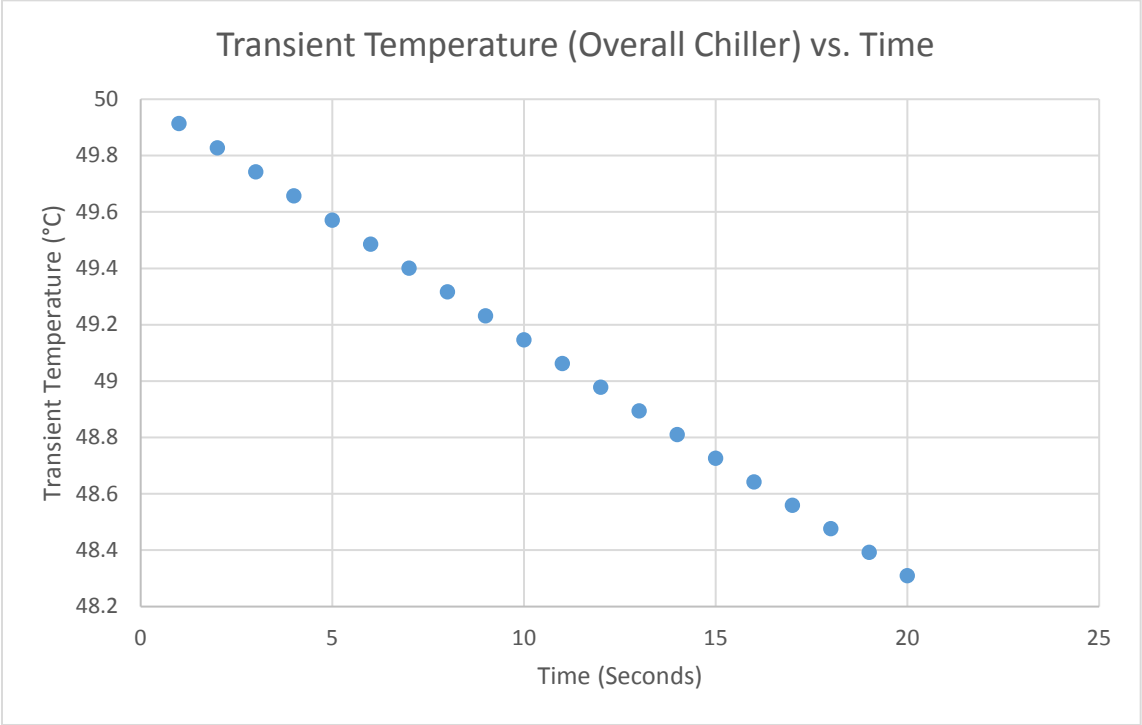

Figure P4: Transient Temperature of the Overall Coolant vs. Time after 20 seconds starting at $50°C$

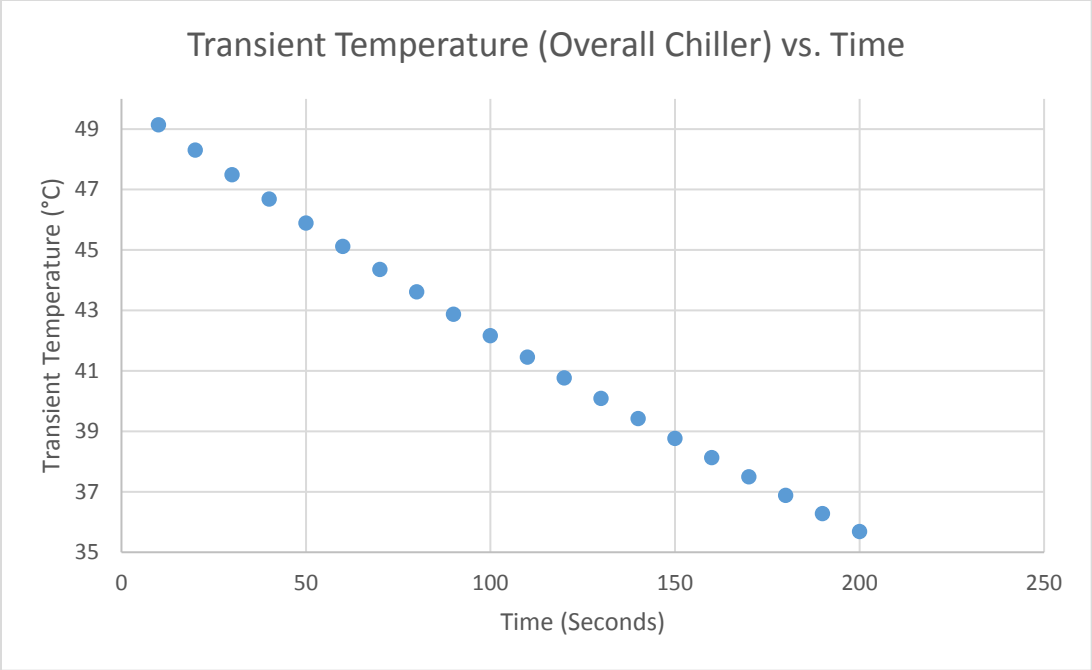

Figure P5: Transient Temperature of the Overall Coolant vs. Time after 200 seconds starting at $50°C$

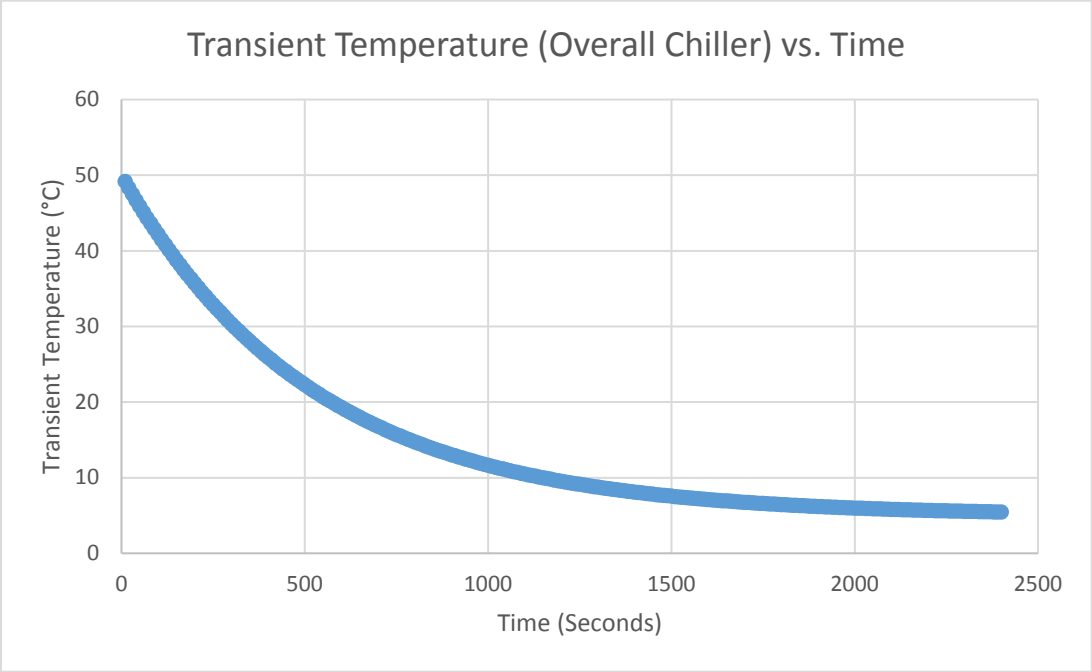

Figure P6: Transient Temperature of the Overall Coolant vs. Time after 2,400 seconds starting at $50°C$

APPENDIX Q: **TRANSIENT TEMPERATURE OF THE BOTTOM COOLANT VS. R1**

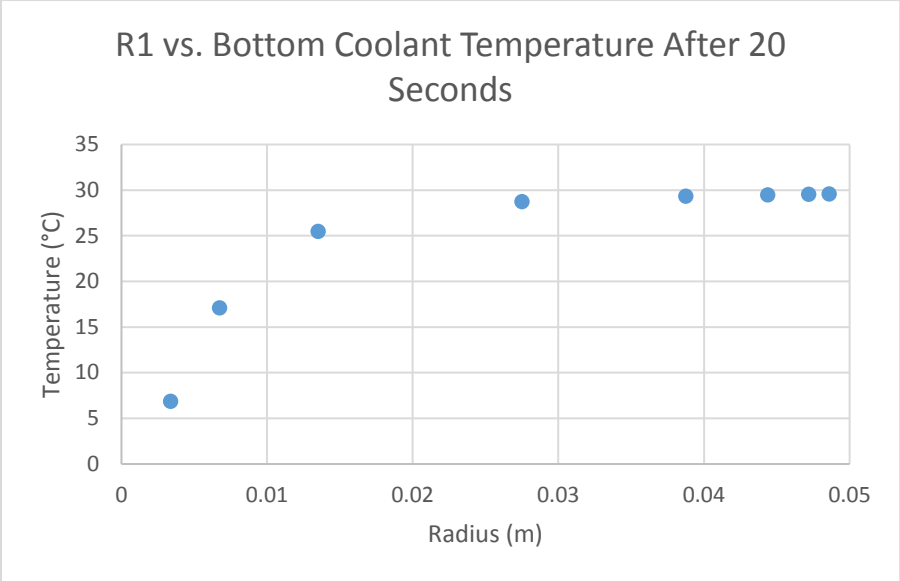

Figure Q1: Transient Temperature of the Bottom Coolant based on different iterations of r1 after 20 seconds at $30°C$

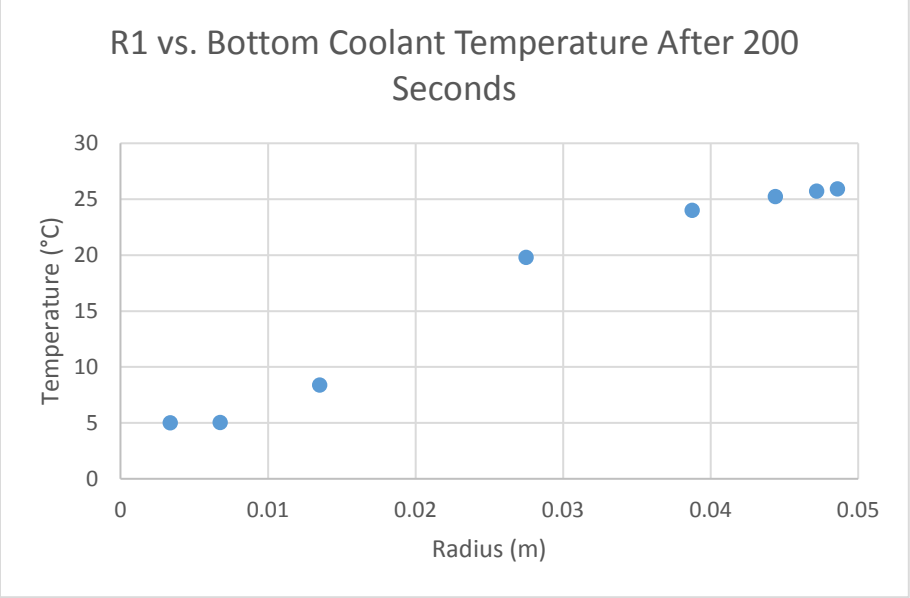

Figure Q2: Transient Temperature of the Bottom Coolant based on different iterations of r1 after 200 seconds at $30°C$

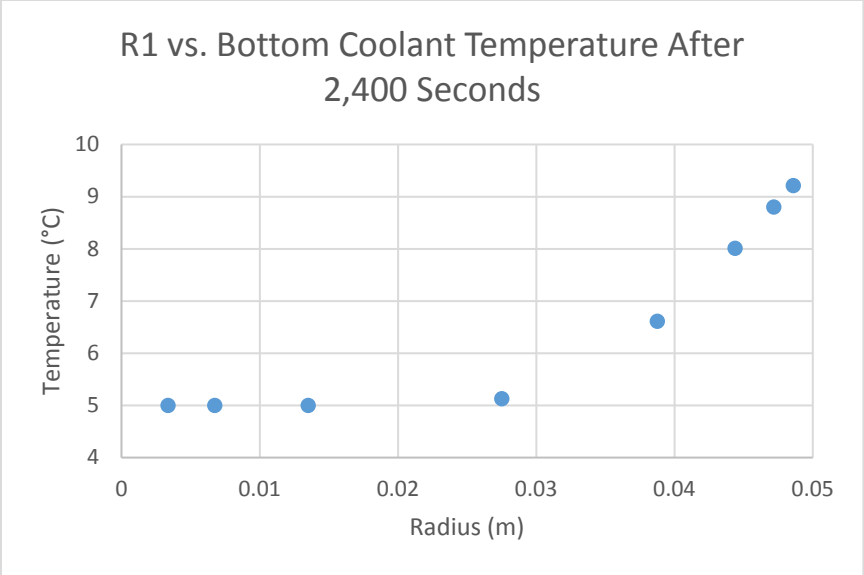

Figure Q3: Transient Temperature of the Bottom Coolant based on different iterations of r1 after 2,400 seconds at $30°C$

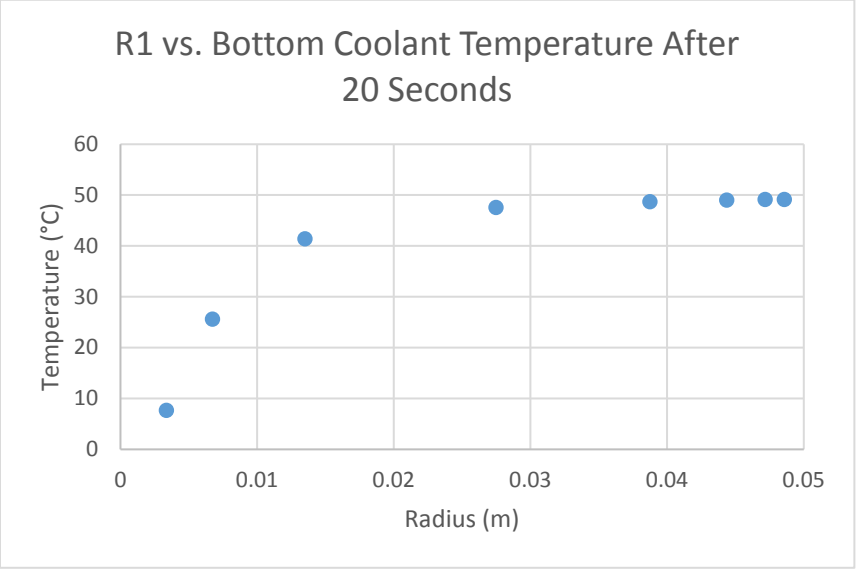

Figure Q4: Transient Temperature of the Bottom Coolant based on different iterations of r1 after 20 seconds at $50°C$

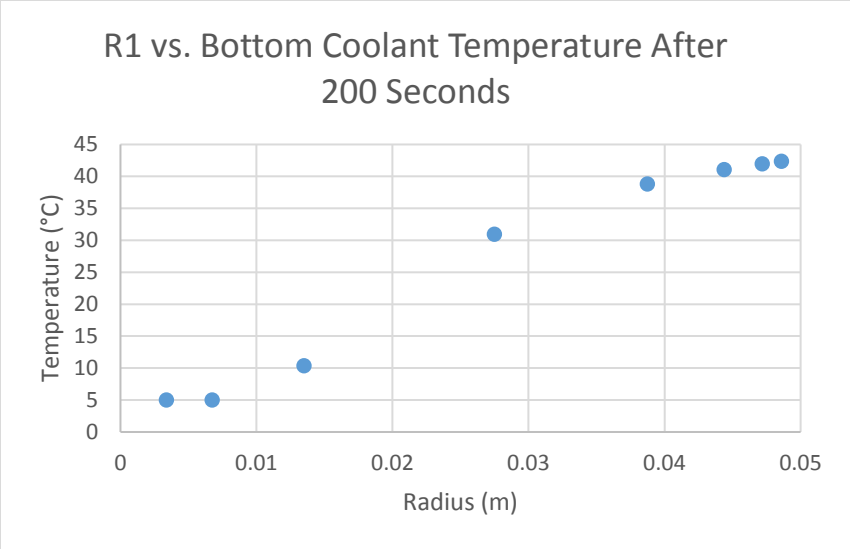

Figure Q5: Transient Temperature of the Bottom Coolant based on different iterations of r1 after 200 seconds at $50°C$

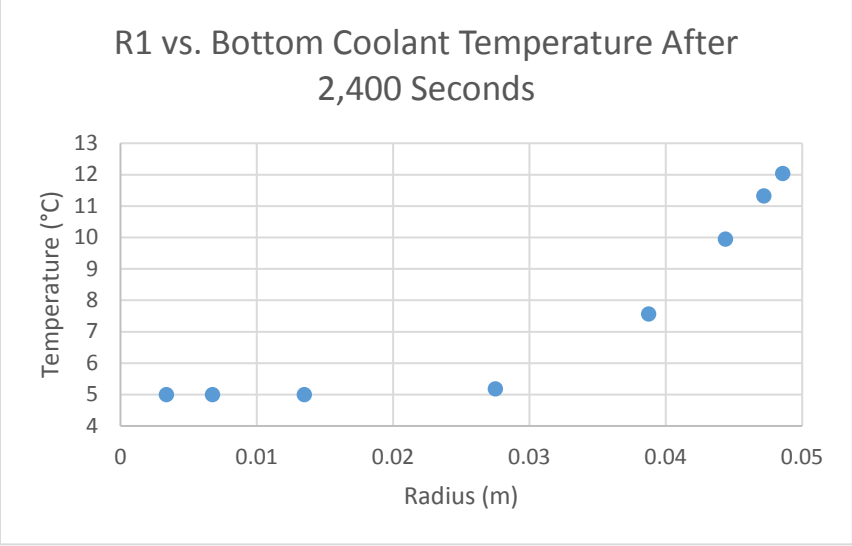

Figure Q6: Transient Temperature of the Bottom Coolant based on different iterations of r1 after 2,400 seconds at $50°C$

APPENDIX R: **TRANSIENT TEMPERATURE OF THE TOP COOLANT VS. R1**

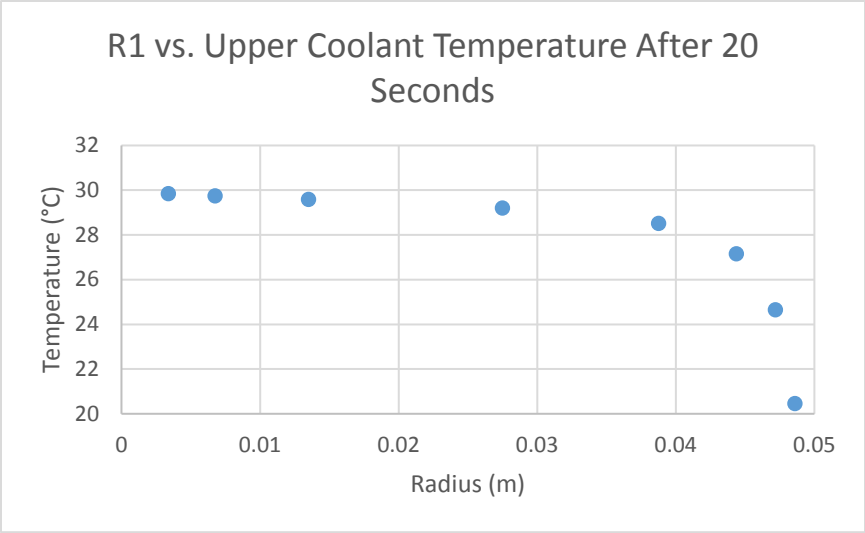

Figure R1: Transient Temperature of the Top Coolant based on different iterations of r1 after 20 seconds at $30°C$

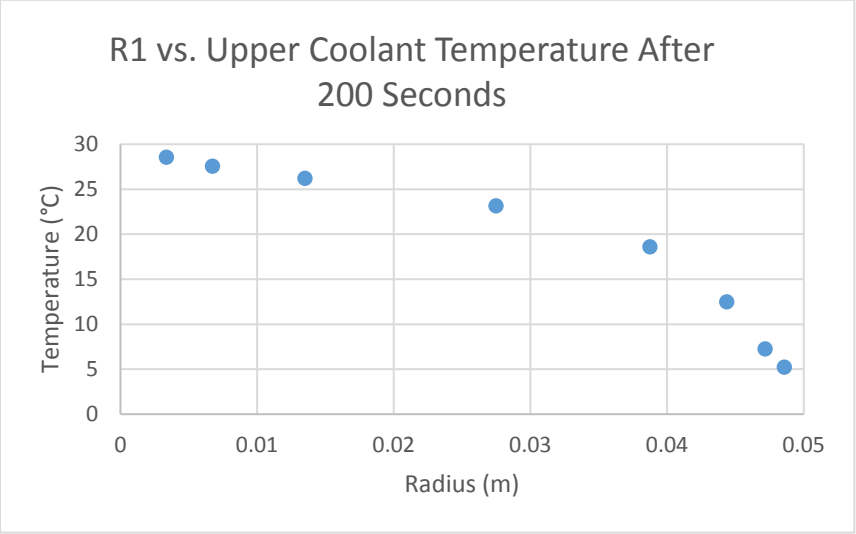

Figure R2: Transient Temperature of the Top Coolant based on different iterations of r1 after 200 seconds at $30°C$

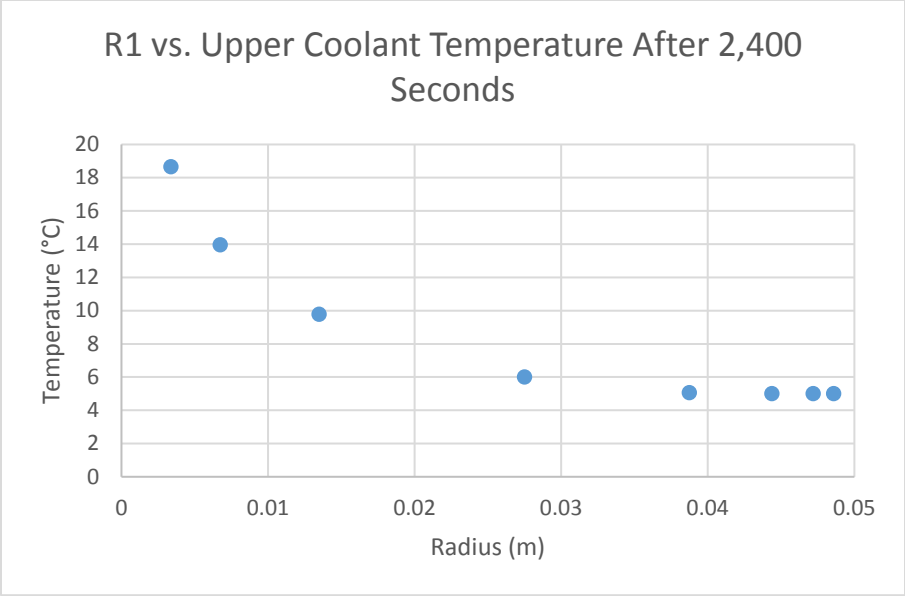

Figure R3: Transient Temperature of the Top Coolant based on different iterations of r1 after 2,400 seconds at $30°C$

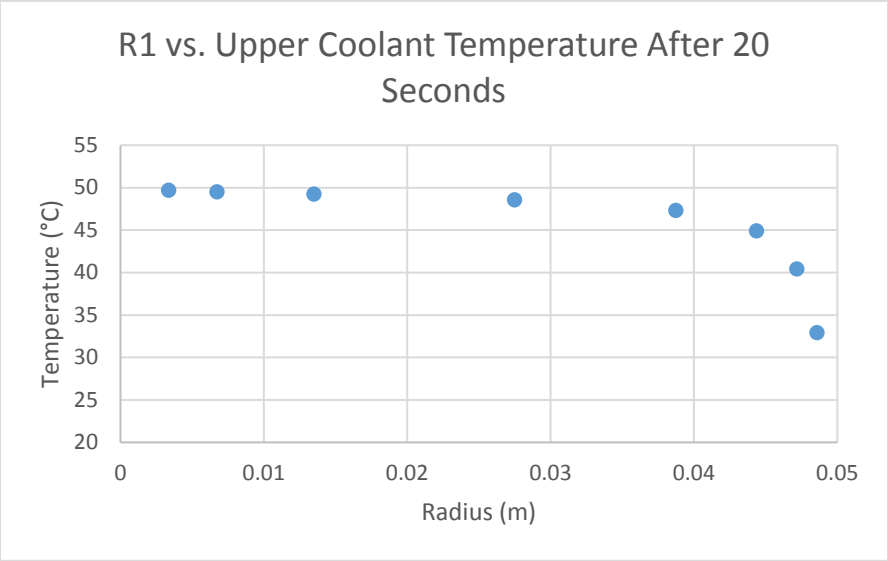

Figure R4: Transient Temperature of the Top Coolant based on different iterations of r1 after 20 seconds at $50°C$

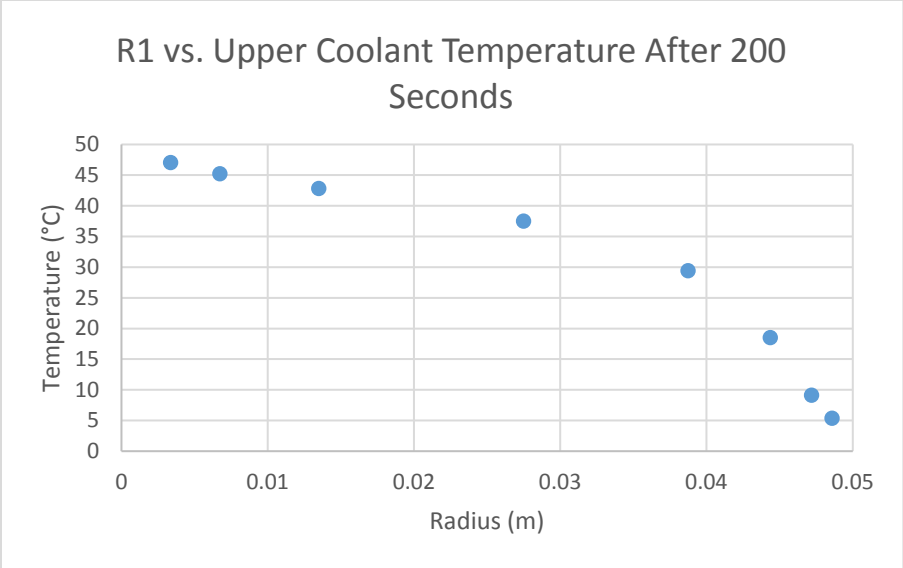

Figure R5: Transient Temperature of the Top Coolant based on different iterations of r1 after 200 seconds at $50°C$

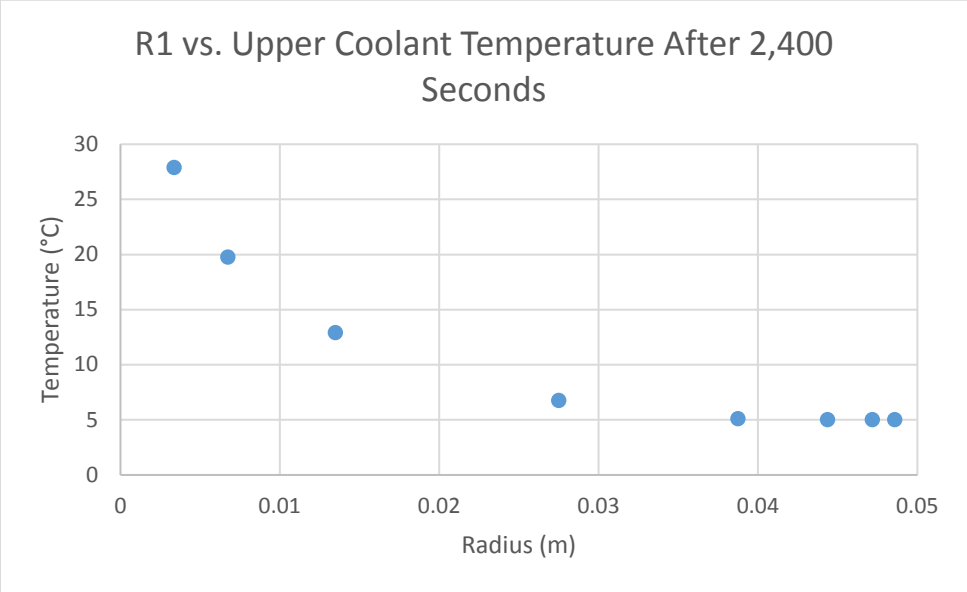

Figure R6: Transient Temperature of the Top Coolant based on different iterations of r1 after 2,400 seconds at $50°C$

APPENDIX S: **TRANSIENT TEMPERATURE OF THE OVERALL COOLANT VS. R1**

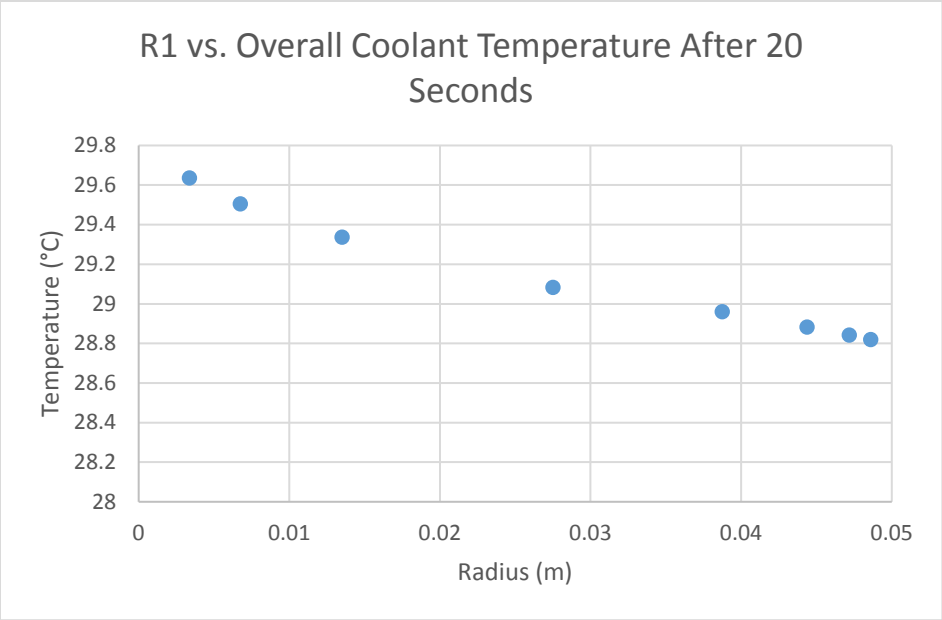

Figure S1: Transient Temperature of the Overall Coolant based on different iterations of r1 after 20 seconds at $30°C$

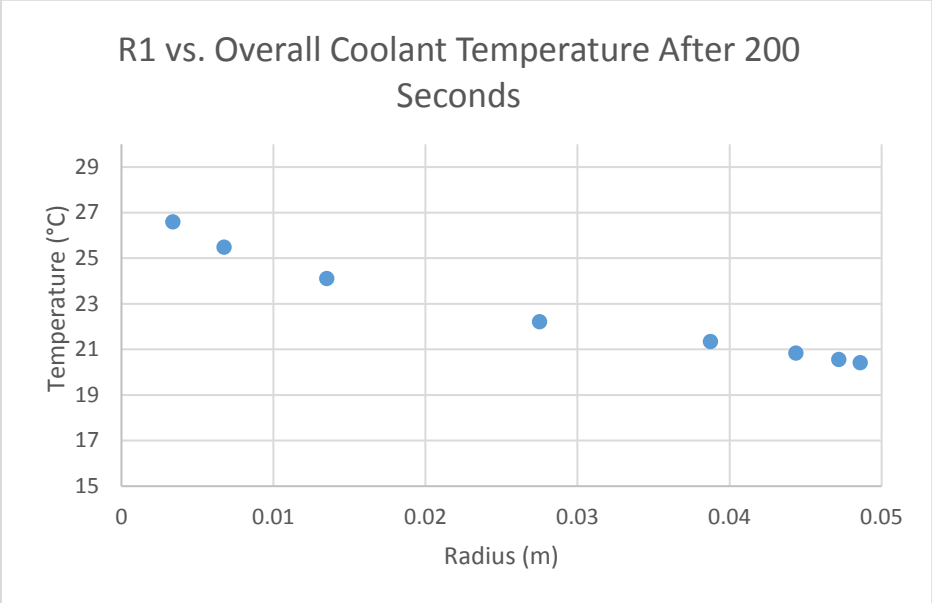

Figure S2: Transient Temperature of the Overall Coolant based on different iterations of r1 after 200 seconds at $30°C$

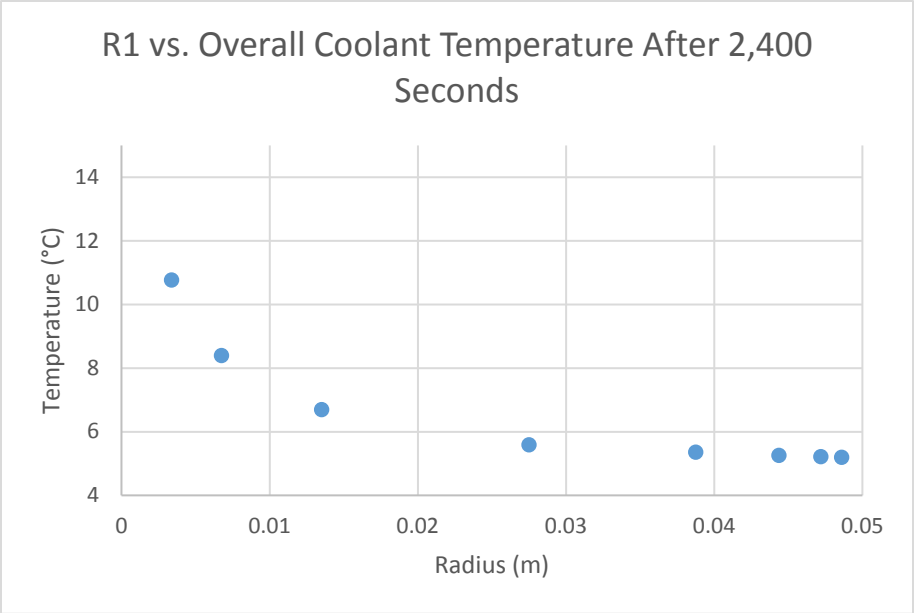

Figure S3: Transient Temperature of the Overall Coolant based on different iterations of r1 after 2,400 seconds at $30°C$

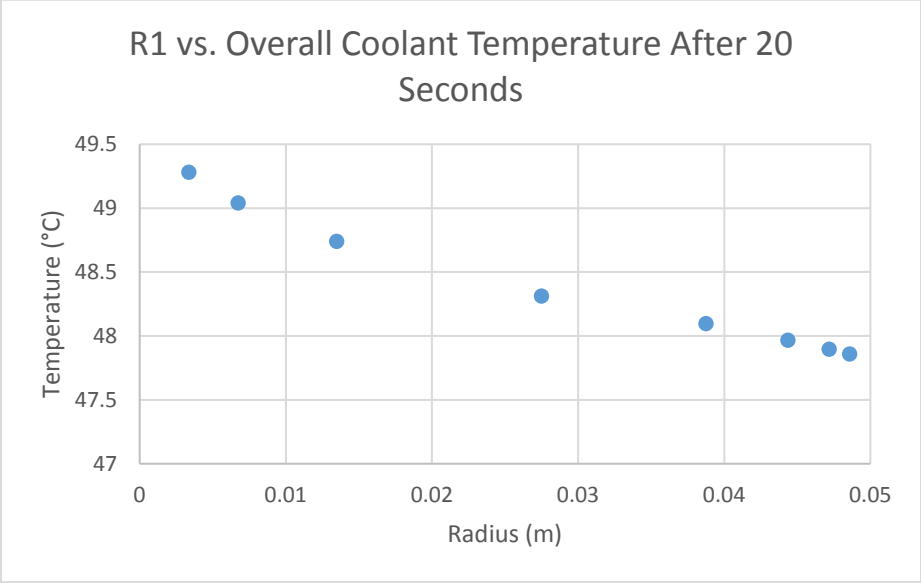

Figure S4: Transient Temperature of the Overall Coolant based on different iterations of r1 after 20 seconds at $50°C$

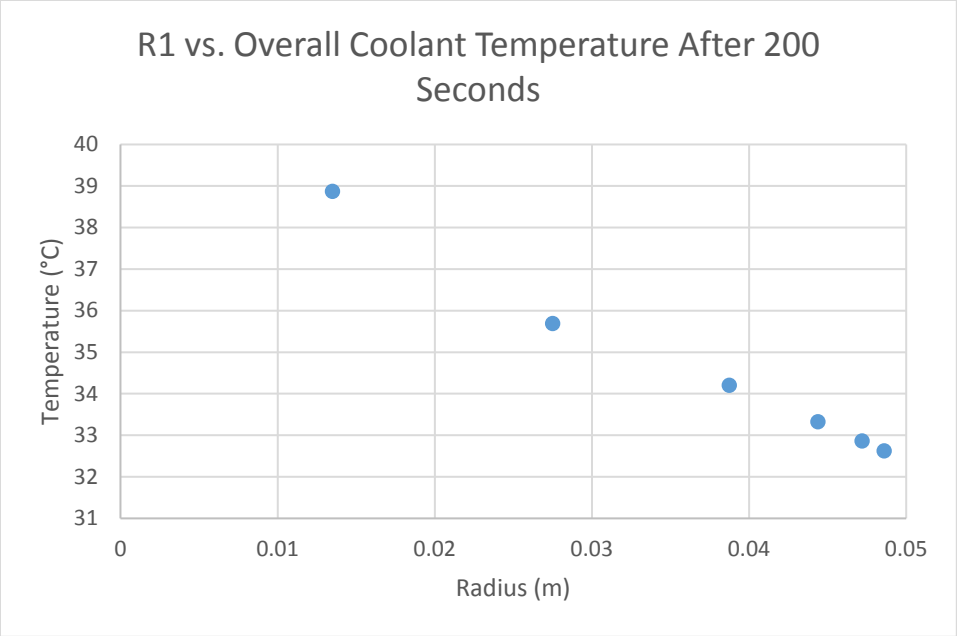

Figure S5: Transient Temperature of the Overall Coolant based on different iterations of r1 after 200 seconds at $50°C$

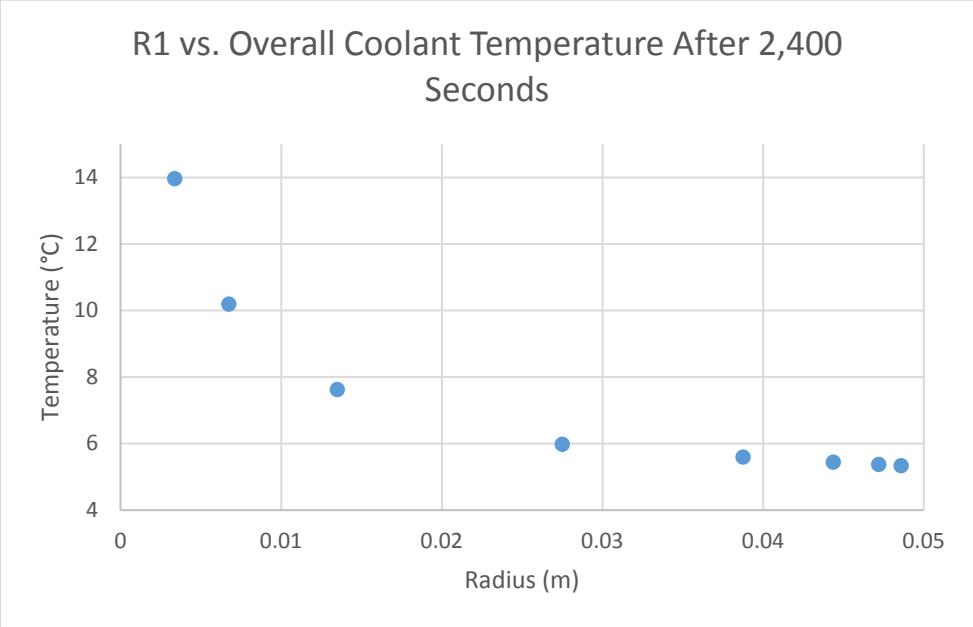

Figure S6: Transient Temperature of the Overall Coolant based on different iterations of r1 after 2,400 seconds at $50°C$